Understanding gene and protein function of MYB93 in tomato and *Arabidopsis*

by

Xulyu Cao

A thesis submitted to

The University of Birmingham

For the degree of

DOCTOR OF PHILOSOPHY

School of Biosciences

The University of Birmingham

July 2021

Abstract

AtMYB93 functions as a negative regulator of lateral root development in *Arabidopsis*. The focus of this study is to identify *MYB93* orthologues in tomato and study their function. I have identified three *SlMYB93*s in tomato, which are *SlMYB93-1*, *SlMYB93-2* and *SlMYB93-3*. Overexpress of *Sl*MYB93-1 and *Sl*MYB93-2 in Arabidopsis exhibit reduced lateral root density, suggests that *Sl*MYB93-1 and *Sl*MYB93-2 have similar function on lateral root development with *At*MYB93 in Arabidopsis.

By analysing RNAseq data of Atmyb93 mutant, I have identified 255 differentially expressed genes, which function in various aspects plant growth, such as sugar transport, flavonoid metabolism, cell wall development. Further analysis has identified *AtGH9C3* and *AtCASPL1D2* have *At*MYB93 binding motifs in their promoter regions., which makes them likely to be direct target genes of *At*MYB93. It is hypothesised that *At*MYB93 controls lateral root development by regulating *AtGH9C3* and *AtCASPL1D2* expression. Interestingly, AtMYB93 is upregulated in response to deficiency, and S deficiency also inhibits lateral root development in Arabidopsis. *At*MYB93 is potentially identified as a lateral root inhibitor in response to S deficiency.

Acknowledgement

I would like to thank Dr Juliet Coates for giving me this opportunity to do my PhD with her supervision and for her immense support and encouragement on my personal and academic life throughout my PhD. I would also like to thank Dr Clare Clayton, Dr Fatemeh Ghaderi and Dr Alexandros Phokas for their valuable advice and help during my PhD.

I would like to thank friends and colleagues in Gibbs and Sanchez-Moran labs for their help] and make second floor an enjoyable place to work. A huge thank you goes to Dr Mark Bailey, Dr Anne-Marie Labandera Nadeau and Dr Alice Derbyshire for their advice and support, which has encouraged me during PhD.

Thanks to friends in Brady lab in UC, Davis for their help and advice. In particular, the guidance of Mona Gouran in doing hairy root transformation in tomato. And a big thank you to Dr Chao Bian for helping me settle down in Brady lab. I would also like to acknowledge Prof Siobhan Brady for her kind support on my research visit in her lab.

Thanks to Karen Staple and Andrian Breckles for their help with growing plants in glasshouse.

Finally, a massive thank you to my Mom, Dad, Grandparents for their unconditional love and support!

I would like to acknowledge the Chinese Scholarship Council (CSC) for funding my PhD project and Universita 21 (U21) and the Society for In Vitro Biology for funding my trip to in UC, Davis.

Table of Contents

TABLE OF FIGURES

TABLE OF TABLES

Chapter Ⅰ: Introduction

1.1. Food Security

1.1.1 Importance of food security

Food is the essential substance to provide energetic and nutritional supports to human activities (Mann and Truswell, 2007). It is also fundamental human right to access adequate food and be free from hunger, which promoted public recognition of food security (UN 1948). As ever-increasing global population grows and climate changes, food security has been threatened and discussed around the world.

The first world-wide discussion was held in early 1930's due to the starvation during the World War One. It was the first time to introduce the world food problem and emphasised the vital position of food for human health (D. John Shaw, 2007). The Food and Agriculture Organisation of the United Nation (FAO) was found in October 1945 to organise and assist 194 member states to defeat hunger and achieve food security worldwide.

The initial concept of food security was then recognised as the right to food in the Universal Declaration of Human Rights by the United Nation (UN) in 1948 (UN, 1948). The term "food security" was first officially defined in the 1974 World Food Summit as "availability at all times of adequate world food supplies of basic foodstuffs to sustain a steady expansion of food consumption and to offset fluctuations in production and prices." (UN, 1975) which emphasis the availability and supply of food to meet growing food consumption. In 1996, the conception of food security had developed with addition of demand and access issues at World Food Summit. And the latest definition was established by the United Nations' Committee on Word Food Security in 2003, as the "means that all people, at all times, have physical, social, and economic access to sufficient, safe, and nutritious food that meets their food preferences and dietary needs for an active and healthy life." It is consisted of four key

components, including food availability, food access, food utilisation and stability (Fraanje and Lee-Gammage 2018).

1.1.2 Challenges for food security

It was reported that 25.9 percent of the world population or 2 billion people around the world had experienced either severe or moderate food insecurity in 2019. According to FAO reports since 2017, there are many threats on the way to achieve food security, such as climate changes, economic regression and the COVID-19 pandemic (FAO, 2020).

1.1.2.1 Climate Changes

Climate change has been a major challenge to food security since mid-20th century, from which extreme weather happened more frequently, such as droughts, floods and heat waves (Gregory *et al*., 2004). In 2016, the strong El Niño event significantly influenced the climates in various parts of the world, including Africa, Central America, Southeast Asia, Australia and a number of Pacific islands (Zhai *et al*., 2016). A severe drop in food production and disruption in food access were also caused by this El Niño event, which was considered as one of the three strongest El Niño event since 1950. (FAO, 2020) According to FAO, Due to the droughts from 2011 to 2016, 124 million people in 51 countries were suffering in severe food insecurity. Comparing to droughts, over-average rainfall or floods also induce food insecurity. It was considered as “the most recurring, widespread, disastrous and frequent natural hazards of the world” (Odufuwa *et al*., 2012). The most immediate impact of floods is destruction of farmlands, which undermines the farm yields and harvests, decreasing the food availability to local households or the whole country. (Devereux, S, 2007) Many African and Southeast countries are particularly vulnerable to flooding. In 2012, South eastern Nigeria was attacked

by the floods, which was noted as the worst one in over past 40 years with over 4701 square kilometres of urban and rural lands submerged (Ojigi, M.L *et al*., 2013). Over 7.7 million people were affected due to the massive destruction of the farmland and houses, which also affected their accommodation, specially food security status (Akukwe *et al*., 2020). Myanmar also suffered from the severe flood in 2015 with 1.29 million acres of farm lands inundated and 687200 acres damaged (Foodlist, 2015).

1.1.2.2 Population explosion

Growth rate of the global population has been increasing significantly since the 19th century and reaching high peak of 2.1% in the 20th century with population of around 6 billion. Although growth rate decreased 1.08% in 2019, it was still advised by UN that the world population will reach 9 billion by 2045, which indicated the increasing demand of the basic needs like food, water and land (UN, 2019). In 2009, the FAO predicted that the 70% more food production would be needed to meet increasing demand of food globally by 2050 (FAO, 2009). Although food production growth rate increased faster than world population growth rate since 1960, uneven distribution of the population around the world does not match with the global food production map (Van Bavel, 2013). Some regions with more rapid population growth and less food production cannot even feed themselves. For example, Sub-Saharan Africa (SSA) was considered as one of those regions and predicted to be unable to be self-sufficient on cereal (approximately 80%) by 2050 due to the uneven growth between the population and cereal yield (Van Ittersum *et al*., 2016). Thus, food imports have become particularly vital to food security in those countries (Hall *et al*., 2017).

Apart from insufficient food supply, unfair food distribution is another challenge for food security in countries with rapid population rate. According to UN, some African countries such

as Malawi and Zambia were predicted to have a five-time population growth between 2015 and 2100, (UN, 2015) which will alleviate the efforts devoted to eliminating poverty and inequality in those regions. Therefore social-economic inequality induced unfair food distribution by making accessing food difficult for low-income families. Although It was commonly known that global food production should be currently sufficient or even exceed the demand of the world's population, food insecurity condition such as hungers and malnutrition still exist in many less developed areas with fast growing population. (Van Bavel, 2013)

1.1.2.3 Soil degradation

Soils are the most common and valuable resources in the world, as soils provide a wide range of ecosystem services for humans, including production of 98.8% food for humanity, filtering and recycling water and nutrients, detoxification of the contaminants and wastes. Thus, healthy soils are essential for ensuring normal human life (FAO, 2015). In 2015, the UN stated that "*soils constitute the foundation for agricultural development, essential ecosystem functions and food security and hence are key to sustaining life on Earth*". (UN, 2015) However, soils are currently non-renewable resources, as their regeneration is slower than the soil degradation, which is caused by soil erosion, nutrients depletion, salinity and contamination. (Lal *et al*., 2015) Recent findings indicate that 33% of global soils are affected by different levels of degradations, which have severely bad influence on human life in different aspects (FAO, 2011).

Food insecurity is one of the major problems caused by soil degradation, which affects all four fundamental components of food security (food availability, food access, food utilisation and stability) (Fraanje and Lee-Gammage, 2018). Soil erosion is the core issue of land degradation,

which can be classified into three groups including water erosion, wind erosion and tillage erosion, which indicates its correlation with climate changes and human activities (Balasubramanian, 2017). Soil erosion leads to loss of the most nutritious topsoil layer containing organic matters, which not only provide plants with micro- and macro nutrients, also ensure the water holding capacity in soil (Pimentel and Burgess, 2013). Recent findings estimate that average global soil erosion rate is ~1.4t ha^{-1} yr^{-1}, which is much higher than natural erosion rate (~0.03t ha^{-1} yr^{-1}) in some places lack human activities. (Wuepper *et al*., 2020) Reduction on quantity and quality of soil adversely affects crop yield and nutritious crop productions and eventually threats the global food security.

Apart from the erosion of soil, soil security is also affected by salinity, acidification and contamination (Kopittke *et al*., 2019). All three issues are also related to human activities, mainly because of the industrialisation and urbanisation. They contribute to production of contaminated wastes, which were then either buried in soil or released in water or air. (Song Y *et al*., 2017) The contaminated soil, water and air affect plant growth and pose a threat to food safety as well as a threat to global food security. For examples, soil salinity due to the irrigation with poor quality water stresses the plant and affects plant growth and crop yield. According to FAO, soil salinity caused 0.3 to 1.5 million ha of farmland loss, and another 20 to 40 million ha of farmland with less productivity every year around the world. (FAO and ITPS, 2015)

Poor quality of water and soil also contribute to other soil security issues. Because of the contaminated wastes from human activities, water and soil can be contaminated with inorganic (heavy metals and metalloids) and organic (herbicides and pesticides) contaminants, which are applied in agriculture. Those contaminants can be absorbed and accumulated in plant, which are toxic to both plants and animals with plant-based diet,

including humans. (Kopittke, P.M et al., 2019) In USA, 1375 sites are listed as the sites with known or threatened releases of hazardous substances, pollutants or contaminants. (USEPA, 2021). In 2015, 80000 sites were recorded as contaminated sites in Australia and 19% of farmland in China was estimated as polluted. (Kopittke, P.M et al., 2019)

Soil insecurity has profoundly negative impacts on agriculture and is recognised as one of the major challenges of the global food security. Economics of Land Degradation (ELD) initiative showed that, with ~52% of farmland suffering severe or moderate soil degradation, it was estimated that soil degradation annually cost US$6.3 to 10.6 trillion for loss of its ecosystem services. And it was also predicted that soil degradation would lead to decreasing food productivity (~12%) and increasing food prices in 2030. (Noel, 2016)

1.1.2.4 COVID-19

Coronavirus disease 2019 (COVID-19) was first identified in December 2019 and recognised as a pandemic by World Health Organisation (WHO) on 11th March 2020. According to the European Centre for Disease Prevention and Control (ECDC), COVID-19 is easily spreading from person to person through respiratory droplet caused by coughing, sneezing and exhaling. As of 30th March 2021, over 124 million confirmed cases and 2.79 million deaths of COVID-19 have been reported worldwide and numbers are still growing (Lau *et al*., 2020). To contain and slow down the spreading of virus, wide range of lockdown has been introduced in most of the countries. As of 28th April 2020, 54% of global population (~ 4.2 billion) were on the complete or partial lockdowns, and almost all global population was affected by local restrictions. (IEA, 2020)

The COVID-19 pandemic is not only a public health crisis, it has also triggered global food insecurity. According to the World Food Program (WFP), “COVID-19 is threatening to affect

millions of people already made vulnerable by food insecurity and malnutrition." (WFP, 2021) Although no major food shortage has been reported yet, food security has been challenged in its all four fundamental components (food availability, food access, food utilisation and stability) during the pandemic (FAO, 2020).

Due to the global human mobility restrictions, less workers are allowed to work, which has severely affected the food supply chains (Aday and Aday, 2020). On one hand, the agricultural production has significantly decreased during the lockdowns. The lockdown policies caused labor shortages in labor-intensive agricultural activities such as sowing, planting and harvesting. During the lockdown, some farmers could miss the right time on sowing or planting the crops, which could affect both their incomes and food supply for the next season. On the other hand, food distribution was also jeopardised by the limited transport choices (Aday and Aday, 2020). During the national lockdown in China, transferring medical teams and supplies from other provinces to different cities in Hubei province was prioritised, and only drivers and trucks with specific certifications were allowed to work (Pu *et al*., 2020). It directly broke the food supply chains, which then caused a dramatic drop of the agricultural products in the market. During the epidemic, the marketing quantity of grain, vegetables, fruit and animal products were all decreased over 50% in the first week (24th Jan -30th Jan, 2020) after lockdown in China. (Pu *et al*., 2020) and It was reported by WTO that COVID-19 led to 5.3% reduction on trade in merchandise goods in 2020 (WTO, 2021).

1.1.3 Importance of plant science

Plants as an important part of our world, not only serve as the basis of the food chains in nature, they also provide habitats for some organisms, such as insects, birds, monkeys. The photosynthesis of plants helps to maintain atmosphere by absorbing carbon dioxide and

water and producing oxygen, which is vital to survival of terrestrial organisms (Harvey *et al*., 2006; Gross *et al*., 2014; Sharkey, 2020). Plants are also widely used in our life such as medicine, wood, paper, clothes and some crops are also reported to prevent soil erosion and land degradation (Muoni *et al.*, 2020; Sahu *et al*., 2020; Park *et al*., 2021).

In order to understand mechanism during plant growth and development, modern botany was on the rise in Ancient Greece, which makes it one of the oldest sciences, including plant biochemistry, plant physiology, plant morphology, plant pathogen, plant evolution and genetics (Rapp *et al*., 2005; Gross *et al*., 2014; Taiz *et al*., 2015; Heldt and Piechulla, 2021). These discoveries will potentially be adopted in application to, such as crop improvement, speed breeding, protect soil to help with challenges for food security. For example, the recent study reported that overexpression of human RNA demethylase *FTO* enhanced leading to root growth, yield and drought tolerance in both rice and potato by inducing demethylation of RNA N6-methyladenosine (Yu *et al*., 2021). Waston *et al*., (2018) developed optimal protocol to accelerate growth of wheat for breeding by comparing plant growth under different conditions, such as night period length, temperature, light density, plant density. And rapid breeding enables the rapid crop improvement.

Root as the underground part of plants plays a vital role in plant development and survival by controlling water and nutrients uptake. And it also helps plant anchorage to the soil, which is an important trait to for both plant growth and soil protection (Petricka *et al*., 2012). Flexibility of root morphology also enables plants adaption in response to different abiotic or biotic stress (Jia *et al*., 2008). Thus, studying molecular basis of root development in plants is critical to crop improvement and environment protection, such as heavy metal or pollute uptake, soil remediation and nutrient cycling (Tangehu *et al*., 2011Lux *et al*., 2012; Zhang *et al*., 2020)

1.2 Root development

1.2.1 Root structure of model plants Arabidopsis and tomato

1.2.1.1 *Arabidopsis*

Arabidopsis thaliana has been recognised as the most widely studied flowering plant, due to its features, such as small size, short lifecycle, small genome (125 Mb), high yield of seed production from self-fertilisation and easy access to various mutants. *Arabidopsis* as a model organism is used in a wide range of fields including plant science, genetics and evolution (Koornneef *et al*., 2010). With the development of sequencing techniques, the first *Arabidopsis* genome sequence was established in 2000 (Kaul et al., 2000). After that, more information on and resources for *Arabidopsis* have been collected, analysed and combined, which included development of different 'omics' databases based on the *Arabidopsis* reference genome, such as genomics, transcriptomics, proteomics and metabolomics (Crandall *et al*., 2020).

1.2.1.2 Tomato

Tomato (*Solanum lycopersicum*) is a major crop and one of the most popular vegetables in the world (Kimura *et al*., 2008). Tomato also plays important role in scientific research of the Solanaceae family as a model plant, which not only functions in the scientific field like *Arabidopsis*, but also serves as a promoter of plant breeding for crop improvement, due to its production of fleshy tomato fruits (Ranjan *et al*., 2012). The tomato genome sequence (950 Mb) was first published in 2012, which provided genomic fundamentals for Solanaceae family research (Iorizzo *et al*., 2012). The tomato cultivar used in this project is the dwarf "Micro Tom", which was first bred by crossing "Florid Basket" and "Ohio4013-3" and it is a good model plant for tomato research, according to its traits: small size, short lifecycle and a large

collection of mutants compared to other tomato cultivars such as “Money Maker” and “Ailsa Craig” (Ezura *et al*., 2009; Shikata *et al*., 2016). The mutations in *DWARF* (*D*) and *SELF-PRUNING* (*SP*) were identified in “Micro Tom”, which were suggested to be major genes for dwarf and determinate phenotype in “Micro Tom” (Meissner et al., 1997). Previous studies showed that tomato *SELF-PRUNING* (*SP*) was identified as ortholog of *TERMINAL FLOWER1* (*TFL1*) in *Arabidopsis*, which controlled switching between vegetative and reproductive phases in tomato shoots (Pnueli *et al*., 2001), and tomato *sp* mutant exhibited determinate phenotype as “Micro Tom” (Pnueli *et al*., 1998). In Arabidopsis Recent study showed that this process was balanced by antagonism between TFL1 and FLOWER LOCUS T (FT) mediated by their competition to bind to bZIP transcription factor FD (Zhu *et al*., 2020). The tomato DWARF (D) was identified as a P450 protein catalysing C-6 oxidation of 6-deoxocastasterone during brassinosteroids (BRs) biosynthesis, and mutation of D leads to reduced content of BRs and reduced response to GA in “Micro Tom”, which play an important role in plant growth and development (Bishop *et al*., 1999; Bajguz *et al*., 2020). With the presence of these mutations described above, biosynthesis and response of two major plant hormones were affected, which may lead to dwarf phenotype and may also affect development of lateral root in “Micro Tom”. Thus, proper control experiments should be applied to ensure the reliability of the studies.

Recently, *Agrobacterium*-mediated hairy root transformation in tomato provided a fast and stable tool for studying cell-type specific gene expression, molecular networks, root cells development and secondary metabolites biosynthesis, compared to traditional transformation (Shanks *et al*., 1999; Ron *et al*., 2014). Due to the introduction of Root inducing (Ri) plasmid, hairy root tissues have potential to grow root infinitely (Shanks *et al*., 1999). Thus, it would not be used to study root structure and morphology, especially, regulation of

lateral root development in this study. Hairy root transformation would be expected to generate CRISPR lines of SlMYB93 in tomato root, which would be used for suberin staining to study function of SlMYB93 on suberin deposition in tomato roots.

1.2.1.3 Root structure

Both *Arabidopsis* and tomato are good models for dicot root research, as they share a similar root structure and cell organisation, except that tomato has an extra layer of exodermis cells between the epidermis and cortex (Zobel *et al*., 2016; Alaguero-Cordovilla *et al*., 2018; Kajala *et al*., 2021). The radial cellular organisation of mature root Arabidopsis is shown in Figure1., which generally consists of 8 different types of cells including epidermis, cortex, endodermis, pericycle, protoxylem, metaxylem, phloem and procambium, ordered from the outer layer to the inner. These cells are distributed evenly surround the radial axis of the root with rotational symmetric patterns (Dolan et al., 1993; Miyashima and Nakajima, 2011). Longitudinally, the primary root is divided into four sections: the root cap, meristem zone, elongation zone and maturation zone, in which the same type of cells may exhibit different developmental functions (Singh et al., 2017). To further study root zones, Brady *et al*., (2007) dissected the primary root into 12 sections and performed microarray expression analysis of genes in different cell types from different longitudinal sections, which plays an important role in root developmental research by establishing expression profiles of genes during root growing in both time and space dimensions.

1.2.2 Primary root development

The primary root as the first and most basic component of root system determines the depth of root penetration in the soil (Qin *et al*., 2019). The *Arabidopsis* primary root derives from a single cell named the hypophysis during embryogenesis, which generates the root apical meristem after several rounds of cell divisions, differentiations and expansions. The root apical meristem is responsible for forming the whole root system (Scheres *et al*., 1994; Benfey *et al*., 2000). After germination, continuous growth of primary root depends on two major developmental processes: cell divisions in the root apical meristem and cell elongations in the elongation zone (Tian *et al*., 2014).

1.2.3 Adventitious root development

Adventitious roots (ARs) are formed postembryonically and are defined as the root developing from any non-root tissues, which represents a plant's adaptability to dynamic environments (Bellini et al., 2014). This type of root is named differently in different plant species, such as crown roots in cereal, nodal roots in strawberry, which are also induced and grown in different manners (Steffens *et al*., 2016). For example, AR in *Arabidopsis* initiate from shoot-root junction. Crown roots of rice and wheat derive from stems below the soil and can be induced by flooding or nutrient deficiency. Nodal roots in strawberry form from nodes that can be induced by heavy metal stress or flooding (Steffens *et al*., 2016). Little is known about AR initiation, due to lack of AR markers and difficulties in observation under normal conditions (Osmont *et al.*, 2007; Omary *et al*., 2020). In *Arabidopsis*, AR induced by cutting emerge from pericycle cells in the hypocotyl, growth of which is similar to that of lateral roots (Sukumar *et al*., 2013). Like regulation of growth of other root types, it was also reported that the hormones auxin and jasmonic acid play important roles in AR formation.

Auxin-inducible genes, *GH3*s, (*GH3.3*, *GH3.5* and *GH3.6*) were reported to regulate AR formation by controlling the JA-responsive COI1 signalling pathway (Gutierrez *et al*., 2012).

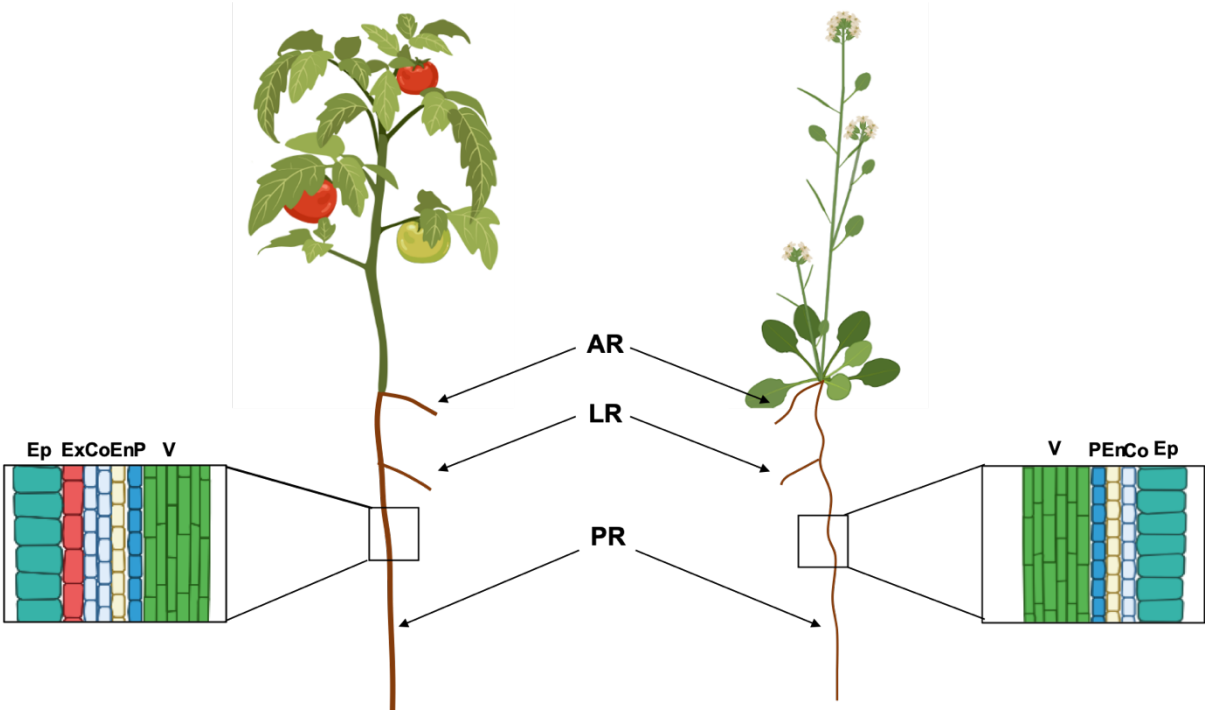

Figure 1.1 root system and root anatomy in tomato and Arabidopsis.
Root systems of both tomato and Arabidopsis are consisting of primary root (PR), lateral root (LR) that emerges from primary root and adventitious root (AR) that grows at shoot-root junction. Longitudinal sections of both primary roots are on the both sides of the plants. Ep, epidermis; Ex, exodermis; Co, cortex; En, endodermis; P, pericyle; V, vasculature. The figure was drawn in Biorender.

1.2.4 Lateral root development

Lateral roots (LR), key organs for plant anchorage and survival, are initiated from pericycle cells of the primary root in most dicots. The development of LRs has been divided into 8 stages (Malamy and Benfey, 1997). Lateral root primordium (LRP) initiation starts with a decision about where it will be located, which is controlled by the auxin maxima in basal meristem (de Smet *et al*., 2014) (Figure1.2). In the first two stages of LRP initiation, two types of cell division occur successively, which divide cells into 8-10 short cells anticlinally and periclinally into two layers. Then cells further anticlinally divide in the pericycle layer and form a dome shape lateral root primordium, which then penetrates the overlaying cell layer (endodermis, cortex and epidermis) and emerges from primary and becomes lateral root (Casimiro et al., 2003).

1.2.4.1 Lateral root initiation

In *Arabidopsis*, lateral roots are initiated from specified pericycle cells which are located in front of the two xylem poles (Péret *et al*., 2009). These xylem pole pericycle cells are still active in cell division after their differentiation and they function as additional meristem cells in the primary root. This enables flexibility of lateral root formation in response to changing environments (Vangheluwe *et al*., 2021). Longitudinally, lateral root formation generally happens in a transition region between the meristem zone and the elongation zone in the primary root, which was reported to be controlled by auxin accumulation (De Smet *et al*., 2007). It is reported that root clock and programmed cell death of lateral root cap cells contributed to auxin oscillations, which regulated formation of LRPs in *Arabidopsis* (Xuan *et al*., 2016; Penrianez-Rodriguez *et al*., 2021). The auxin accumulation in specified xylem poles determines the lateral root founder cells in pericycle, which are adjacent to these xylem poles

These lateral root founder cells form lateral root primordia after several rounds of asymmetric divisions, which develop lateral roots (Du *et al*., 2018). Apart from Auxin, enviromental condition was reported as the regulator of lateral root formation, such as nutrients, abiotic and biotic stress (Forde, B. and Lorenzo, H. 2001; Seo *et al*., 2009; Kong *et al*., 2020; Wu *et al*., 2020).

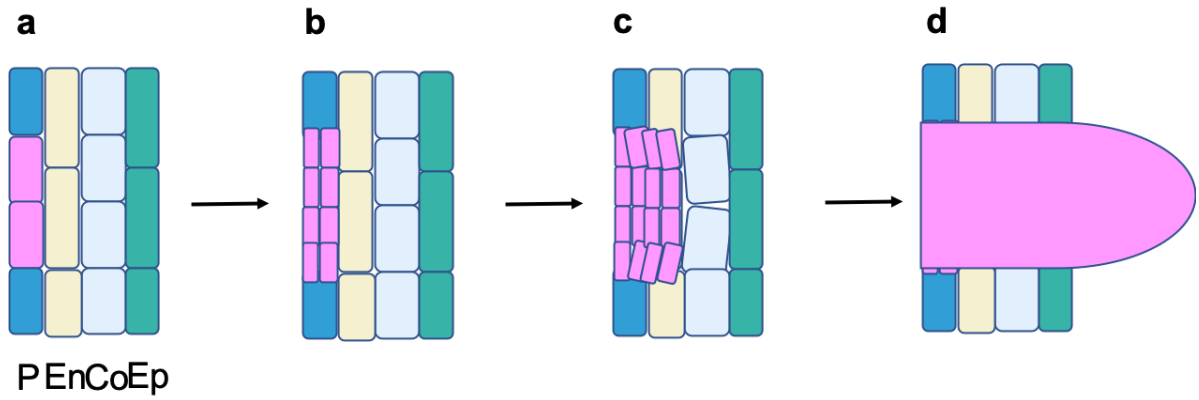

Figure 1. 2 Stages of lateral root development longitudinally. (a) and (b), first two steps of lateral root primordia (LRP) initiation.
Lateral root founder cell in pericycle divides into 8-10 cells after anticlinally and periclinally divisions. (c) the dome-shaped LRP forms by further divisions, which flattens the overlapping endodermal cell till it gets through. (d) LRP emerges through the cortex and epidermis by loosening cell adherence and growing through intercellular space and become a new lateral root with apical meristem activity. P, pericycle; En, endodermis; Co, cortex; Ep, epidermis.

1.2.4.2 Lateral root emergence

After lateral root initiation, the lateral root primordium needs to penetrate three layers of cells (endodermis, cortex and epidermis) above to emerge from primary root. This process involves interactions between the lateral root primordium and neighbouring cells overlapping the lateral root primordium. To minimise the damage to primary roots, these overlaying endodermal cells continuously become thinner, while the lateral root primordium grows radially. With the fusion of plasma membrane and degradation of the Casparian strip, the lateral root primordium grows through the overlaying endodermal cells (Vermeer *et al*., 2014). As for the cortex and epidermis, the lateral root primordium grows out from the intercellular space by pushing overlapping cells away and becoming a lateral root (Péret *et al*., 2009). The newly emerged lateral roots have similar apical meristem activity as primary roots, enabling elongation of lateral roots (De Smet *et al*., 2006). Tomato root has different anatomical structure, which contains one more layer of exodermis between epidermis and cortex (Kajala et al., 2021). Thus, unlike *Arabidopsis*, LRPs would need to penetrate 5 layers of cells (one layer of endodermis, two layers of cortex, one layer of exodermis and one layer of epidermis) during lateral root emergence in tomato. Exodermis was reported to present in 93% of angiosperms, which forms apoplastic barriers (Casparian strip and suberin lamellae) in response to different stress, such as drought, salinity, heavy metal and nutrient stress (Perumalla *et al*., 1990; Hose et al.,2001) In *Phragmites australis* and rice, Armstrong *et al*. (2005) showed that sulphide induced exodermal suberin deposition and lignification leading to interal aeration and reduced water and nutrients uptake, which result in inhibition of lateral root emergence.

1.3 Macronutrients and root development

Root systems are pivotal for plant growth and survival. They not only help by anchoring plants in the soil, but are also responsible for water and nutrient uptake for plant development (Roger *et al*., 2015). Nutrients present in the soil are essential for shoot growth and root branching. In vascular land plants, different root system architectures (RSA) are induced by different nutrient stress conditions. Here I will discuss RSA of *Arabidopsis* under different macronutrient stress conditions (Figure 1.3) and the effect of each macronutrient on root development such as nitrogen, phosphorous, potassium and sulphur.

1.3.1 Nitrogen

Nitrogen (N) can be taken up and utilised by plants in different forms, including inorganic (nitrate and ammonium) and organic (amino acids and peptides). Plants supplemented with different concentrations of N adopt different RSAs. In *Arabidopsis*, growth of PRs and LRs was dramatically repressed under N deficiency (10 μM, 110 μM), and low to medium levels of N availability (275 μM and 550 μM) promoted PR elongation and LR branching, while high levels of N availability (10000 μM and 11400 μM) inhibited elongation of LRs (Araya *et al*., 2014; Gruber *et al*., 2013). In addition, nitrate treatment can both promote and inhibit growth based on the experimental designs (Vidal *et al*., 2010; Araya *et al*., 2014; Gruber *et al*., 2013; O'Brien *et al*., 2016; Naulin *et al*., 2020). It was reported that PR elongation was inhibited by auxin accumulation in root tips, which was regulated by a nitrate-responsive auxin receptor AFB3 (Vidal *et al*., 2010). Recent studies also showed that elongation of PRs in the wild-type Col-0 *Arabidopsis* ecotype was induced by supplementation of 5mM KNO_3, which resulted from enhanced cell division and elongation, regulated by nitrate-induced cytokinin synthesis (Naulin *et al*., 2020).

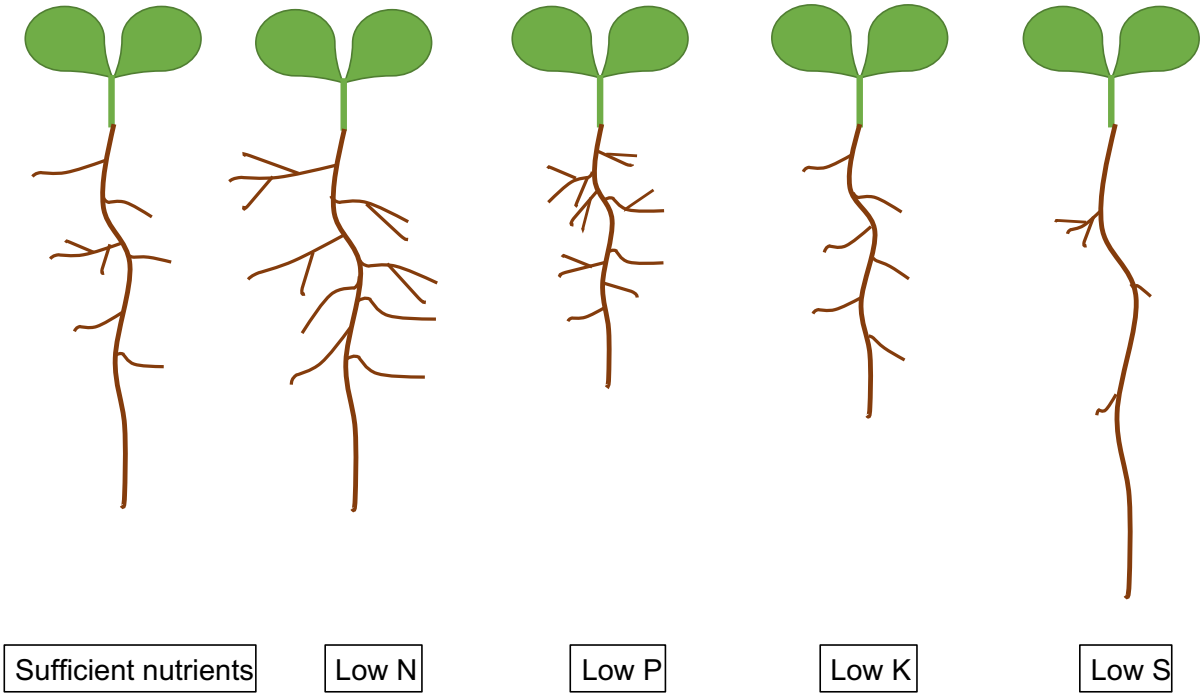

Figure 1.3 Effect of macronutrient deficiency on root development.
Low nitrate (low N), length and density of 1st and 2nd order lateral root increase. Low phosphate (low P), length primary root and 1st order lateral root decrease and 1st and 2nd order lateral root increase. Low potassium (low K), length of primary root and 1st order lateral root decrease. Low sulphate (low S), primary length increases and both length and density of 1st order lateral root decrease. Figure was drawn based on data from Gruber *et a*l., 2013

LR development is generally more sensitive to variation in N availability compared to that of the PR in *Arabidopsis* (Araya *et al*., 2014; Tian *et al*., 2014). LR development was inhibited by both high levels of N availability and severe N deficiency in plants, and enhanced under low and moderate N availability. Previous studies examining the relationship between nitrate signalling and lateral root development has identified proteins such as CLAVATA3/ESR-related-CLAVATA 1(CLE-CLV1), TRYPTOPHAN AMINOTRANSFERASE RELATED 2 (TAR2), ARABIDOPSIS NITRATE RELATED 1 (ANR1) (Gan *et al*., 2005; Gan *et al*., 2012; Araya *et al*., 2014; Ma *et al*., 2014). Araya *et al*., (2014) defined a CLES-CLV regulatory module controlling lateral root development under limited nitrate supply. Overexpression of CLE3 significantly inhibited LR growth, whereas a loss of function CLV mutant showed increased LR growth. Ma *et al*., (2014) identified another mechanism, by which the auxin biosynthesis gene TAR2 expression was up-regulated by N deprivation leading to accumulation of auxin in developing LRs. ANR1, a MADS box transcription factor, was reported as a positive regulator of LR elongation in response to localised N availability (Zhang and Forde 1998), overexpression of ANR1 in Arabidopsis improved LR branching by increasing LR length and number of 2^{nd} order LRs (Gan *et al*., 2012).

Previous studies also reported that sufficient inorganic N regulated *Arabidopsis* root development in complementary manners, by which nitrate promoted LR elongation, whereas ammonium stimulated LR branching (Lima *et al*., 2010). Meier *et al*., (2020) recently reported that LR branching was finely controlled by localised ammonium supply, which triggered accumulation of shoot-derived auxin in the root. Radial diffusion of auxin from vascular cells to the outer cells overlapping lateral root primordia was mediated by the auxin influx carrier LAX3. Further studies found that activity of auxin transporter (PIN-FORMED 2) PIN2 was

modulated in response to different N resources, which then regulated root development by controlling auxin transport direction in the root tip (Ötvös *et al*., 2021).

1.3.2 Phosphorous

Phosphorous (P) is the second most abundant macronutrient in plants, while availability of phosphate (Pi), the available form of P in soil, is finite due to its sorption in soil (Holtan *et al*., 1988). RSA of *Arabidopsis* under low P is shown in Figure 1.3. In general, phosphate (Pi) deficiency inhibits growth of PR and promotes density and branching of LRs and root hairs enabling plant adaptation to access P in the topsoil (Niu *et al*., 2013). Modifications of RSA in response to Pi deficiency has been also observed in other species, such as maize (*Zea mays*), wheat (*Triticum aestivum*) and lupin (*Lupinus albus*). In maize, Pi deficiency has either positive or negative effect on lateral root development across various genotypes (Zhu *et al*., 2007; Postma *et al*., 2014; Jia *et al* 2018). Soumya *et al*., (2021) recently reported that low P availability induced lateral root branching by increased formation of 1st, 2nd and 3rd lateral roots. P deficiency stimulates formation of proteoid (cluster) roots in white lupin, which are involved in desorption of the unavailable P and degradation of organic N in soil (Müller *et al*., 2015; Fujiishi *et al*., 2019).

Pi deficiency-responsive regulators have been reported in *Arabidopsis*, that modulate the root structure in response of low P. LOW PHOSPHOROUS 1 and 2 (LPR1 and LPR2) encode ferroxidases involved in primary root inhibition under Pi deficiency (Müller *et al*., 2015). Mutants of *LPR1* and *LPR2* exhibited significant reduction in both PR length and LR density under low P indicating cross talk between phosphorous and iron signalling pathways in root development (Svistoonoff *et al*., 2007). *PHOSPHATE STARVATION RESPONSE1* (*PHR1*) overexpression lines showed more lateral roots whilst fewer were present in mutant lines

when subjected to low P availability (Huang *et al*., 2018). Further studies reported that transcription of PHR1 was positively regulated by AUXIN RESPONSE FACTOR 7 and -19 (ARF7 and ARF19). Overexpression of *PHR1* in the *arf7*/*arf19* double mutant partially rescued its lateral root impairment phenotype under low P availability (Huang *et al*., 2018). Expression of plasma membrane H^+ ATPase genes *ARABIDOPSIS* H^+*-ATPase* 2 and -7 (*AHA2* and *AHA7*) was upregulated under low P treatment (Yuan *et al*., 2017). Loss of function *aha2* mutants exhibited significant reduction in the elongation rate of PR, due to the inhibition of the proton flux within the root elongation zone, while mutation of *AHA7* led to reduction in root hair density which also correlated with lower proton flux in *aha7* mutant compared to wild type (Yuan *et al*., 2017).

1.3.3 Potassium

Potassium (K) together with N and P are widely present in fertilisers applied to improve agricultural production (Sogn *et al*., 2018). K as an essential macronutrient for plant growth and metabolism is also the most abundant cation in plants, essential for various metabolic processes including enzyme activation, protein synthesis, photosynthesis and maintaining turgor (Marschner, 2010). *Arabidopsis* RSA under K deficiency is shown in Figure 1.3. Low K availability represses elongation of both PRs and 1st order LRs, but promotes formation of 2nd order lateral roots (Gruber *et al*., 2013). Studies also show that root hair elongation is also induced to enhance K uptake under limited K supply (Zhao *et al*., 2017; Feng *et al*., 2021).

Several phytohormone-related genes have been proposed to participate in RSA modulation in response to K deficiency. For instance, the auxin responsive transcription factor AUXIN RESPONSE FACTOR 2 (ARF2) was reported to participate in root structure modification in response to K starvation by inhibiting expression of the HIGH AFFINITY K^+ TRANSPORTER 5

(*AtHAK5*). Overexpression of *At*HAK5 enhanced tolerance to low K availability with longer PRs and root hairs compared to wild type, while the loss function of *Athak5* mutant showed opposing phenotypes (Zhao *et al*., 2017). A recent study identified *At*MYB77 as a transcriptional activator of *At*HAK5 in response to K deficiency (Feng *et al*., 2021).

It has been reported in *Arabidopsis*, that reactive oxygen species (ROS) are involved in the K-deprivation response pathway by inducing expression of a peroxidase RARE COLD INDUCIBLE 3 (RCI3). Both overexpression and mutation of *RCI3* showed significantly decreased PR length suggesting a role in root growth under low K availability (Kim *et al*., 2010). Low K availability induced degradation of the auxin efflux carrier PIN-FORMED 1 (PIN1) mediated by the K^+ channel ARABIDOPSIS K^+ TRANSPORTER 1 (AKT1), which inhibited root growth by reducing auxin accumulation at root tips (Li *et al*., 2017).

1.3.4 Sulphur

Sulphur (S) is an essential macronutrient for plant growth and development (Dan *et al*., 2007). S is taken up by plants in the form of sulphate, which is required for synthesis of cysteine, methionine and other metabolites including glutathione, glucosinolates and Acetyl CoA (Gläser *et al*., 2014; Kacjan *et al*., 2021). Sulphur also functions in many plant developmental processes, in photosynthesis, and in enzyme activation (Wulff-zottele *et al*., 2010; Kessler *et al*., 2006). RSA in S deficiency is shown in Figure 1.3. In *Arabidopsis*, elongation of PRs and 1^{st} order LRs was induced by low S supply, while 1^{st} order lateral root density was repressed under limited S treatment (Gruber *et al*., 2013). Sulphur was reported to have mild effects on root development compared to other macronutrients, and S-responsive root development was also associated with changes of auxin distribution and accumulation (Gruber *et al*., 2013).

Sulphur deprivation induces expression of SULPHATE TRANSPORTERs (SULTRs) to maintain sulphur homeostasis (Yoshimoto *et al*., 2002). Low sulphur supply also stimulates expression of NITRILASE 3 (NIT3) leading to increases in total IAA levels in the root, which promotes lateral root branching in *Arabidopsis* (Kutz *et al*., 2002). Another study showed that SULPHUR LIMITATION 1 (SLIM 1) was identified as a transcription factor which regulated both sulphate uptake and glucosinolate degradation in low sulphur conditions, resulting in shortened primary roots in the *slim1* mutant under sulphur deficiency (Maruyama-Nakashita *et al*., 2007).

Transcriptomic analysis of *Arabidopsis* grown under sulphur deficient conditions identified sulphur-responsive genes, including 21 auxin-related genes such as *IAA17*, *IAA9*, *IAA28* (Nikiforova *et al*., 2003). This indicates auxin may play an important role in the modulation of root development in response to sulphur deficiency. A number of R2R3 MYB transcription factors have been also implied in response to sulphur deficiency such as *At*MYB9, *At*MYB52, *At*MYB93, which further extends the sulphur deficiency responsive molecular network (Bielecka *et al*., 2015). *At*MYB93 expression was also reported to be upregulated in responsive to N deficiency, which suggest that plant may share similar mechanism in response to different nutrient deficiency (Bielecka *et al*., 2015).

1.4 MYB family in plant

1.4.1 MYB transcription factors

The *MYB* family of genes first discovered in 1982, is one of the largest gene families in all eukaryotes. MYB genes were defined by conserved DNA binding domains and each domain has three evenly spaced tryptophan residues (Klempnauer *et al*., 1982; Gabrielsen *et al*., 1991; Ogata *et al*., 1994; Jia *et al*., 2004; Dubos *et al*., 2010). Most MYB proteins function as transcription factors with different numbers of MYB domain repeats. According to the the number and localization of the conserved DNA binding domains, the MYB transcription factors are divided into four types: 4R-MYB (containing four conjoined DNA binding domains); 3R-MYB (R1R2R3-MYB); R2R3-MYB and MYB-related protein (containing one or two interval domains) (Paz-Ares *et al*., 1987; Rosinski *et al*., 1998; Jin *et al*., 1999). In *Arabidopsis*, *MYB* genes are involved in various processes regulating plant growth, including plant metabolism, cell differentiation and stress response, hence MYB proteins are crucial for plant development and survival in different environments (Rabinowicz *et al*., 1999; Stracke *et al*., 2001; Velasco *et al*., 2007; Du *et al*., 2009; Feller *et al*., 2011).

1.4.2 Structure and transcriptional function of MYBs

In *Arabidopsis*, 197 *MYB* genes were identified, which making MYBs one of the largest transcription factor families. MYB proteins regulate the transcription of downstream target genes by binding to their promoter regions, shaping signalling pathways such as metabolite biosynthesis, cell cycle regulation. *At*MYB46 and *At*MYB83 activate other downstream MYB transcription factors (*At*MYB58, *At*MYB63 and *At*MYB85) to regulate lignin biosynthesis (Ko *et al*., 2009). Yang *et al.*, (2017) reported that *At*MYB26 directly induces expression of *NAC SECONDARY WELL THICKENING PROMOTING FACTOR 1* and *2* (*NST1* and *NST2*), which are

important for secondary well thickening in anther walls and siliques. Planchais *et al.*, (2002) found that transcription of *CYCB1;1* was activated through *At*MYB59 binding to TF elements in its promoter region, crucial in controlling cell cycle progression. In *Artemisia annua*, *Aa*MIXTA1 was found to positively regulate glandular secretory trichomes (GSTs) initiation by activating expression of cuticle biosynthesis related genes, such as *AaKCS5*, *A*aABCG12, *AaCER1*, *AaCYP77A1* and *AaCYP86A1* (Shi *et al*., 2018).

Some MYBs also act as transcriptional repressors. *At*MYB4, possessing a conserved EAR repression motif, negatively regulates accumulation of sinapate ester sunscreens for UV protection by inhibiting transcription of *CINNAMATE-4-HYDROXYLASE*(*C4H*) in *Arabidopsis* (Jin *et al*., 2000). When *Arabidopsis* was exposed to UV-B, *AtMYB4* expression was also down regulated, activating biosynthesis of sinapate ester by derepressing C4H (Jin *et al.*, 2000). Park *et al.*, (2008) found that *At*MYB60 inhibited anthocyanin biosynthesis by repressing transcription of dihydroflavonol 4-reduatase (DFR) in lettuce leaves. In loquat (*Eriobotrya japonica*), *Ej*MYB1 and *Ej*MYB2 act as an activator and a repressor respectively, which compete to bind to AC elements within promoter regions of lignin biosynthesis genes to regulate fruit flesh lignification.

1.4.3 Function of R2R3 MYBs

R2R3-MYBs consist of two conserved DNA binding domains (R2 and R3 repeats). 126 of the 197 MYBs in *Arabidopsis* fall into the R2R3 structural class, making it the most common group (Yanhui *et al*., 2006), indicating their importance in plant growth and development. Two conserved DNA binding domains are located at C-terminus of R2R3 MYBs, approximately 50 amino acids in length. Each DNA binding domain comprises a secondary structure of three α-helices separated by three tryptophan residues and three- dimensional folding of the last two

helices forming a “helix-turn-helix” (HTH) structure, a common structure in DNA binding proteins. The HTH structure is important for DNA recognition and binding, factilitating R2R3 MYBs to play key roles in the cellular regulation of plant growth and survival.

1.4.3.1 R2R3MYBs in plant development

In *Arabidopsis*, AtMYB36 is expressed specifically in the pericycle cells and modulates the cell proliferation/differentiation transition in the root meristem (Liberman *et al*., 2015). *At*MYB59 is highly expressed in roots and inhibits root growth by modulating cell division in roots (Mu *et al*., 2009). *At*MYB77, which targets auxin response genes, was identified as a promoter of lateral root development in *Arabidopsis* (Shin *et al*., 2007). *At*MYB23 was found to participate in cell patterning in root epidermis development, affecting both density and distribution of root hairs (Kang et al., 2009). Kirik et al., (2005) also found that *At*MYB23 expressed in developing trichome cells and an *Atmyb23* mutant had fewer trichome branches, suggesting that *At*MYB23 also plays a role in trichome development in shoots. *At*MYB91/AS1 also participates in leaf development (Byrne *et al*., 2000). A group of MYBs involved in anther development has also been reported, including *At*MYB21, *At*MYB24 and *At*MYB57 (Cheng *et al*., 2009).

MYBs also control developmental processes in other plants. For instance, in tomato, the *BL* gene (a R2R3 MYB) has been proposed to regulate lateral shoots, and loss function of *BL* significantly inhibited lateral shoot development (Schmitz *et al*., 2002). *Sl*AN2 and *Sl*MYB70 were found to function in fruit development in tomato, with overexpression of *Sl*AN2 leading to faster fruit softening and ripening (Meng *et al*., 2015). In contrast, overexpression of *Sl*MYB70 led to delay of fruit ripening in tomato (Cao *et al*., 2020). *Sl*MYB70 was identified as a transcriptional repressor, targeting ethylene biosynthesis genes. In alfalfa, *Ms*MYB112

silencing lines had more shoot branches indicating a function in shoot branching (Gao *et al*., 2018).

1.4.3.2 Regulation of primary and secondary metabolism

R2R3 MYB factors are also associated with the control of the primary and secondary metabolism. *At*MYB11, *At*MYB12 and *At*MYB111 control flavonol biosynthesis by regulating the expression of flavonoid early biosynthetic genes including *CHALCONE SYNTHASE* (*CHS*), *CHALCONE ISOMERASE* (*CHI*), *FLAVONOL 3-HYDROXYLASE* (*F3H*) and (*FLAVONOL 3'-HYDROXYLASE*) *F3'H* (Stracke *et al*., 2010). A MYB-BHLH-WDR (MBW) complex consisting of a series of R2R3 MYBs (*At*MYB75, *At*MYB90, *At*MYB113, *At*MYB114 and *At*MYB123) and bHLHs (bHLH001, bHLH002 and bHLH042) plays a key role in metabolism. The MBW complex regulates biosynthesis of anthocyanins and proanthocyanins by controlling *DIFHYDRFLAVONOL-4-REDUCTASE* (*DFR*), *LEUCOANTHOCYANIDIN DIOXYGENASE* (*LDOX*) and *ANTHOCYANIDIN REDUCTASE* (*ANR*) (Xu *et al*., 2015). Zhou *et al*., (2017) reported that *At*MYB3 worked as a transcriptional repressor of *C4H* and inhibited phenylpropanoid biosynthesis in *Arabidopsis*. Repressor activity of *At*MYB3 was enhanced by interaction with two LNK proteins (NIGHT LIGHT-INDUCIBLE AND CLOCK-REGULATED 1 and 2, LNK1 and LNK2). *At*MYB99 was found to regulate primary metabolism and phenylpropanoid biosynthesis by targeting promoters of *TRANSKETOLASE 2* (*TK2*) and genes involving in phenylpropanoid pathway including *PAL*s (*PHENYLALANINE AMMONIA LYASE*, *PAL1*, *PAL2* and *PAL4*), *LAP*s (*LESS ADHESIVE POLLEN*, *LAP5* and *LAP6*) and *UGT*s (*UDP-GLUCURONOSYLTRANSFERASE*, *UGT72B1*, *UGT73B2* and *UGT79B6*) (Battat *et al*., 2019). In tomato, *Sl*MYB12 controls the biosynthesis of the flavonoid that determines the colour of the tomato fruit. Silencing of *Sl*MYB12 in

tomato led to reduction of naringenin chalcone in fruit peels, which caused a pink-coloured tomato fruit phenotype (Ballester *et al*., 2010).

1.4.3.3 MYB proteins in plant hormone responses

Plant hormones are a group of simple organic biochemicals including auxin, abscisic acid (ABA), gibberellic acids (GA), ethylene, cytokinins (CK), which are crucial for regulating plant growth and survival under different conditions (Vedamurthy *et al*., 2021).

Several studies have indicated MYB proteins play an important role in hormone signalling in plants. *At*MYB77 works as a transcriptional activator of auxin response genes, such as *IAA1*, *IAA19*, *PIN1*, *GH3.2*, *GH3.3*, *SAUR-AC1*, *HAT2* (Shin *et al*., 2007). In addition, direct interaction of *At*MYB77 with AUXIN RESPONSE FACTOR (ARFs) proteins has been demonstrated to enhance activation of auxin response gene expression (Shin *et al*., 2007).

ABA and GA act as antagonistic regulators, controlling various developmental processes in higher plants. Abe *et al*., (2003) found *AtMYB2* expression is induced by ABA and *At*MYB2 overexpressing lines were hypersensitive to ABA. Further studies suggest that *At*MYB2 activates expression of ABA-induced gene *RD22* through a MYB binding motif in its promoter, and identified *At*MYB2 as an activator in ABA signalling (Abe *et al*., 2003). Similarly, *At*MYB52 was identified as upregulated in the ABA-hypersensitive mutant *ahs1* when compared to wild type, which suggests that *At*MYB52 is involved in the ABA response (Park *et al*., 2011). In tomato, ABA-Induced MYB1 (*Sl*AIM1) was also involved in the ABA responses to alleviate effect of the abiotic stress and biotic stress (AbuQamar *et al*., 2009).

The R2R3 MYB transcription factor, GAMYB, was reported to promote α-amylase synthesis in aleurone cells of barley (Gubler *et al*., 1995). GAMYB expression is regulated by both GA and ABA. GA induced transcription of GAMYB, while ABA partially blocked its transcription, which

suggests it functions within cross talk of GA and ABA (Gubler *et al*.,2002). In *Arabidopsis*, both *At*MYB21 and *At*MYB24 have been shown to interact with the five GA signalling repressors, DELLAs, (REPRESSOR OF GA_{1-3}, RGA; GIBBERELLIC ACID INSENSITIVE DWARF 1, GAI; RGA-Like 1, RGL1, RGL2 and RGL3) and with JASMONATE ZIM-DOMAIN (JAZ) proteins (JAZ1, JAZ8 and JAZ11), respectively, which inhibit transcription activity of *At*MYB21 and *At*MYB24, leading to repression of stamen filament elongation (Cheng *et al*., 2009; Song *et al*., 2011; Huang *et al*., 2020).

1.4.3.4 Abiotic stress responses

MYB genes have been shown to be induced by different abiotic stresses, including drought, cold, high salinity, heavy metal (Roy *et al*., 2016). In *Arabidopsis*, it was reported that 51% of MYBs were upregulated by drought stress and 41% are downregulated (Zimmermann *et al*., 2004; Abe *et al*., 2003; Jung *et al*., 2008; Gao *et al*., 2014). With mutations leading to sensitivity, expression of *At*MYB96 is induced by both drought stress and ABA, which reduced stomatal opening and lateral root formation to enhance drought resistance in plants (Seo *et al*., 2009).

*At*MYB15 functions in cold stress responses. Loss of *Atmyb15* led to increased expression of downstream cold-responsive genes *C-REPEAT BINDING FACTOR*s (*CBF*s, *AtCBF1*, *2* and *3*), which are responsible for enhancing cold tolerance in *Arabidopsis* (Agarwal *et al*., 2006). In apple, *Md*MYB15, *Md*MYB23 and *Md*MYB308L were identified as cold-responsive MYB transcription factors, *Md*MYB23 and *Md*MYB308L were demonstrated to act as transcriptional activators of *Md*CBF1 and *Md*CBF2 to increase cold tolerance in plants (An *et al*., 2018; An *et al*., 2020).

Expression of *At*MYB49 was induced by heavy metal Cadmium (Cd) (Zhang *et al*., 2019). AtMYB49 bound to the promoters of bHLH38 and bHLH101 transcription factors activating their expression and leading to subsequent expression of *IRONREGULATED TRANSPORTER 1* to enhance Cd uptake. The transcription factor *At*MYB49 also positively regulates expression of *HIPP22* and *HIPP44* (*HEAVY METAL-ASSOCIATED ISOPRENYLATED PLANT PROTEIN*), leading to increased accumulation of Cd (Zhang *et al*., 2019). Previous studies showed *Os*MYB45 was functional in response to toxic Cd stress, and mutation of *OsMYB45* resulted in hypersensitivity to Cd suggested its potential role in Cd stress resistance (Hu *et al*., 2017).

*At*MYB20 and *At*MYB111 were both identified as positive regulators of the salt stress response. *At*MYB20 functions as a transcriptional repressor of two salt-induced ABA-responsive genes, *ABI1* and *ABI2* (*ABA INSENSITIVE 1* and *2*) and *AtPP2CA* (*TYPE 2C SERINE/THREONINE PROTEIN PHOSPHATASE*), which accelerates salt tolerance in plants (Cui *et al*., 2013). It is reported that the salt-induced transcription factor *At*MYB111 positively modulated the salt tolerance of plants, which was dependent on its function in flavonol metabolism (described above, Section 1.4.3.2) (Li *et al*., 2019). In rice, *Os*MYB91 was reported to function in response to salt stress, and overexpression of *Os*MYB91 exhibited enhanced salt tolerance (Zhu *et al*., 2015).

1.4.3.5 Biotic stress responses

Biotic stress in plants includes infections by pathogens, attacks by insects, animals and competition with weeds (Dreher *et al*., 2007). Plants respond to biotic stress to block invasion of pathogens and minimise the damage caused by other living organisms (Morkunas *et al*., 2018). In *Arabidopsis*, *At*MYB52 and *At*MYB122 encode activators of indole-3-yl methylglucosinolate (I3G) biosynthesis, which promote synthesis of active antimicrobial

compounds in response to *Botrytis cinerea* infection (Xu *et al*., 2016). *At*MYB122 together with *At*MYB34 and *At*MYB51 also participate in defense against another fungal pathogen *Plectosphaerella cucumerina*. The *Atmyb34*/*Atymyb51*/*Atmyb122* triple mutant showed susceptibility towards *P.cucumerina* (Frerigmann *et al*., 2016). *At*MYB15 was reported to control lignification of cell walls during the immune response to pathogens, increasing disease resistance (Chezem *et al*., 2019). *At*MYB15 was also important for the pathogen-induced defense response EFFECTOR TRIGGERED IMMUNE (ETI) to restrict programmed cell death and block invasion of the pathogens in *Arabidopsis* (Kim *et al*., 2020). *At*MYB30 was reported to promote programmed cell death known as the hypersensitive respose in plants, to increase resistance against pathogen attack (Vailleau *et al*., 2002). *Os*MYB30, *Os*MYB55 and *Os*MYB110 also enhanced resistance to pathogens by inducing synthesis of hydroxycinnamic acids (HCCAs) in rice (Kishi-Kaboshi *et al*., 2018). *BOTRYTIS-SUSCEPTIBLE 1* (*BOS1*) encodes an R2R3 MYB transcription factor protein which plays a role in response to *Botrytis cinerea* infections via a JA-dependent disease signalling pathway (Mengiste *et al*., 2003). De Vos *et al*., (2006) reported that *At*MYB102 contributed to basal resistance to the insect *Pieris rapae*, mutation of *At*MYB102 facilitated enhanced growth and development of *Pieris rapae* larvae compared to wild type. *At*MYB12 functions in phenylpropanoid and flavonol metabolism and was also reported to enhance insect resistance in plants when overexpressed (Misra *et al*., 2010).

1.5 The S24 clade of R2R3-MYBs in *Arabidopsis*: AtMYB53, AtMYB92 and AtMYB93 have roles in root development and suberin deposition.

*At*MYB92 was first identified as an interactor with ARM (armadillo) repeats of lateral root inhibitors ARABIDILLOs in *Arabidopsis* (Coates *et al*., 2006; Gibbs et al 2014). Phylogenetic analysis indicated that *AtMYB92* and two other homologues, *AtMYB53* and *AtMYB93*, all clustered within a distinct subgroup of R2R3-MYBs, the S24 clade (Stracke *et al*., 2001; *Du et al*., 2018). Furthermore, all three MYBs were found to interact with ARABIDILLO ARM repeats (Gibbs et al 2014), and expression profiles of them showed that they all were enriched for expression in roots (Winter *et al*., 2007; Gibbs *et al* 2014). In particular, *AtMYB93* transcripts were only detected in roots indicating that *AtMYB93* is a root-specific gene (Gibbs *et al*., 2014). *At*MYB93 was classified as an R2R3 type MYB transcription factor in *Arabidopsis thaliana*, which contains two conserved helix-turn-helix motifs, namely R2 and R3 repeats (Kranz *et al*., 1998). Within the *Arabidopsis* R2R3 MYB family, *At*MYB93 *At*MYB53 and *At*MYB92 share another conserved domain (LIQMG^{F}/$_{I}$DP^{M}/$_{V}$TH$_{X}$PRTD) downstream of the R3 repeat (Stracke *et al*., 2001). Further analysis of amino acid sequences of those three proteins revealed another conserved region, ^{I}/$_{L}$FssLsQL^{M}/$_{I}$sLs$_{X}$NL^{R}/$_{K}$g$_{X}$^{V}/$_{I}$^{D}/$_{E}$qqQFp, where x is any amino acid and lowercase letters represents two occurrences of those amino acids (Gibbs *et al*., 2014). Presented here is the schematic representation of *At*MYB93, *At*MYB53 and *At*MYB92, which shows the domain structures of those proteins and highlights the identified conserved motifs. Apart from the conserved N-termini, the rest of the sequences does not align clearly between the three proteins, which indicates that the C-termini of these proteins are more divergent (Figure 1.4)

Among these three MYBs, *AtMYB93* has root-specific expression and its promoter is only active in endodermis cells overlapping the lateral root primordium (LRP) at the early stage of

lateral root development (Gibbs *et al*., 2014). Lateral root density was significantly higher in the *Atmyb93* mutant compared to wild-type plants, and *AtMYB93*-overexpressing lines showed the opposite phenotype with significantly fewer lateral roots. Moreover, it was reported that the proportion of LRPs at late stages was higher in the *Atmyb93* mutant than in wildtype plants. On the contrary, more early stage LRPs were spotted in *At*MYB93-overexpressing lines, which indicated *At*MYB93 inhibited the rate of the LRP progression (Gibbs *et al*., 2014). Thus, *At*MYB93 is a flowering plant-specific MYB protein, which acts as a negative regulator of lateral root development in *Arabidopsis* (Gibbs *et al*., 2014).

Recent studies show all three MYBs in S24 subgroup bind to the promoter of the fatty acid synthesis-related gene *BIOTIN CARBOXYL CARRIER PROTEIN 2* (*NbBCCP2*), acting as transcriptional activators (Baud and Lepiniec, 2009). Further studies reported that transient overexpression of *At*MYB92 in tobacco leaves also induced expression of lipogenic genes *ACYL CARRIER PROTEIN1* (*Nb*ACP1) and *LIPOAMIDE DEHYDROGENASE1* (*NbLPD1*) and suberin biosynthetic genes including *ALIPHATIC SUBERIN FERULOYL TRANSFERASE* (*NbASFT*), *3-KETOACYL-COA SYNTHASE* (*NbKCS1*), *CYTOCHROME P450* (*NbCYP86B1*), *GLYCEROL-3-PHOSPHATE DEHYDROGENASE 1* (*NbGPDHc1*) and *GLYCEROL-3-PHOSPHATE ACYLTRANSFERASE 4, 5* (*NbGPAT4* and *5*), which led to enhanced suberin deposition (~50 fold) (To *et al*., 2020). Shukla *et al*., (2021) also reported that *At*MYB53, *At*MYB92 and *At*MYB93 were necessary for suberin deposition in endodermis. Ectopic expression of *At*MYB53, *At*MYB92 and *At*MYB93, respectively in all endodermal cells induced suberin deposition in endodermis and a *myb41/myb53/myb92/myb93* quadruple mutant abolished suberin deposition in roots (Shukla *et al*., 2021), although no change in lateral root density was seen in these mutants.

The orthologue of *At*MYB93 was also identified in apple, *Md*MYB93, which was also characterised as a regulator of suberin deposition in russeted apple skin (Legay *et al*., 2015). Transient overexpression of *Md*MYB93 in *Nicotiana benthamiana* leaves induced expression of suberin related genes, such as *NbKCS2*, *NbGPAT5*, *NbCYP86A1* and *NbASFT*. Gas chromatography- mass spectrometry (GC-MS) analysis of tobacco leaves expressing *Md*MYB93 also showed large accumulations of suberin and its precursors (Legay *et al*., 2015).

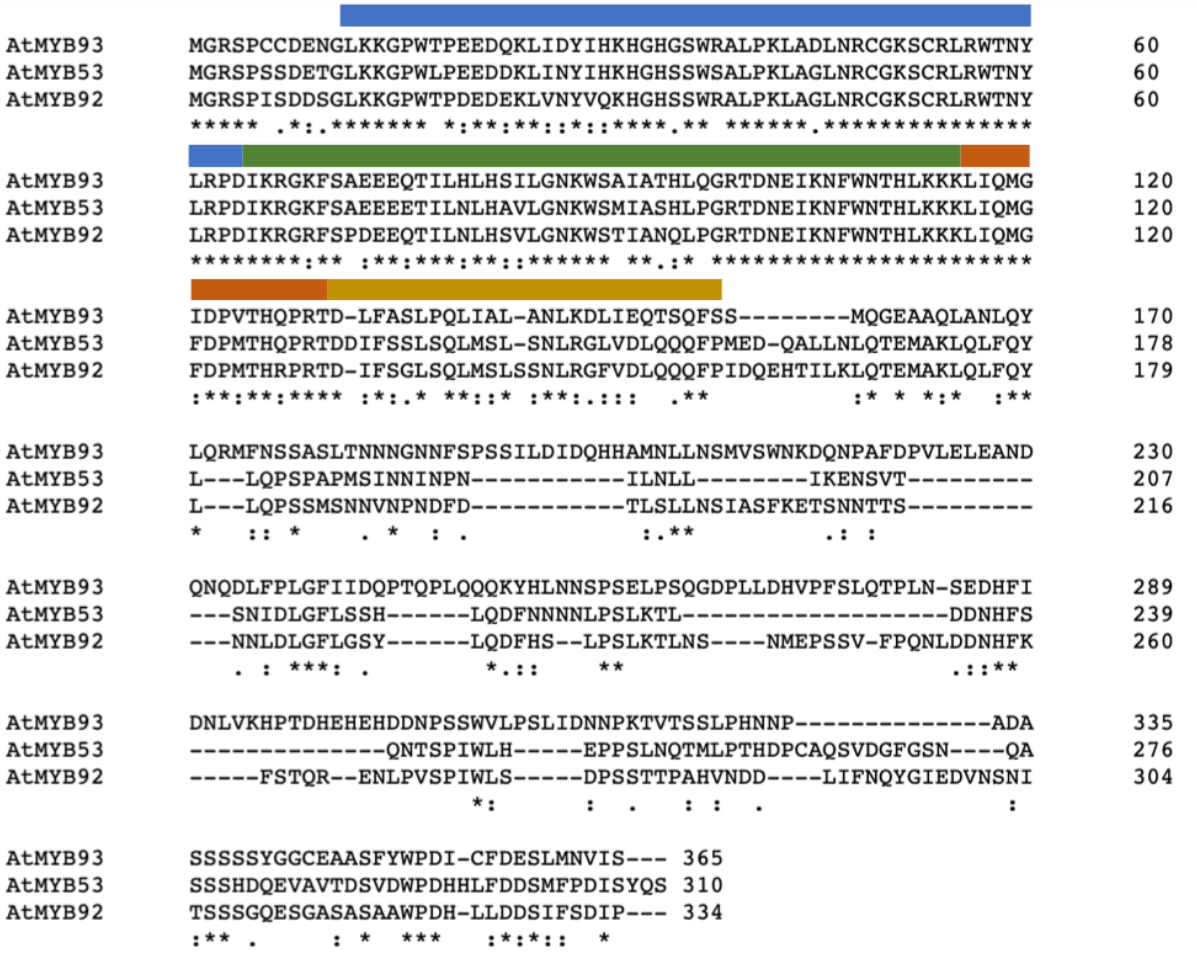

Figure 1.4 Alignment of amino acid sequences of *At*MYB93, *At*MYB53 and *At*MYB92.
Alignment of full-length amino acid sequences of *At*MYB93, *At*MYB53 and *At*MYB92 using ClustalW with character counts in Clustal Omega, EMBL-EBI (https://www.ebi.ac.uk/Tools/msa/clustalo/). R2 and R3 MYB repeats were denoted by the blue bar and green bar, respectively. A further conserved motif followed by R3 repeats were denoted by orange bar and yellow bar (Kranz *et al*., 1998; Gibbs *et al*., 2014). ‘ * ’ indicates identical amino acid among three proteins; ‘ : ’ and ‘ . ’ indicate conservative and semi-conservative mutations; blank indicates non-conservative mutations.

1.6 Study objectives

Previously, *At*MYB93 has been identified as a negative regulator of lateral root development in *Arabidopsis*. Loss of *At*MYB93 function enhanced lateral root density and overexpression of *At*MYB93 led to not only fewer lateral roots, but also enhanced suberin deposition in *Arabidopsis* (Gibbs *et al*., 2014; Shukla *et al*., 2021). Legay et al., (2016) also reported that *Md*MYB93 was involved in suberin deposition in russeted apple fruit skin, which affects the firmness of fruit, a good trait to be applied in agriculture to extend shelf-life. These studies extended our understanding of MYB93 in plant development and can be applied to fundamental crop improvement in the future.

Informed by the previous studies of MYB93s, we hypothesised that tomato orthologues of MYB93, *Sl*MYB93s, will have a similar function as *At*MYB93 and *Md*MYB93 in lateral root development and fruit development in tomato. Thus, the main objectives of this project were to:

1. Identify MYB93 orthologues in tomato and investigate their function *in planta*.
2. Further investigate the role of *At*MYB93 regulating lateral root development in *Arabidopsis* by determining the molecular mechanisms by which *At*MYB93 carries out its functions.

Chapter Ⅱ : Materials and methods

List of abbreviations

BSA	Bovine serum albumin
DMSO	Dimethyl sulfoxide
dNTPs	Deoxynucleotides
EDTA	Ethylenediaminetetraacetic acid
IAA	Indole-3-acetic acid
KT	Kinetin
LB broth/agar	Luria-Bertani broth/agar
LiAc	Lithium acetate
MES	2-(N-morpholino) ethanesulfonic acid
MS mediuam	Murashige and Skoog medium
PVDF	Polyvinylidine fluoride
SDS	Sodium dodecyl sulphate
TBS	Tris buffered saline
TBST	Tris buffered saline with 0.1%tween 20
TE	Tris-base, EDTA
TEMED	Tetramethylethylenediamine
2,4-D	2,4-Dichlorophenoyacetic acid

2.1 Bacterial and yeast strains

2.2.1 Bacterial strains

***Escherichia coli* DH5α** (*fhuA2 lac*(del)U169 *phoA glnV44* Φ80' *lacZ*(del)M15 *gyrA96 recA1 relA1 endA1 thi-1 hsdR17*) was used for standard cloning procedures and was grown in shaking liquid L-broth (LB, appendix 1) culture for ~ 16 h at 37°C at ~200 rpm. DH5α grown on LB-agar plates (Appendix 1) were incubated at 37°C for ~16 h.

***Agrobacterium tumefaciens* strain GV3101** is derived from a C58 background (Hellens et al., 2000), which carries a rifampicin resistance gene for selection of bacteria. GV3101 was grown in liquid culture for ~48 h at 28°C in the shaker at ~200 rpm. GV3101 grown on LB-agar plates were incubated at 28°C for ~48 h.

***Agrobacterium rhizogenes* ATCC 15834** is closely related to *Agrobacterium tumefaciens*, but *A. rhizogenes* contains a hairy root-inducing (Ri) plasmid instead of a tumour-inducing (Ti) plasmid (Tepfer et al., 1987; Ron et al., 2014). *A rhizogenes* was grown in liquid LB culture with required antibiotics for ~48 h at 28°C in the shaker at ~200rpm. *Agrobacterium rhizogenes* grown on LB-agar plates were incubated at 28°C for ~48 h.

2.1.2 Yeast strains

***Saccharomyces cerevisiae* AH109**, *MATa*, *trp1-901*, *leu2-3*, 112, *ura3-52*, *his3-200*, *gal4Δ*, *gal80Δ*, *LYS2::GAL1UAS-GAL1TATA- HIS3*, $GAL2_{UAS}$-$GAL2_{TATA}$-*ADE2*, *URA3::MEL1* $_{UAS}$-$MEL1_{TATA}$-*lacZ*, *MEL1*, was grown in liquid YPDA culture (Appendix.1) for ~48 h at 28°C shaking at ~200 rpm. AH109 grown on YPDA agar plates (Appendix.1) were incubated at 28°C for at least 48h (Jame et al., 1996).

2.2 Plant materials

***Arabidopsis*:** *Arabidopsis thaliana* Columbia-0 (Col-0) ecotype.

Tomato: *Solanum lycopersicum* cv. Micro-Tom (Micro-Tom).

Solanum lycopersicum cv. M82 (M82).

Tobacco: *Nicotiana benthamiana*.

2.3 Plant growth conditions

All plants were germinated and grown in Levington M3 compost/vermiculite mix which was well-watered.

Arabidopsis

Seeds were sowed on Levington M3 compost/vermiculite mix in standard greenhouse conditions (~22°C with a day length of 16 h). Sterile seedlings were transferred into Levington M3 compost/vermiculite mix and grown in the same conditions.

Tomato

Seeds were sowed on Levington M3 compost/vermiculite mix in the incubator setting with 24°C and 16 h day length. Sterile plants were transferred into Levington M3 compost/vermiculite mix covering with cling film to help them grow better in the unsterile environment.

Tobacco

Seeds were sowed in Levington M3 compost/vermiculite mix in the incubator (Sanyo) setting with 24°C and 16 h day length.

2.4 Cloning vectors

pGBKT7 (Clontech) is a 7.3kb yeast vector enabling fusion protein expression. pGBKT7 contains the *ADH* promoter (P_{ADH1}) and GAL4 DNA binding domain. In addition, it also carries a T7 promoter, c-myc epitope tag and a multiple cloning site (MCS). The transcription termination signals of T7 and *ADH1* are located downstream of the MCS. pGBKT7 contains a kanamycin resistance gene for selection in *E.coli* and *TRP1* as a nutritional marker in yeast.

pGADT7 (Clontech) is a 7.9kb yeast expression vector to express the protein of interest fused with the GAL4 activation domain (GAL4 AD). The transcription of GAL4 AD is driven by the *ADH1* promoter and terminated at the *ADH1* terminator (T_{ADH1}). The protein of interest is introduced into the multiple cloning site (MCS) with an HA tag fused to the C-terminus. The T7 promoter located upstream of the HA tag controls the transcription and translation of the HA tagged protein *in vitro*. The vector carries ampicillin resistance gene *(Amp^r)* for selection in *E. coli* and nutritional marker (*LEU2*) for selection in yeast.

pSKint is a ~3kb precursor vector for introducing an RNAi hairpin structure into a final plant binary vector, with an *Arabidopsis ACTINII* intron in nucleotide position 1 to 155. Two multiple cloning sites with different restriction sites are located on either side of the intron. pSKint vector carries an ampicillin resistance gene for selection in *E.coli* (Guo *et al*., 2003).

Modified pBI121 (mpBI121) is a 12.8kb plant binary vector based on pBI121 (Clontech) with some modifications within the left border and right border carried out by the Liu lab (Yongsheng Liu, personal communication) (Cao *et al*., 2012). mpBI121 carries more restriction sites than pBI121, including *Kpn*I, *Sal*I and *Xho*I. In addition, two versions of mpBI121 exist, mpBI12135S and mpBI121TFM7, carrying either the CaMV 35S promoter or the fruit specific

promoter TFM7 upstream of the MCS, respectively, enabling either constitutive or fruit-specific expression. Another modification is the deletion of the *GUS* reporter gene and leaving only a NOS terminator at the end of the MCS. Thus, the vector enables expression of cloned genes in plants. mpBI121 also contains a kanamycin resistance gene *nptII* for selection in the transformation in tomato.

pYPQ131 is a 3.8kb Golden gate (REF) entry vector for generating constructs for the CRISPR/Cas9 system. pYPQ131 carries a tetracycline resistant gene (*TcR*) for selection in bacteria. The guide RNA (gRNA) cassette is located in downstream of *TcR*, and is used to introduce gRNA into the vector between RNA Pol Ⅲ promoter and terminator. Two *Bsa*I sites with specific cutting sequences are on both sides of the gRNA cassette for Golden Gate cloning. The replication origin gene (pUC ori) is downstream of the gRNA scaffold to allow high-copy replication and maintenance in *E. coli*. Both pYPQ132 and pYPQ133 have the same backbone as pYPQ131 vector with different *Bsa*I cutting sites (Engler *et al*., 2008).

pMR278 is a 5.7kb golden gate vector to assemble three different gRNAs before they are introduced into final vector pMR286 for the CRISPR/Cas9 system. pMR278 carries both kanamycin and gentamycin resistance genes for selection in *E. coli*. The replication of the plasmid starts from replicon (pMB1 ori), which ensures high-copy replication and maintenance in *E. coli.* Three gRNA scaffold sites driving by individual *Arabidopsis thaliana* *At*U6-1 promoter are located in downstream of replicon. The different gRNA cassettes are cloned into those gRNA scaffold sites by golden gate cloning. Gateway recombination site attL1 and attL2 are on the both sites of assembled gRNAs, which are used for introduction into pMR286.

pMR286 is a 15kb plant binary Gateway vector for CRISPR/Cas9 system. (Leibman-Markus, M *et al*., 2018). Within the left border and right border of the T-DNA region, the Cas9 gene is driven by the *PcUbi* promoter (from *Petroselinum crispum*) with upstream localisation of the *NeoR*/*KanR* gene for selection in plants. A Gateway cassette with attR1 and attR2 sites is downstream of the Cas9 gene, used for cloning in the gRNAs under control of the *AtU6-1* promoter from pYPQ131. pMR286 carries a spectinomycin resistance gene outside the T-DNA insertion region, used for selection in *E. coli*.

pDonor (Zeo) is a 4.3kb gateway entry vector. The gene of interest will replace the sequences within gateway cassette sites attP1 and attP2 via a BP reaction. The vector contains chloramphenicol resistance gene driven by a chloramphenicol transferase (*cat*) promoter and bacterial toxin (*ccdB*) that help with selection of empty vector in *E. coli.* The replication origin gene (ori) allows high-copy replication and maintenance in *E. coli*. pDonor/Zeo also carries a Zeocin resistance gene (*BleoR*) located at the upstream of ori, used for selection in *E. coli.*

pEarleyGate 104 is a 12kb plant binary Gateway vector to express a protein of interest fused with yellow fluorescence protein (eYFP). Within the T-DNA repeat, the plasmid contains a bialophos resistance gene for selection in plants driven by a *MAS* promoter and terminated at a *MAS* terminator. A CaMV 35S promoter located at upstream of eYFP controls the transcription and translation of the fused protein of interest, which terminates via an *OCS* terminator. The protein of interest will be introduced to replace the sequence between Gateway cassette attR1 and attR2, which contains a chloramphenicol resistance gene driven by the lac UV5 promoter and the bacterial toxin (*ccdB*) that helps with selection of the empty vector in *E. coli.* The vector replicates autonomously in *E. coli* and *Agrobacterium* from ori

and the *Pseudomonas* plasmid pSV1 genes (pSV1 ori, pSV1 RepA and pSV1 StaA). It also carries Kanamycin resistance gene (*KanR*) allowing for selection in bacteria.

2.5 Isolation of nucleic acids

2.5.1 Isolation of plasmid DNA from *E. coli*

Plasmid DNA was extracted using an ISOLATE II Plasmid Mini Kit (Bioline). According to manufacturers' instructions, 5-10 mL bacterial overnight culture was used for plasmid DNA extraction depending on the copy number of plasmids. Bacterial pellets were collected by centrifuging in microcentrifuge tubes and resuspended in a buffer containing RNaseA to degrade RNA. Bacteria were then lysed with addition of lysis buffer containing sodium dodecyl sulfate (SDS). Neutralisation buffer was added in samples to precipitate protein and chromosomal DNA by centrifugation at 15000× g. Supernatants from the spun samples were loaded onto a silica membrane on a spin column after centrifugation, which allowed plasmid DNAs bind to the membrane. The silica was then washed with wash buffer supplemented with ethanol, and plasmid DNAs were then eluted in Tris-EDTA (TE) buffer.

2.5.2 Isolation of genomic DNA from plants

Genomic DNA was extracted using an ISOLATE II Genomic DNA Kit (Bioline) according to manufacturers' instructions. 100 mg plant tissues were harvested and homogenized with plastic micropestles (Carl Roth) in 1.5 mL microcentrifuge tubes. DNA was then extracted according to manufacturer's instructions. Ground tissues were pre-lysed using a buffer containing proteinase K to digest contaminating proteins. Samples were then incubated at 56°C for 1-3 hours until the tissues were completely lysed. Prior to DNA binding, supplements of 210 μL ethanol were applied to samples to adjust the DNA binding conditions. Samples were then loaded and centrifuged through silica membrane-containing columns to bind DNA onto the silica membranes. Samples were washed with wash buffer containing ethanol and eluted in elution buffer (TE Buffer) to release DNA from the silica membrane. DNA

concentration and quality were then measured on a Nanodrop spectrophotometer and DNA was diluted with DNase-free water for cloning.

2.5.3 Isolation of RNA from plant tissues

Total RNA was extracted from ~30 mg collected plant tissue using an ISOLATE II Plant Mini Kit (Bioline) following the manufacturer's protocol. Plant tissues were harvested and homogenised in liquid nitrogen using ceramic mortars and pestles cleaned with RNase remover (Bioline). Samples were then transferred to RNase-free microcentrifuge tubes and lysed using lysis buffer supplied with β-mercaptoethanol to denature proteins. Lysates were then filtered through spin columns to remove cell debris and filtrates were transferred to new microcentrifuge tubes and mixed with 70% (v/v) ethanol. RNA was absorbed onto a silica membrane by centrifugation through a second silica-based column. Before the samples were washed with Wash Buffer containing ethanol, DNase I solution was applied to the silica membranes to avoid DNA contamination. RNA was eluted with RNase-free water and stored at -80 °C.

2.5.4 cDNA synthesis

Complementary DNA (cDNA) was synthesised from RNA using the SuperScript™ III First-Strand Synthesis System (Invitrogen) according to the manufacturer's instructions. RNA was denatured with a supplement of 1μL Oligo(dT)20 (50μM) and 1μL dNTPs(10mM) by incubating at 65 °C for 5 min. cDNA synthesis mix containing 200 U reverse transcriptase and 40 U RNaseOUTTM which prevents RNA degradation was added into RNA sample. The reaction was started by incubating the sample at 50 °C for 50 min, and the sample was then incubated at 85 °C for 5 min to terminate the reaction. Template RNA in the sample was

removed using 2 U RNase H and incubation at 37 °C for 20 min. cDNA was ready for RT-PCR or cloning and was stored at -20 °C

2.5.4 Isolation of DNA fragments from agarose gels and PCR reactions

Single bands were separated and isolated on agarose gels and were excised via placing the gel on a UV transilluminator for visualisation. Agarose gel slices were collected in microcentrifuge tubes and the nucleic acid in the gel was then extracted using the ISOLATE II PCR and Gel Kit (Bioline) according to manufacturer's instructions. Gel slices were completely dissolved in Binding Buffer containing pH indicator by incubating at 50 °C for 10 min. Samples were then loaded and centrifuged through silica columns to bind DNA fragments on the silica membranes. DNA fragments were washed with wash buffer containing ethanol and eluted in elution buffer. The same kit and similar protocols were applied for PCR product purification.

2.5.5 Rapid genomic DNA extraction for hairy root tissues genotyping

1 cm root tissues were collected and ground in 1.5 mL microtubes with pestles. Samples were vortexed for 5 seconds after addition of 400 μL extraction buffer. Following centrifugation at 12000g (5 minutes at room temperature), 300 μL supernatants were transferred into the fresh 1.5 mL microtubes with 300 μL isopropanol. DNA pellet was harvested by centrifuging at 12000 g for 5 minutes and dried by incubating the open tubes at room temperature overnight. The pellets were then dissolved in 100 μL water and 1 μL DNA was used for genotyping PCR.

2.6 Manipulation of bacteria and yeast

2.6.1 Preparation of *E. coli* competent cells for heat shock transformation

An *E. coli* (DH5α) glycerol stock was streaked out on an LB agar plate and incubated at 37 °C overnight. A single DH5α colony was inoculated into 10 mL LB broth medium and incubated at 37 °C with shaking at 200 rpm overnight. The overnight culture was then added into 250 mL SOB medium in a 1 Litre conical flask and grown at 18 °C with shaking at 200 rpm until an OD of 0.6 was reached. The culture was immersed in ice for 10 min and bacteria were collected by centrifuging at 3000 rpm at 4 °C for 10 min. The bacterial pellet was then resuspended in 80 mL ice-cold TB buffer (Appendix.2) and incubated in ice for 10 min. The bacteria were then spun down by centrifugation at 3000 rpm at 4°C for 10 min and resuspended with 20 mL refrigerated TB buffer and 1.5 mL DMSO. 100 μL aliquots were loaded into refrigerated 1.5 mL centrifuge microtubes and frozen in liquid nitrogen. Competent cells were stored at -80 °C.

2.6.2 *E. coli* transformation

E. coli heat shock competent cells were thawed on ice and mixed with ligation products or plasmid DNA. This mixture was then incubated on ice for 20 min and heat shocked at 42°C for 90 seconds in a water bath. The mixture was then incubated on ice for another 5 min and 700 μL LB medium was added. The bacterial resuspension was incubated at 37 °C with shaking at 200 rpm for 2 hours. Bacteria were harvested by centrifugation at 4000 rpm for 5 min and 100 μL LB was used to resuspend the bacterial pellet before spreading it on a LB agar plate with required antibiotics. The plate was incubated at 37 °C for 12 hours, and colony PCR was applied to screen for positive colonies. Positive *E. coli* colonies were inoculated into an overnight culture then stored in 50% glycerol at -80 °C.

2.6.3 Preparation of *Agrobacterium tumefaciens* competent cells for electroporation

Agrobacterium tumefaciens (GV3101) was streaked out on an LB agar plate with rifampicin (25 mg/L) and incubated at 28 °C for 48 hours. A single colony was inoculated in 10 mL LB liquid medium with rifampicin (25 mg/L) and grown at 28 °C with shaking at 200 rpm for 48 hours. The culture was then poured into 250 mL LB liquid medium in a 1 litre conical flask and incubated at 28 °C with shaking at 200 rpm until an OD of 0.5-1 was reached. The culture was submerged in ice for 15-30 min and bacterial cells were pelleted by centrifuging at 3000 rpm at 4 °C for 10 min. The pelleted cells were washed with 250 mL refrigerated water twice and resuspended in 10 mL ice cold 10 % glycerol. Bacteria were then collected using centrifugation at 3000 rpm at 4 °C for 10 min and resuspended with 2 mL ice cold 10 % glycerol. 100 μL aliquots were added to 1.5 mL centrifuge microtubes and frozen in liquid nitrogen. The competent cells were stored at -80 °C.

2.6.4 Transformation of *Agrobacterium* by electroporation

Agrobacterium electrocompetent cells were thawed on ice and mixed with 1- 100ng plasmid DNA. The mixture was incubated on ice for 20 min and loaded slowly into a pre-chilled electroporation cuvette. Prior to placing cuvette in the electroporator (BioRad), the surface of the cuvette's electrodes was dried. The electroporation was set with the following parameters: 2.5 kV, 25 μF capacitance and 400 Ω resistance. Immediately after electroporation, 700 μL LB medium was added into the electroporation cuvette and mixed well with the bacteria. The mixture was then transferred into a new 1.5 mL centrifuge microtube, which was then incubated at 28 °C with shaking at 200 rpm for 2 hours. The *Agrobacterium* was spun down at 4000 rpm for 5 min and 600 μL supernatant was removed.

The bacterial pellet was resuspended in the remaining supernatant and spread on the LB plate with appropriate antibiotics. The plate was incubated at 28 °C for 48 hours, colonies were inoculated for plant transformation after screening by colony PCR. *Agrobacterium* was then stored in 50% (v/v) glycerol at -80 °C.

2.6.5 Yeast two hybrid assay

The specific yeast strain was streaked out on YPDA plate and incubated at 30°C till the single yeast colonies were available for transformation. The single yeast colony was inoculated in 100 µL yeast transformation solution in 2ml centrifuge tube and 2µg of each plasmid was added in the tube. All tubes were incubated at 37°C for 45 min and the contents in tubes were transferred and spread on double drop out selective media plates (-Leu/-Trp). The plates were incubated at 30°C until transformants were observed (typically 2-3 days). Single colonies of each transformation were inoculated in 50 µL sterile water, 5 µL of which was then dropped on quadruple drop out plates (-Ade/-His/-Leu/-Trp). The quadruple plates were then incubated in 30°C for 2-3 days to test interaction between two candidate proteins.

2.7 Manipulation of plants

2.7.1 *Arabidopsis* floral dip

Arabidopsis seeds were scattered in 8 cm pots, and 3 to 5 plants per pot were retained after germination. Around 4 weeks later, the main inflorescence spike of each plant was cut, allowing secondary buds to form, which were subjected to floral dip. The *Agrobacterium* was prepared in the week before the plants were ready to dip. The pre-transformed *A. tumefaciens* (Section 2.6.4) was restreaked from the glycerol stock on to an LB plate with kanamycin and rifampicin, from which a single colony was picked and inoculated in 5mL LB liquid medium supplemented with kanamycin and rifampicin. After 48 h (28°C, 200 rpm) incubation, the culture was added into 500mL fresh LB liquid medium supplemented with kanamycin and rifampicin and incubated overnight (28°C, 200 rpm). The *A. tumefaciens* was harvested by centrifugation (5000rpm, 15min) and bacterial pellet was resuspended in 250mL 5% sucrose solution supplement with 125µL Silwett L-77 (Duchefa). Before floral dipping, the opened buds on all the inflorescence spikes were cut, leaving only closed buds. These buds were dipped and gently rotated in the bacterial suspension for 30s. Plants were then covered with cling films and placed in dark for 24 h before put back in the normal growth condition. Primary transformant (T1) Seeds were harvested after ~2 months.

2.7.2 Arabidopsis seeds sterilisation and selection

Arabidopsis seeds were surface sterilised with 1mL 10% bleach (Parazone ™ (Jeyes)) on rotator at 24rpm for 10 min in 1.5mL Eppendorf tubes, which were then washed with 1 mL sterilised water on rotator at 24rpm, 10 min for 3 times. Sterilised seed were used for selection or lateral root assay by loading seeds on ½ MS agar plates with or without appropriate antibiotics (Appendix.1).

2.7.3 Tomato tissue culture

The tomato variety *Solanum lycopersicum*. cv. Micro Tom (Micro Tom) was used in all experiments, unless otherwise indicated. Micro Tom seeds were directly seeded in the pots with substrates and placed in the glass house (16h light and 8h dark, 22°C). For transformation experiments Micro Tom seeds were soaked in water and incubated at 37°C for 1 h. Seeds were sterilise in a laminar flow hood (Section2.7.3) and placed in Magenta pots (Sigma-Aldrich) with ½ Murashige and Skoog (MS) MS media (Appendix 1). After that all the pots were placed in the incubator (25°C, 70% to 80% relative humidity) in the dark for the first two days. If the majority of seeds germinated, pots were transferred in a 14-h/10-h photoperiod, 25°C in light and 20°C in dark, 70% to 80% relative humidity, and light intensity of approx. 300 µmol photons m^{-2} s^{-1}. After *Agrobacterium* infection experiments (section 2.7.3), all the cotyledons were grown on co-incubation media and then selection media (Appendix 1), which were placed in the incubator (14-h/10-h photoperiod, 25°C in light and 20°C in dark, 70% to 80% relative humidity, and light intensity of approx. 300 µmol photons m^{-2} s^{-1}).

2.7.4 Tomato tissue culture and transformation

Tomato seeds were surface sterilized with 20% Bleach (Parazone ™ (Jeyes)) for 20 min, washed with 30 mL autoclaved water 3 times, and dried on autoclaved filter papers. Seeds were then washed with more water in the fresh sterilized falcon tubes, and changed the tubes for at least 3 times to clean up the bleach residues completely. After sterilization, seeds were dried on the autoclaved filter papers, and then placed on 1/2 MS medium supplemented with 2% sucrose (Appendix 1). After 2 days cold treatment at 4°C and 2 to 3 days dark treatment

at 22°C, the germinated tomato seeds were set in a long-day growth room (16h light/ 8h dark) for 4 to 5 days.

The cotyledons of the tomato seedlings were cut and evenly wounded with tweezers on the underside of the leaves before incubating them on Pre media (Appendix 1) for 2 days. Meanwhile *Agrobacterium* transformed with the required constructs was streaked from the glycerol stock (section 2.6.4) and cultured in 10mL LB liquid with kanamycin and rifampicin to OD ~1.0. *Agrobacterium* was collected and resuspended in 30-40mL Induction Media (IM) until an OD of ~0.1 was reached. All the pre-cultured cotyledons were soaked in the IM for 20 min, and the liquid residue on the surface of the leaves was removed before transferring the cotyledons into Co (Co-incubation) media. After 2 days incubation in Co media, the media was changed to K60 media for selection. Green callus grew after 3 weeks' culture and was selected with a high concentration of kanamycin in the media K65. 2 to 3 months later, the differentiated shoots arising from the callus were grown on in larger containers with K70 media. The callus at the bottom of the large shoots was cut and removed, and the shoots were transferred to rooting medium. The rooted tomato plants arising from this process were transferred into soil covered with a plastic transparent cover, to help the young plants grow well in the open-air environment.

All the media and solutions for tissue culture were prepared in advance, described in Appendix 1.

2.7.5 Tomato hairy root transformation

In addition to using *Agrobacterium tumefaciens* to transform the tomato plant genome, *Agrobacterium rhizogenes* was applied in the tomato hairy root transformation process to induce the production of hairy roots and rapidly generate transgenic materials.

Tomato seeds were sterilised following (seeds sterilise protocol, Section 2.7.3) and grown on MS agar (Appendix 1) plates for 7 days after germination. *Agrobacterium rhizogenes* containing the constructs of interest were inoculated in NB liquid with appropriate antibiotic (Appendix 1) until reaching an optical density at 600nm (OD600) of 0.2-0.4. Cotyledons of tomato seedlings were ready for transformation when they showed complete expansion, but no true leaves had emerged. Cotyledons were cut from seedlings and soaked in 20 mL MS liquid medium to prevent them drying out. After all the cotyledons were harvested, they were then transferred and immersed in *Agrobacterium rhizogenes* solution for 20 mins. After infection, liquid on the surface of these explants was dried with sterile filter papers. Explants were then transferred on co-culture media in the dark with the lower epidermis facing upwards. After 3-days of co-cultivation, cotyledons were then gently placed flat on the selection media with lower epidermis facing upwards. Hairy roots that emerged from different cotyledons or different positions on the same cotyledons were excised and transferred onto new selection media separately for amplification. Ten independent hairy roots were subcultured for each construct. Genotyping and other experiments were applied after root amplification.

2.7.6 Lateral root assay

Arabidopsis seeds were sterilised with 20% bleach (Parozone ^{TM} (Jeyes)) solution for 10 min, and then washed 3 times with autoclaved water for 10 min to remove the bleach residue. Seeds were plated in rows on 1/2 MS medium in square petri dishes, in a line approximately 1cm from the top of the plate when standing vertically. After that, petri dishes were taped with Micropore tape (3M) and incubated at 4℃ for around 48h. Then the seedlings in petri dishes were grown vertically under normal *Arabidopsis* growth conditions (section 2.3).

Lateral roots were counted on the 7th, 8th and 9th days after transfer to the growth room. A photo of each plate was also taken on the same days, and primary root length of each seedling was calculated using the freehand line-drawing and measuring tools in Image J. The lateral root density was calculated by the calculation below.

$$\textbf{Root density} = \frac{\textbf{lateral root number}}{\textbf{primary root length}}$$

2.7.7 Transient expression in tobacco leaves

Agrobacterium with constructs of interest was streaked on LB agar plates with appropriate antibiotics and grown in 28 ℃ for 48h. Single colony of each sample was inoculated and grown in LB liquid media with appropriate antibiotics in 28 ℃ for 48h, which was used for making *Agrobacterium* overnight culture by adding 10% (v/v) old culture into new media. After overnight growing in 28 ℃, 2 mL Agrobacterium cells were spinning down in 2 mL Eppendorf tubes by centrifugation at 5000 rpm for 5min. Cell pellets of each sample was then resuspended in 1 mL infiltration buffer with pipette and centrifuged at 5000 rpm for 5min. Pellets of each sample was resuspended in 1 mL infiltration buffer. OD value of each sample was measured using spectrophotometer, which was used for dilution of resuspended cells to OD of ~0.7. Diluted resuspended cells were then used for infiltration lower face of 6-week-old tobacco leaves by using 1 mL syringes. Infiltrated tobaccos were then grown in glasshouse for 48h to allow expression of proteins. Infiltrated leaves were then used for confocal and protein extraction.

2.7.8 Preparation of plant samples for ion analysis

Wild type and transgenic tomatoes seeds were sowed in compost and grown in the glass house. True leaves were of each plant were harvested for genomic DNA extraction, which were used as templates for genotyping. (Section 2.7.5) Leaves of transgenic tomatoes were harvested and dried in oven at 50 ℃ for 48h. In order to meet minimum weight requirement (~0.2g dry weight) of ICP-MS analysis, around 20g fresh weight tomato leaves need to be collected for each genotype.

2.8 Gene Cloning

2.8.1 Golden gate cloning

Golden gate cloning was used to assemble three different gRNAs for CRISPR/Cas9 system. gRNAs were cloned into different entry vectors separately by conventional cloning (Section 2.8.3). Then the three correct entry vectors with different gRNAs were mixed with the Golden gate destination vector, supplemented with Type IIS enzyme *Bsm*BI and T4 DNA ligase. Reactions were incubated in a PCR machine using a program with 37°C and 16 °C for 10 cycles (Section 2.8.8.3).

2.8.2 Gateway cloning

Genes of interest were firstly introduced into Gateway entry vectors by either conventional cloning or TA cloning. Gene cassettes in entry clones were then cloned into Gateway destination vector by site-specific recombination. Destination vectors encodes the different antibiotic resistant gene to entry vectors, which avoid plasmid contamination during the *E. coli* transformation (Section 2.8.8.4).

2.8.3 Conventional cloning

DNA fragments of interest were obtained from an organism with unique restriction sites on both sides of DNA fragments. Restriction enzymes which can recognise those restriction sites were used to cut circular empty vector and formed sticky ends on both sides. The same restriction enzymes were then applied to DNA fragments to obtain the same sticky ends. Linearised vectors and digested DNA fragments were ligated by T4 DNA ligase (New England Biolabs). Ligation products were then introduced into *E. coli DH5*α and positive colonies screened on the LB agar plates with appropriate antibiotics.

2.8.4 Polymerase chain reaction (PCR)

Polymerase chain reaction (PCR) is a common technique used in molecular biology. PCR was applied to amplify DNA fragments of interest from plant gDNA and RNA for molecular cloning, sequencing or detection of product.

In PCR, DNA polymerase enzymes were key components to make new strands of DNA from plasmid DNA, genomic DNA and cDNA. *Taq* polymerase (PCR Biosystem) was used for colony PCR, plant genotyping and Reverse-Transcription PCR (semi-quantification PCR). High fidelity enzymes Phusion™ DNA Polymerase (New England Biolabs) or Q5® High Fidelity DNA Polymerase (New England Biolabs) were used for gene cloning, as these enzymes generate blunt-end PCR products with fewer errors then products generated by *Taq* polymerase.

PCR reactions were set up based on manufacturer's instructions. Primers were designed by hand and supplied by Eurofins; a list of primers is given in Appendix 3. For gene cloning, PCR products were purified as in section 2.5.4.

2.8.5 Thermocycling conditions for PCR

All PCRs were performed in PCR machines (Techne). The temperature used in the initial DNA denaturation stage is 94-98 °C depending on the DNA polymerase used. The number of cycles for next three stages is 30-35 depending on the procedure. First stage in cycler is denaturation stage was carried out at the same temperature used in the initial stage for 10s to denature at template DNA and primers. The subsequent annealing stage was performed for 30s, and temperature was set based on the GC content of primer pairs, which was calculated following equation:

$$annealing\ temperature = [4 \times (number\ of\ G\ or\ C) + 2 \times (number\ of\ A\ or\ T)]$$

The extension stage in each cycle was carried out at 72 °C and the extension time was set depending on the different DNA polymerases and size of the DNA fragments, according to manufacturers' instructions.

2.8.6 Agarose gel electrophoresis

0.8%-1% (m/v) agarose gels were used in this project. Agarose was added into 1×TAE solution (Appendix.2) and dissolved by heating in a microwave till the solution became clear. Agarose solution was then poured into a gel mould with an appropriate comb after the solution had cooled down to around 55°C. Gels were allowed to set for 20 min and submerged in a gel tank filled with 1×TAE solution. Prior to loading samples, 6 × loading buffer with the DNA dye GelRed (Biotium) was mixed with samples and DNA ladders. Samples were then loaded into wells alongside a DNA ladder and run at 110 V for 30 min. Gels were imaged using a BioRed Gel Doc viewer.

2.8.7 Genotyping PCR

Genomic DNA extracted from transgenic plant was used as templates for genotyping PCR. The PCR reaction was set up as follow:

Genomic DNA (~50 ng/ μL)	1 μL
2 × RedMix (Biolab)	10 μL
Genotyping forward primer (100μM)	1 μL
Genotyping reverse primer (100μM)	1 μL
ddH_2O	7 μL

Total	20 μL

The thermocycling condition of genotyping PCR was set up referring to Section 2.8.5. And transgenic plants were genotyped by performing Agarose gel electrophoresis of PCR products. (Section 2.8.6) After imaging the gel, the expected bands indicated existence of transgene in plant.

2.8.8 CRISPR/Cas9 T-DNA vector cloning

2.8.8.1 Single guide RNA (sgRNA) design

sgRNAs were designed in CRISPR-P V2 (http://crispr.hzau.edu.cn/cgi-bin/CRISPR2/CRISPR) with settings (snoRNA promoter: U6, target genome: Solanum lycopersicum (SL2.5)). The target sequence in FASTA format was entered into the database for designing and three best sgRNAs were selected based on Score, location, GC content (40%-60%) and off-target sites.

2.8.8.2 Cloning sgRNAs into expression vectors

2.8.8.2.1 gRNA expression vector linearisation

gRNA expression vectors (pYPQ131, pYPQ132 and pYPQ133) were separately linearised by digesting with *Bsm*BI. Digestion reactions were set up as follows:

gRNA expression vectors (90 ng/μL)	32 μL
10×CutSmart Buffer	4 μL
*Bsm*BI (10000 U/mL)	2 μL

ddH_20	2 μL
Total	40 μL

Reaction products were then purified using the Bioline Gel & PCR purification kit (section 2.5.4) after incubation at 37 °C for 3 hours. DNA concentrations were quantified using a Nanodrop spectrophotometer.

2.8.8.2.2 sgRNA oligos phosphorylation and annealing

To clone sgRNA oligos into gRNA expression vectors, sgRNA forward and reverse oligos were phosphorylated and annealed by using T4 Polynucleotide Kinase (New England Biolabs). Reaction settings were as follows:

sgRNA oligo forward (100 μM)	1 μL
sgRNA oligo reverse (100 μM)	1 μL
10 × T4 Polynucleotide Kinase Buffer	1 μL
T4 Polynucleotide Kinase(10000 U/mL)	0.5 μL
ddH2O	6.5 μL
Total	10 μL

Reactions were performed in the PCR machine using the following program:

37 °C	30 min
95 °C	5 min
↓ (5 °C/min)	14 min
25 °C	∞

2.8.8.2.3 Ligation and *E. coli* transformation

Annealed sgRNA oligos were diluted in ddH2O with 1:200 dilution. And linearised gRNA expression vectors were ligated with diluted annealed sgRNA oligos using T4 ligase.

Linearised gRNA expression vectors	1 μL
diluted annealed sgRNA oligos	1 μL
10 × T4 Ligase Buffer	1 μL
T4 Ligase (400000 U/mL)	0.5 μL
ddH_2O	6.5 μL
Total	10 μL

Ligation reactions were incubated at room temperature for one hour and ligation products were then transformed into *E. coli* DH5α. Vectors with guide RNAs were verified by sequencing with primer pTC14-F2 (Appendix 3).

2.8.8.3 Golden Gate assembly of three guide RNAs

Correct plasmids from section 2.8.8.2.3 were introduced into pMR278 via a Goldev Gate reaction, which was set up as follows:

pMR278 (100ng/ μL)	1.5 μL
pYPQ131 (100ng/ μL)	1 μL
pYPQ132 (100ng/ μL)	1 μL
pYPQ133 (100ng/ μL)	1 μL
10 × T4 Ligase Buffer	1 μL

T4 Ligase (400000 U/mL)	0.5 μL
*Bsa*I (10000 U/mL)	0.5 μL
ddH_2O	3.5 μL
Total	10 μL

Reactions were performed in the PCR machine with the thermotical program as follow:

37 °C	5 min	10 cycles
16 °C	10 min	
50 °C	5 min	
80 °C	5 min	
Hold at 10 °C		

Reaction products were then introduced into *E. coli* DH5α and plated on the LB agar medium with appropriate antibiotic. Colony PCR and restriction digestion were applied for screening, and positive clones were verified by sequencing.

2.8.8.4 Gateway assembly of multiplex CRISPR-Cas9 system into a binary vector

Gateway LR reactions were set up as follows:

pMR286 (100ng/ μL)	2 μL
pMR278 with three sgRNAs (100ng/ μL)	2 μL
5×LR Clonase II emzyme mix	1 μL
Total	5 μL

Reactions were incubated at room temperature overnight and introduced into *E. coli* DH5α. Transformed cells were then plated on the LB agar medium with appropriate antibiotic. Colony PCR and restriction digestion were applied for screening, and positive clones were verified by sequencing.

2.9 Manipulation of protein

2.9.1 Protein extraction from plants

Tissues were collected and ground in liquid nitrogen by using precool mortar and pestles. 1 mL cold protein extraction buffer (Appendix.2) was added in mortar and well-mixed with samples before they got defrosted. Then samples were filter with microcloth before transferred into 1.5 mL Eppendorf tubes, which were centrifuged at 15000 g, 4 °C for 45 min. The supernatants were collected in new Eppendorf tubes, which were then used for Bradford assay and western blot.

2.9.2 Bradford assay

250µL Bradford reagent from company was mixed with 4µL protein sample in 96 wells plate. And the OD value of each sample was read in machine at 570nm wavelength. In particular, BSA was used to generate standard curve before measuring the samples.

2.9.3 SDS-Polyacrylamide Gel Electrophoresis (SDS PAGE): gel construction

The BIORAD Mini-PROTEAN Handcast System was used to cast 12 % polyacrylamide gels. The casting mould was assembled before resolving gel and stacking gel solutions without TEMED were prepared (Appendix.2). The resolving gel was poured into mould immediately after mixing with TEMED and isopropanol was added on the top of the resolving gel to get rid of air bubbles. The isopropanol was removed carefully with filter papers after polymerisation of the resolving gel. Stacking gel solution was then mixed with TEMED and poured on the top of solid resolving gel in the mould. A sample comb was inserted into the stacking gel solution in the mould without creating air bubbles. SDS PAGE gel was used for electrophoresis after complete polymerisation of stacking gel.

2.9.3 Western Blot

2.9.3.1 SDS PAGE: gel electrophoresis

SDS PAGE gels were assembled in the electrophoresis chamber filled with 1× Running Buffer. The sample comb was then removed before samples were loaded in the wells of the SDS PAGE gel. 120V voltage was applied to the electrophoresis chamber for 90 min to migrate protein samples in the SDS PAGE gel vertically. The SDS PAGE gel was then used for membrane transferring or Coomassie blue staining.

2.9.3.2 Transfer of proteins to a membrane

The SDS PAGE gel after electrophoresis was removed from the electrophoresis chamber. A PVDF (Polyvinylidine fluoride) membrane was cut and prepared by wetting in methanol and the resolving gel was soaked in 1× Transfer Buffer without stacking gel. Filter papers and fibre pads were wet in the 1× Transfer Buffer and used to assemble the 'transfer sandwich' with filter papers surrounding the gel and PVDF membrane. The sandwich was then loaded in the transfer cassette which was placed in the transfer tank filled with ice cold 1× Transfer Buffer. 25V voltage was applied to the transfer tank at 4 °C for 12-16 hours to transfer proteins from the gel to the membrane. The transferred membrane was soaked in 5% skimmed milk poweder dissolved in 1× TBST Buffer (Appendix.2) for an hour to prevent non-specific binding of antibodies to the membrane.

2.9.3.3 Antibody hybridisation to membrane

Based on optimised conditions, antibodies were added into either 5% skimmed milk in 1× TBST Buffer or 1% BSA solution. The transferred membrane was washed with TBS solution (5min, 3 times) before incubation with primary antibody for 1 h at room temperature. The membrane was then washed with TBST solution (5min, 3 times) before incubation with the secondary antibody. One hour later, the washing procedure was repeated with TBST, and the membrane was ready for film development.

2.9.3.4 Enhanced chemiluminescence (ECL)

ECL western blotting substrate (Thermo Scientific) was used to detect the horseradish peroxidase (HRP) on the secondary antibody. Detection Reagent 1 and Detection Reagent 2 were mixed at a ratio of 1:1. The volume of the ECL substrate depended on the size of the PVDF membrane. ECL substrate was added to the blot and incubated for 1 minute. Excess reagent was drained, and the blot covered with a clear plastic sheet protector was fixed in a film cassette. Hyperfilm (Amersham) was placed on the ECL treated blot, and the exposure time was set according to the amount of the target protein. The film was developed by the X-o-graph processor.

2.9.3.5 Comassie blue staining

The PVDF membrane was submerged in Coomassie Blue staining buffer (Appendix.2) with shaking at low speed for 30 min. The membrane was then rinsed with water and soaked in destaining buffer (Appendix.2) with shaking at low speed for 15 min. The membrane was washed with water and air dried in a laminar flow hood for 5 min.

2.10 Appendix 1: growth media

All media were prepared with filtered water from water purification system and sterilised at 15 psi and 121 °C for 15-20 minutes.

Bacterial growth media

LB broth

Tryptone	10 g/L
Yeast extract	5 g/L
NaCl	10 g/L

LB agar plate

LB broth plus 10 g/L agar

SOB

Tryptone	20 g/L
Yeast extract	5 g/L
$MgSO_4$	0.96 g/L
NaCl	0.5 g/L
KCl	0.186 g/L

Required antibiotic was added for selection based on antibiotic resistance. Antibiotics were mixed with cooled media (no more than 50°C) at required concentrations: kanamycin, 50 μg/mL; ampicillin, 50μg/mL; rifampcin, 50μg/ mL.

Yeast growth media

YPDA

Yeast extract	10 g/L
Peptone	20 g/L
Glucose	20 g/L
Adenine hemisulfate	40 mg/L

YPDA agar plate

YPDA plus 20 g/L agar (Sigma)

SD drop-out broth

Yeast Nitrogent without amino acids (Sigma)	6.8 g/L
Drop-out mix	Depends on different mixes
Glucose	20 g/L
Adenine hemisulfate	40 mg/L

SD drop-out agar

SD drop-out broth plus 20g/L agar (Sigma)

Yeast transformation solution (600 µL)

1M LiAc	200 µL
50% PEG3350	400 µL
β-mercaptoethanol	4 µL

Arabidopsis growth media

½ Murashige and Skoog (MS) agar:

2.2g/L MS basal salts (Sigma)

pH 5.6-5.8 with KOH

10g/L agar (Sigma)

MS basal salts with or without sulfur from Cassion were applied in Arabidopsis growth media for sulfur stress experiments.

Tomato tissue culture media

Solution I	100 mL
Glycine	2g
Vitamin B1	0.1g
Vitamin B6	0.5g
Nicotinic acid	0.5g

PB Buffer	60mL
NaH_2PO_4	3.90g
K_2HPO_4	0.87g

AB Salt solution	100mL
MS	2.2g
Solution I	500µL
KT (2mg/mL)	25µL

2,4-D (1mg/mL)	100µL
Acetosyringone (10mg/mL)	735µL
Agar	4g
Induction Solution	100mL
AB salt	5mL
Sucrose	1g
Water	90mL
Filter-sterilized solutions below are added into autoclaved solution above.	
0.625M MES Buffer	2mL
PB Buffer	2mL
ACE (10mg/mL)	400 µL

Pre Media	500mL
MS	2.2g
Solution I	500µL
6-BA (1mg/mL)	500µL
IAA (1mg/mL)	20µL
Agar	4g

Co Incubation Media	500mL
MS	2.2g
Solution I	500µL

KT (2mg/mL)	25μL
2,4-D (1mg/mL)	100μL
ACE (10mg/mL)	735μL
Agar	4g

K60 (K65, K70) Selection Media	500mL
MS	2.2g
Solution I	500μL
6-BA (1mg/mL)	500μL
Carbenicillin (100mg/mL)	2500 μL
Kanamycin (50mg/mL)	600 μL, 650 μL, 700 μL
IAA (1mg/mL)	20μL
Agar	4g

Rooting Media	500mL
MS	2.2g
Solution I	500μL
Carbenicillin (100mg/mL)	2500 μL
Kanamycin (50mg/mL)	700 μL
IAA (1mg/mL)	1000μL
Agar	2.5g

*For all the culture medium preparation, MS medium should be made and autoclaved before other filter sterilized ingredients are added.

Tomato hairy root tissue culture media

MS liquid and agar media:

4.4g/L MS basal salts (Cassion)

pH 5.6-5.8 with KOH

10g/L agar (Sigma)

NB broth:

8g/L Difco Nutrient Broth

NB agar:

23g/L Difco Nutrient Agar

Co-culture and selection media:

4.43g/L MS with vitamins

0.5g/L MES

30g/L Sucrose

10g/L Agar

pH 5.8 with 1M KOH

200 mg/L Cefotaxime and Kanamycin are supplemented for selection media.

2.11 Appendix 2: General solutions

Agarose gel electrophoresis solution

5 × TBE:

0.45 M Tris

0.45 M Boric acid

12.5 mM EDTA

Competent *E. coli* cell solutions

TB buffer:

500 mM KCl

200 mM MOPS

160 mM $MnCl_2$

40 mM $CaCl_2$

pH 6.7 with KOH and sterilise with syringe filter

Western blotting solutions

Protein extraction buffer:

50mM Tris-HCl pH7.5

150mM NaCl

5mM MgCl2

10% (v/v) glycerol

1mM EDTA

0.5% NP-40

1 protease inhibitor cocktail tablet (Roche) per 10 mL

10 × Running Buffer:

250mM Tris base

1900 mM Glycine

1% SDS

10 × TBS:

200 mM Tris base

1500 mM NaCl

Coomassie stain:

0.1% Comassive blue R-250

45% Methanol

10% Glacial acetic acid

45% H_2O

5 × SDS loading dye:

5% (v/v) β-mecaptoethanol

0.02% (m/v) Bromophenol blue

30% (v/v) Glycerol

10% (m/v) SDS

250mM Tris-HCl pH 6.8

1 × Transfer buffer:

25mM Tris base

190 mM Glycine

20% (v/v) Methanol

Blotting buffer:

1 × TBS

5 % (w/v) milk powder

Solutions for manipulation of plants

DNA extraction buffer:

200 mM Tris-HCl pH 7.5

250 mM NaCl

25 mM EDTA

0.5% (m/v) SDS

Infiltration buffer:

10 mM MES

10 mM $MgCl_2$

2 µM Acetosyringone

2.12 Appendix 3 Primers

Primers for cloning

Gene	5’ primers	3’ primers
SlMYB93-1 (for pGBKT7)	AAAGAATTCGGAAGATCTCCTTGTTGTGATG	AAAGGATCCTCAAGAAATGTCATGCATGAAG
SlMYB93-2 (for pGBKT7)	AAAGAATTCGGAAGGTCTCCTTTTTGTG	AAAGGATCCCTAGGGAATATCATGGAAGAAGGA
SlMYB93-3 (for pGBKT7)	AAAGGATCCTGGGAAGATCTCCTTGTTGTG	AAAGTCGACTTAAAACTTATCAATGTCTTGG
SlMYB93-1 (for mpBI121)	AAATCTAGAATGGAGGAGCAGAAGCTGAT	AAAGTCGACTCAAGAAATGTCATGCATGAAG
SlMYB93-2 (for mpBI121)	AAATCTAGAATGGAGGAGCAGAAGCTGAT	AAAGTCGACCTAGGGAATATCATGGAAGAAGGA
SlMYB93-1-1 (psKint)	AAAGTCGACCTAGGAAACAAATGGTCTGCAAT	AAAAAGCTTTGAGGGTGTAGGTAGTGGTG
SlMYB93-1-2 (psKint)	AAAGGATCCCTAGGAAACAAATGGTCTGCAAT	AAATCTAGATGAGGGTGTAGGTAGTGGTG
SlMYB93-2-1 (psKint)	AAAGTCGACACCGATATATTTAACAGCTTGCCTC	AAAAAGCTTTAGGAGGAAGTTGCCATGGAG
SlMYB93-2-2 (psKint)	AAAGGATCCTAGGAGGAAGTTGCCATGGAG	AAATCTAGAACCGATATATTTAACAGCTTGCCTC
SlMYB93-1 (for pDonor(Zeo))	GGGGACAAGTTTGTACAAAAAAGCAGGCTTCATGGGAAGATCTCCTTGTT	GGGGACCACTTTGTACAAGAAAGCTGGGTCTCAAGAAATGTCATGCATGA
SlMYB93-2 (for pDonor(Zeo))	GGGGACAAGTTTGTACAAAAAAGCAGGCTTCATGGGAAGGTCTCCTTTTTGTG	GGGGACCACTTTGTACAAGAAAGCTGGGTCCTAGGGAATATCATGGAAGAA

Restriction sites: GAATTC, *Eco*RⅠ; GGATCC, *Bam*HⅠ; TCTAGA, XbaⅠ; GTCGAC, *Sal*Ⅰ; GCGGCCGC, *Not*Ⅰ; AAGCTT, *Hind*Ⅲ.
Adapter primers: GGGGACAAGTTTGTACAAAAAAGCAGGCTTC, attB1; GGGGACCACTTTGTACAAGAAAGCTGGGTC, attB2.

Sequence of sgRNAs for CRISPR cloning

Gene	5’ primers	3’ primers
SlMYB93-1-sgRNA-1	GATTGACAAACATGGTCATGGAAGT	AAACACTTCCATGACCATGTTTGTC
SlMYB93-1-sgRNA-2	GATTGTGAGTGTTTGATGAGGGTGT	AAACACACCCTCATCAAACACTCAC
SlMYB93-1-sgRNA-3	GATTGACTAACAATGGTGCAGATCA	AAACTGATCTGCACCATTGTTAGTC
SlMYB93-2-sgRNA-1	GATTGGGTTTGCTCCTCCAAAGAA	AAACTTCTTTGGAGGAGCAAACCC
SlMYB93-2-sgRNA-2	GATTGTAGGCCTTAAGAAAGGTCCT	AAACAGGACCTTTCTTAAGGCCTAC
SlMYB93-2-sgRNA-3	GATTGCATTGTCGTCTCACCTGTAT	AAACATACAGGTGAGACGACAATGC

Primers for RT PCR

Gene	5’ primers	3’ primers
SlMYB93-1	GGAAACAAATGGTCTGCAATC	GATGAGGGTGTAGGTAGTGGTG
SlMYB93-2	TTGGCAACAAGTGGTCAGC	TCAGCTAAATGGGAGAAATGG
SlMYB93-3	GCTGTCTTAGGAAACAAGTGGTC	CTTGGCTCATAATCCTAAACTCAG
Actin Ⅱ (tomato)	GGTGAAGGCTGGATTTGCT	GAAGTTCTCAAACATAATCTGGGT
ACTIN (*Arabidopsis*)	TCGTACAACCGGTATTGTGCTG	TAACAATTTCCCGCTCTGCTG

Primers for sequencing

Primer name	Primer sequence
M13-F	CGCCAGGGTTTTCCCAGTCACGAC
M13-R	CAGGAAACAGCTATGAC
T7	TAATACGACTCACTATAGGG
3’BD	CGTTTTAAAACCTAACAGTCAC
pTC14-F2	CAAGCCTGATTGGGAGAAAAc

Chapter Ⅲ： Identifying MYB93 orthologues in *Solanum lycopersicum*

3.1 Introduction

As described in Chapter 1, there are many challenges in our agriculture system. To help plants survive those challenges, plant science has been applied to study mechanisms of plant development and responses to different stresses, which can help to develop crop improvement in agriculture.

Root systems are vital to plant growth and development. Roots are not only in charge of the uptake of nutrients and water, they also function as storage organs, such as cassavas, beets and carrots (Giaquinta, 1979; Adetan *et al*.,2003; Szczepanek *et al*., 2020). In addition to the functions described above, lateral roots in the root system are crucial for plant to anchor to substrates, which helps plants to survive from flooding, tornados or soil erosion (Li *et al*., 2017; Berry *et al*.,2020; Yamauchi *et al*., 2021).

Although process of lateral root development in *Arabidopsis* is well studied, how lateral root development is restrained is less established. As Gibbs *et al*., (2014) showed that the promoter of *AtMYB93* is specifically active in several endodermis cells overlapping lateral root primordia in the early stage of lateral root initiation. Since *AtMYB93* was identified as a negative regulator of lateral root development in *Arabidopsis*, it may provide a new angle in understanding the mechanism of lateral root initiation pattern in *Arabidopsis*. Moreover, this information may be applied to crop plants.

From previous publications, *At*MYB93 was identified as a root-specific transcription factor, whose expression was only detected in root tissue (Gibbs *et al*., 2014). While *AtMYB53* and *AtMYB92* were reported to express mainly in root, their expression was also detected in other tissues including bud, flower, leaf, silique and stem (Gibbs *et al*., 2014). *AtMYB93* played a negative role in regulating lateral root development in *Arabidopsis*, as *Atmyb93* knock out lines showed increased LR density compared to wild type (Gibbs *et al*., 2014). *AtMYB92* plays

some role this process but it does not function redundantly with *AtMYB93* as *Atmyb92* mutants do not show a LR phenotype although the *Atmyb93*/*Atmyb92* double mutant showed a higher LR density than the *Atmyb93* mutant (Gibbs *et al*., 2014). These findings suggest correlation of gene expression pattern with function.

The aim of this chapter was to identify MYB93 orthologues in tomato and confirm that these MYB93 orthologues are R2R3-MYBs. A phylogeny tree using amino acid sequences of putative MYB93s from different species was constructed to identify three putative tomato MYB93s. An analysis of the protein sequences of putative MYB93s showed that they have highly conserved R2R3 domains, followed by a further conserved domain with 35 amino acids. Use of Reverse transcription PCR (RT-PCR) showed that all three *SlMYB93*s share a similar expression pattern with *AtMYB93*, mainly in roots.

Reverse genetic methods were used to investigate *SlMYB93* functions. Using the floral dipping method, I generated *SlMYB93*-overexpressing lines in *Arabidopsis* and demonstrated that SlMYB93s can inhibit lateral root development in *Arabidopsis*. Tomato tissue culturing and hairy root transformation was applied to overexpress or knockdown individual *SlMYB93*s in tomato to study their functions. Using hairy root transformation, I generated CRISPR lines of *SlMYB93*s, which will be used to study the functions of *SlMYB93*s in specific tomato root cells.

3.2 Identifying *AtMYB93*-orthologous genes in *Solanum lycopersicum*

3.2.1 Putative *SlMYB93*s

To identify AtMYB93 orthologous genes in *Solanum lycopersicum*, the full length amino acid sequence of *At*MYB93 was used to perform a BLAST search in the tomato genomic sequence database, Solgenomics (https://solgenomics.net/tools/ blast). The closest matches were Solyc04g074170.1.1(4e-^{110}), Solyc04g056310.2.1(2e^{-96}) and Solyc05g051550.1.1(7E^{-96}) followed by other various R2R3 MYB proteins with increasing e-values, which indicated quality of the alignment. A lower e-value indicates a better alignment.

As described before, *At*MYB53 and *At*MYB92 were categorised in the same subgroup with *At*MYB93, which implied that these proteins may have or share similar function. Thus, full length protein sequences of both *At*MYB53 and *At*MYB92 were also to BLAST search in the Sol genomics database. Interestingly, the closest matches were the same as the result of the *At*MYB93 BLAST search, but with different alignment orders. In both the *At*MYB53 and *At*MYB92 BLAST searches, tomato proteins were ranked in the same order and Solyc04g056310.2.1 was closest hit with e-value of 6e^{-93} and 4e^{-93}, respectively. *Solyc05g051550.1.1* and *Solyc04g074170.1.1* were considered as highly similar sequences of *At*MYB53 with e-value of 1e-^{89} for both proteins, and of AtMYB92 with e-value of 2e^{-92} and 3e^{-90}, respectively. These three proteins were also clustered in the same subgroup in tomato R2R3 MYB phylogeny tree, which is similar to the relationship among *At*MYB93, *At*MYB53 and *At*MYB93 (Li *et al*., 2014).

Together with the previous findings, *Solyc04g074170.1.1* was initially identified as a R2R3 MYB transcription factor and it was expected to be an orthologue of *At*MYB93 and potentially have a role in lateral root development in tomato. *Solyc04g056310.2.1* and *Solyc05g051550.1.1* were initially identified as putative orthologues of *At*MYB53 and

*At*MYB92, respectively. These proteins were also subdivided into the same subgroup with *Solyc04g074170.1.1* in a previous phylogeny (Li *et al*., 2014), which indicated similarity among their conserved motifs. Thus, *Solyc04g056310.2.1* and *Solyc05g051550.1.1* may share the similar function as *Solyc04g074170.1.1* in tomato.

3.3.2 Phylogeny tree construction

Although my previous studies have identified three tomato best matched proteins of *At*MYB93 by a BLAST- based method, it was important to confirm the result with a phylogeny-based method. A phylogeny tree of R2R3-MYB transcription factors from tomato and *Arabidopsis* constructed by Li *et al*., (2014) showed all three tomato MYBs (*Solyc04g074170.1.1*, *Solyc04g056310.2.1* and *Solyc05g051550.1.1*) were clustered in the same subgroup, which was identical with the relationship among *At*MYB93, *At*MYB53 and *At*MYB92 in *Arabidopsis*. A further phylogeny tree generated with R2R3-MYB genes from *Arabidopsis*, tomato and rice showed that all three tomato MYBs were clustered in the distinct group with *At*MYB93 (Li *et al*., 2014). And previous studies showed that AtMYB93, AtMYB53 and AtMYB92 shared best three matched genes when blasting in Sol Genomics and similar pattern was also observed in blasting in rice. Thus, we decided that using three best matches of blasting in each species is sufficient to identify AtMYB93 ortholog in tomato and other two matches may or may not be potential orthologues of AtMYB53 and AtMYB92.

In order to confirm the identification of *Solyc04g074170.1.1*, and to extend previous phylogenetic analysis, the full length protein sequence of *At*MYB93 was used for a BLAST search against a database of diverse plant species including monocots, dicots and *Amborella trichopoda*, namely Phytozome v12 (https://phytozome.jgi.do-e.gov/pz/portal.html). Due to the high similarity of conserved motif in these potential orthologues, it is hard to confirm

orthologues of AtMYB93, AtMYB53 and AtMYB92. The best three matched genes with similar structures were chosen as the putative MYB93 orthologues in each species. In total, 118 protein sequences of blast-based putative MYB93s were used to construct the phylogenetic tree (Figure 3.1) by neighbour-joining method based on amino acid sequences in SEAVIEW. In this phylogram, all the MYB proteins from different species were roughly divided into two basic groups, which were monocot groups and dicot groups, indicating that the phylogeny tree constructed was effective.

The putative *Solyc04g074170.1.1*, *Solyc05g051550.1.1* and *Solyc04g056310.2.1* appeared to be localised in the same cluster with *At*MYB93 (At1g34670), and other homologues also shown in phylogeny tree constructed by Gibbs et al., (2014), such as *Pt*MYB93-1 (PtMYB30, PopulusPotri.005G164900.1), *Pt*MYB93-2(PtMYB109, PopulusPotri.002G096800.1), VvMYB93-1(VvMYB93a, VIT_07s0141g00100) and VvMYB93-2(VvMYB93b, VIT_11s0078g00480). Other reported AtMYB93 orthologues were also shown in this new phylogeny tree, such as *Md*MYB93-1(MdMYB93, MDP0000320772) and *St*MYB93-1(StMYB102, PGSC0003DMT400016394) (Legay et al., 2016; Lashbrooke et al., 2016). Thus, Solyc04g074170.1.1 was identified as the closest *Sl*MYB to *At*MYB93. However, in this phylogeny tree, *Solyc05g051550.1.1* and *Solyc04g056310.2.1* were also clustered with *At*MYB93, rather than *At*MYB92 and *At*MYB53, which was identical with the result from Li *et al* (2014) and Du *et al* (2015), indicating that they were more evolutionarily similar to *At*MYB93. The phylogeny tree also showed putative MYB93 orthologues in other species such as *Brassica rapa*, *Glycine max* (soybean), *Ananas comosus* (pineapple) and *Amborella trichopoda*, which is neither monocot nor dicot.

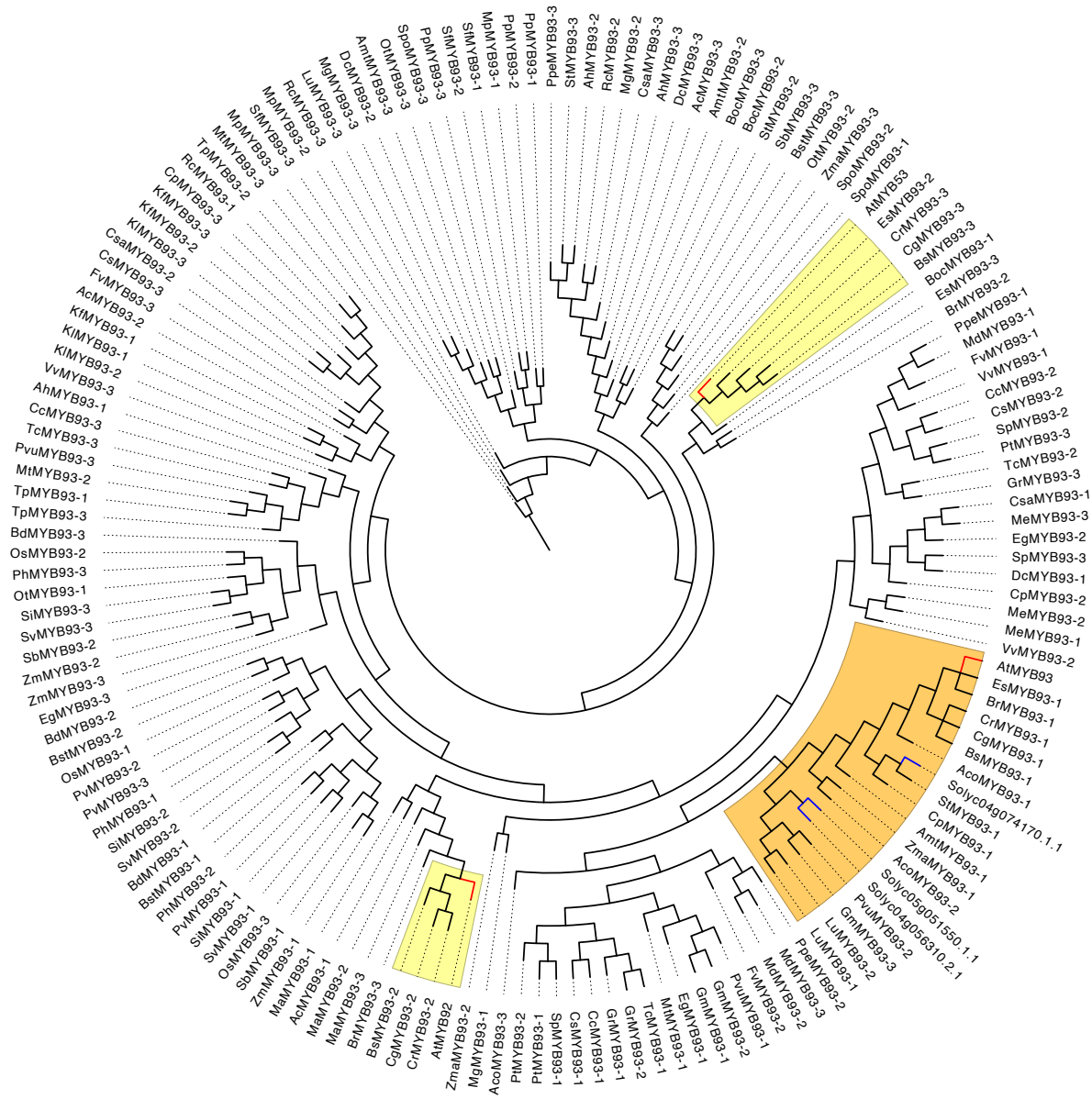

Figure 3.1 Phylogeny tree of putative MYB93s from different species.
Multiple alignment of full length protein sequences of putative MYB93s was performed by using ClustalW in Kalign (EMBL-EBI, https://www.ebi.ac.uk/Tools/msa/kalign/) with default setting. And the phylogeny tree was constructed in SEAVIEW using neighbour-joining method. *Solyc04g074170.1.1*, *Solyc04g056310.2.1* and *Solyc05g051550.1.1* were clustered in the group with *At*MYB93, and the cluster was highlighted in orange. Clusters with AtMYB53 and AtMYB92 were highlighted in yellow. branches of three SlMYB proteins were highlighted in blue, branches of AtMYBs were highlighted in red. *Ac, Aquilegia coerulea; Aco, Ananas comosus; Ah, Amaranthus hypochondriacus; Amt, Amborella trichopoda; At, Arabidopsis thaliana; Bd, Brachypodium distachyon; Boc, Brasica oleracea capitate; Br, Brasica rapa; Bs, Boechera stricta; Bst, Brachypodium stacei; Cc, Citrus clementina; Cg, Capsella grandiflora; Cp, Carica papaya; Cr, Capsella rubella; Cs, Citrus sinensis; Csa, Cucumis sativus; Dc, Daucus carota; Eg, Eucalyputus grandis; Es, Eutrema salsugineum; Fv, Fragaria vesca; Gm, Glycine*

max; Gr, Gossypium raimondii; Kf, Kalanchoe fedtschenkoi; Kl, Kalanchoe laxiflora; Lu, Linum usitatissimum; Ma, Musa acuminate; Md, Malus domestica; Me, Manihot esculenta; Mg, Mimulus guttatus; Mt, Medicago truncatula; Os, Oryza sativa; Ot, Oropetium thomaeum; Ph, Panicum hallii; Pp, Physcomitrella patens; Ppe, Prunus persica; Pt, Populus trichocarpa; Pv, Panicum virgatum; Pvu; Phaseolus vulgaris; Rc, Ricinus communis; Sb, Sorghum bicolor; Sf, Sphagnum fallax; Si, Setaria italica; Sl, Solanum lycoersicum; Sp, Salix purpurea; Spo, Spirodela polyrhzia; St, Solanum tuberosum; Sv, Setaria viridis; Tc, Theobroma cacao; Tp, Trifolium pretense; Vv, Vitis vinifera; Zm, Zea mays; Zma, Zostera marina.

3.4 Expression pattern of *SlMYB93* genes

To determine the expression patterns of *Solyc04g074170.1.1* (Solyc04g074170.1.1), *Solyc04g056310.2.1* (Solyc04g056310.2.1) and *Solyc05g051550.1.1* (Solyc05g051550.1.1), the total RNAs were extracted from different tissues of Micro Tom including roots, stems, leaves, flowers and fruits from different developmental stages (TF: 10dpa, IMG: immature green, MG: mature green, BR: breaker and RR: red ripen). Reverse transcription PCR (RT-PCR) was performed by One-step RT-PCR kit (Bioline) and the relative abundance of these genes' transcripts in different tissues was detected by imaging the gel from the electrophoresis. The housekeeping gene *ACTIN Ⅱ* was used as a control in the comparisons. The results are shown in Figure 3.2.A. The cDNAs of all three tomato genes were amplified and mainly detected in roots and slightly in early developmental stage fruit for *Solyc05g051550.1.1* and *Solyc04g074170.1.1*. The expression pattern detected in this study also matched the expression data from Micro Tom transcriptome database, TOM EXPRESS (http://tomexpress .toulouse.inra.fr) (Figure 3.2.B, C, D).

Like expression of *AtMYB93*, *SlMYB93*s were mainly expressed in root, but slightly expressed in early stage of fruit. However, unlike expression of *AtMYB53* and *AtMYB92*, *Solyc04g056310.2.1* showed root-specific expression character and *Solyc05g051550.1.1* showed similar expression pattern to *Solyc04g074170.1.1*, which suggest that they may play roles in both root and fruit development. Thus, with combination of phylogeny and expression pattern analysis, all three genes were recognised as putative orthologues of *AtMYB93* and renamed as *SlMYB93-1* (Solyc04g074170.1.1), *SlMYB93-2* (Solyc04g056310.2.1) and *SlMYB93-3* (Solyc05g051550.1.1).

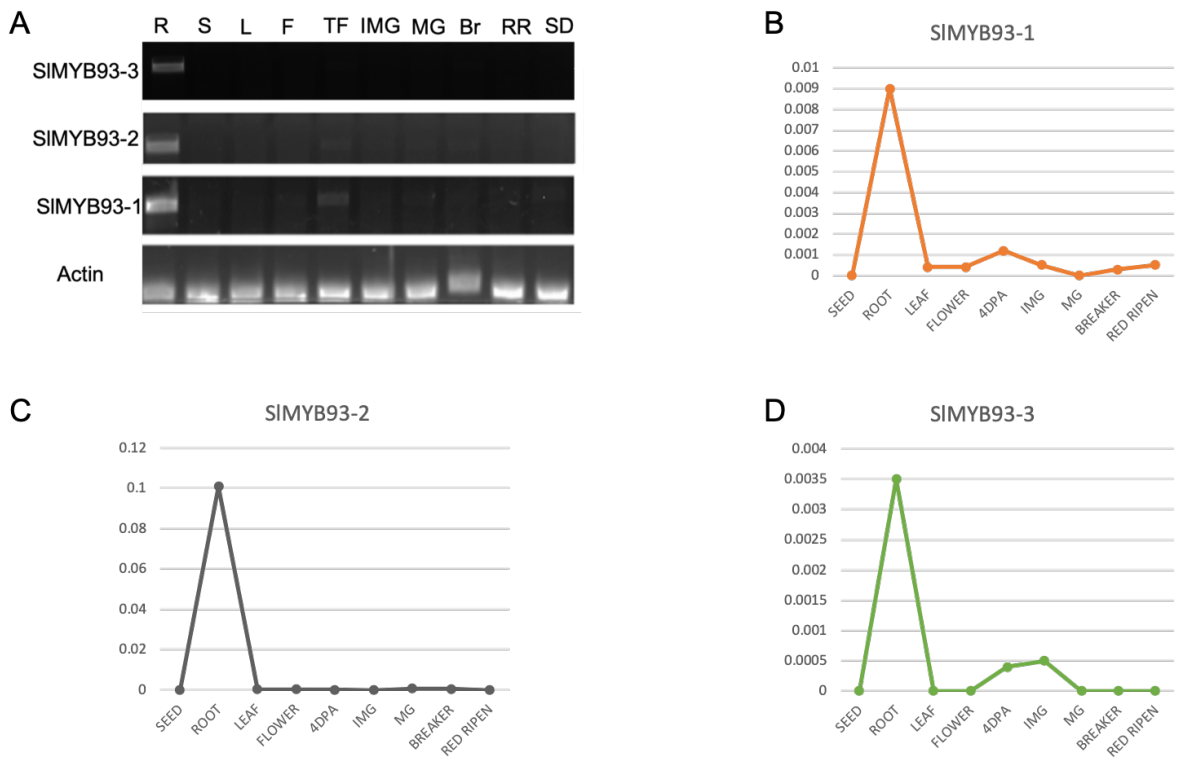

Figure 3.2 Expression pattern of SlMYB93s in tomato.
(A) The detection of *SlMYB93*s in different tomato tissues by RT-PCR. All three *SlMYB93*s have a similar expression pattern; they are found mainly in root and slightly in early stage of fruit. *ACTIN2*, a globally expressed housekeeping gene, was used as a loading control. R, root; S, Stem; L, leaf; F, flower; TF, 4 days post anthesis (DPA) tomato fruit; IMG, immature green; MG, mature green; Br, breaker; RR, red ripen; SD, seed. (B, C and D) Expression profile of *SlMYB93*s from the tomato transcriptome database (TOMEXPRESS). *SlMYB93-1*(Solyc04g074170.1.1) and *SlMYB93-3*(Solyc05g051550.1.1) are found in mainly in the root and weakly express in early stage of fruit. *SlMYB93-2*(Solyc04g056310.2.1) is found exclusively in the root.

3.5 *Sl*MYB93s are R2R3 type MYB proteins

*Sl*MYB93-1 (Solyc04g074170.1.1), *Sl*MYB93-2 (Solyc04g056310.2.1) and *Sl*MYB93-3 (Solyc05g051550.1.1) were identified in previous studies as putative R2R3 type MYB proteins (Li et al., 2014). Among them, only *Sl*MYB93-1 (Solyc04g074170.1.1) was also assigned as the orthologue of *At*MYB93 (At1g34670) based on the better alignment of full-length amino acid sequences. In order to further identify the characters of these three genes, more bioinformatic analysis has been conducted.

Full length amino acids sequences of all three proteins were analysed in Pfam (https://pfam.xfam.org) and SMART (http://smart.embl-heidelberg.de). Analysis in both online resources showed that all three proteins shared conserved domains in the similar position of their N termini (probabilities from $6.4e^{-17}$ to $9.9e^{-15}$), but different conserved domains were recognised in both databases. MYB-like DNA binding domain was characterised at Pfam, which were identified as SANT (switching-defective protein 3(Swi3), adaptor 2(Ada2), nuclear receptor co-repressor (N-CoR) and transcription factor (TF)IIIB) domains in SMART. SANT domain is highly similar with MYB DNA binding domain in sequence and structure, but it is assigned a function in protein-protein interaction rather than protein-DNA interaction as MYB DNA binding domain (Boyer *et al*., 2001).

The full-length sequence and corresponding schematic representation of *Sl*MYB93-1 is shown in Figure 3.3.A, in which two recognised conserved MYB domains are highlighted in both. *Sl*MYB93-2 and *Sl*MYB93-3 exhibit similar structures. In previous studies, R2R3 MYBs in tomato were identified and amino acid sequences of their R2 and R3 repeats were aligned. Based on the frequency of each amino acid at each position, consensus sequences of R2 and R3 domains in tomato was identified by Li *et al*., (2014). The R2 and R3 repeats of the three putative *Sl*MYB93s showed high similarity with these consensus sequences (Figure 3.3B).

An alignment analysis of amino acid sequences of R2 and R3 repeats between *Sl*MYB93-1 and *At*MYB93 was also conducted and showed a highly matched alignment with identity of 95%. The R2 and R3 repeats of *Sl*MYB93-2 and *Sl*MYB93-3 were also aligned with that of *At*MYB93, with identity of 95% and 92% respectively.

To further investigate the conserved features of R2 and R3 domains among these putative *Sl*MYB93s, I performed WebLogo analysis on WebLogo 3 (http://weblogo.threeplusone.com) using aligned amino acid sequences of R2 and R3 repeats of *Sl*MYB93-1, *Sl*MYB93-2 and *Sl*MYB93-3 (Figure 3.3.B) (Crooks et al., 2004). The results showed that they all contain conserved triplet tryptophan residues (W) in each repeat, which help to form a hydrophobic core structure and are vital for structure and function of MYB domains. The first tryptophan residue was replaced by phenylalanine (F) at position 59 in the R3 repeat, which is common in R2R3 MYB family in planta, such as in *Arabidopsis*, rice and Chinese cabbage (Wang et al., 2015)

The amino acid sequences of R2R3 domains from all three *Sl*MYB93s were analysed in SWISS MODEL by using comparative protein structure modelling. The protein structures of all three R2R3 domains were all predicted based on the structure of WEREWOLF(WER) R2R3 domain from X-ray crystallography with sequence identity of 59.46%, 56.76% and 56.76%. (Wang et al., 2020). As shown in Figure 3.3.C, R2R3 domains consisted of two imperfect amino acid sequence repeats. Each repeat contained three tryptophan or hydrophobic residues which evenly spaced in three alpha-helices. The second and third helices of each repeat formed a “helix-turn-helix” structure of HLH DNA binding motif (Wang et al., 2020). The structure prediction suggested that all three putative *Sl*MYB93 genes have conserved structure of their DNA binding domain with R2R3-MYB genes in *Arabidopsis*.

Collectively, I initially identified three *Sl*MYB93s (*Sl*MYB93-1, *Sl*MYB93-2 and *Sl*MYB93-3) in tomato based on phylogeny and expression pattern analysis. Further bioinformatic analysis of these proteins suggest that *Sl*MYB93-1, *Sl*MYB93-2 and *Sl*MYB93-3 are orthologues of *At*MYB93 and are R2R3 MYB transcription factors that may transcriptionally regulate genes involving in root and fruit development in tomato.

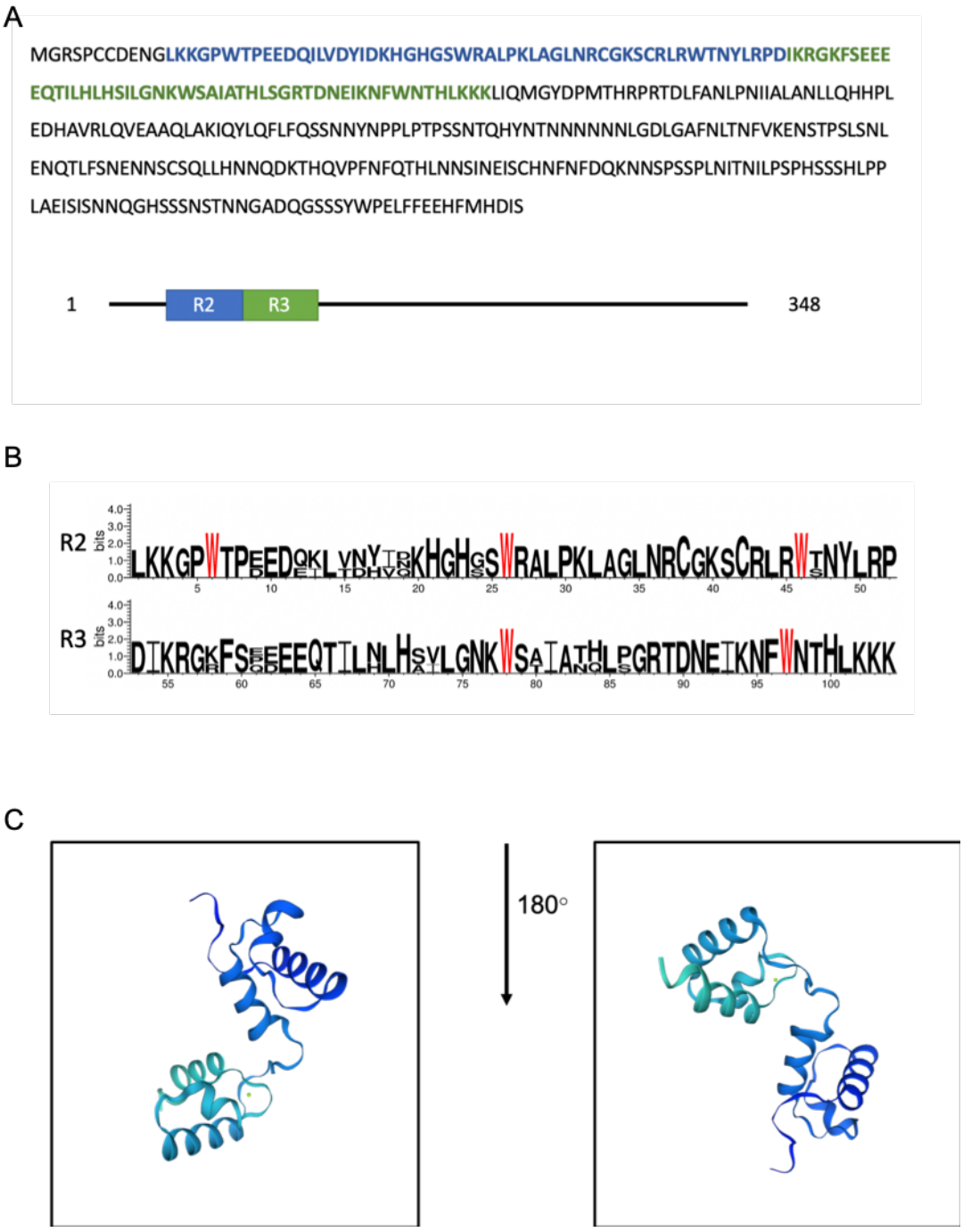

Figure 3.3 Identification and structure predication of R2R3 repeats in *S*lMYB93s.
(A) Full length amino acid sequence of *S*lMYB93-1. R2 and R3 repeats were predicted in Pfam (https://pfam.xfam.org), which were highlighted in blue and green separately. A schematic diagram of *S*lMYB93-1 was shown. (B) Weblogo analysis of predicted R2 and R3 MYB domains of *S*lMYB93s. Size of the amino acid codes indicted their conservation in R2R3 MYB domains. Conserved tryptophan residues (W) were highlighted in red. (C) Template 6kks.1 (R2 and R3 repeats of the *Arabidopsis* R2R3 type protein MYB66) from SWISS-MODEL. All three SlMYB93s shared the same structural prediction.

3.6 Cloning of overexpressing and silencing constructs for *SlMYB93* genes

3.6.1 Deletion in *SlMYB93-3* sequences

Tomato root cDNA was synthesised by reverse transcription of RNA from wild type tomato roots. Full length CDS (Coding DNA Sequence) of three *SlMYB93*s were amplified from tomato root cDNA (Figure 3.4A) by PCR and PCR purification products were introduced into the vector pCR-blunt, which were then sequenced by using general primers M13-F and M13-R. After alignment of sequencing results with sequences from genome database (NCBI, https://www.ncbi.nlm.nih.gov/nucleotide), *SlMYB93-1* and *SlMYB93-2* were completely aligned with reference sequences. However, due to the wrong sequence of Solyc05g051550 in the "Micro Tom" database (NCBI, GenBank: AK319434.1) at the time, in which there were two nucleotides missing in database at position 345-346. So, I failed to acquire full length CDS of *SlMYB93-3* at first and I was acknowledged that the sequence of *SlMYB93-3* I cloned was corrected in the latter of my PhD. Thus, only *SlMYB93-1* and *SlMYB93-2* were further studied in this project from this point on.

3.6.2 Cloning of pBI121::35S:: myc-cSlMYB93s

Full length CDS sequences of *SlMYB93*s without start codons were amplified from wild type tomato root cDNA. To assemble a c-myc tag on the N-terminal (5') end of *SlMYB93*s, both genes were introduced into the vector pGBKT7 with restriction sites for *Bam*HI and *Eco*RI, and the resulting ligation products were then used as templates to amplify *SlMYB9*3s with a fused N-terminal myc tag. Genes with the myc tag were inserted into the binary vector pBI121 with restriction sites *Xba*I and *Sal*I with a CaMV35S promoter at the 5' end and a NOS terminator on the 3' end (Figure 3.4B). Constructs were then introduced into *Agrobacterium tumefaciens* GV3101, which was then used for plant transformation. (Section 2.6.4)

3.6.3 Cloning of pBI121-35S::*SlMYB93*s RNAi construction

The CDS fragments (~300bp) used to design an RNAi construct from both *SlMYB93*s were selected by using the Virus-Induced Gene Silencing (VIGS) tool from the Sol Genome Network (https://vigs.solgenomics.net). Primers were then designed to generate DNA fragments that encode sense and antisense RNA by PCR amplification. The DNA fragments were then cloned into pSK-int at both sides of the intron with appropriate restriction sites to obtain fragments with the structure of *SlMYB93*-intron-*SlMYB93*, which were then cloned into the binary vector pBI121 with restriction sites *Xba*I and *SalI* with a CaMV35S promoter on the 5' side and a NOS terminator on the 3' side (Figure 3.4B). Constructs were then introduced into *Agrobacterium tumefaciens* GV3101, which were then used for plant transformation. (Section 2.6.4)

3.6.4 Generation of a 35S::*Sl*MYB93::YFP fusion protein construct

The full length CDS of *SlMYB93*s were amplified from wild type tomato root cDNA with attB sites at both ends for Gateway cloning. PCR products were assembled into entry vector pDONOR-Zeo by a BP reaction, which was then used for an LR reaction to introduce genes of interest into the plant binary vector pEG104-YFP. The expression of *Sl*MYB93s YFP fusion protein was driven by CaMV35S promoter and terminated by NOS terminator (Figure 3.5B). Constructs were then introduced into *Agrobacterium tumefaciens* GV3101, which was then used for transient expression in tobacco leaves.

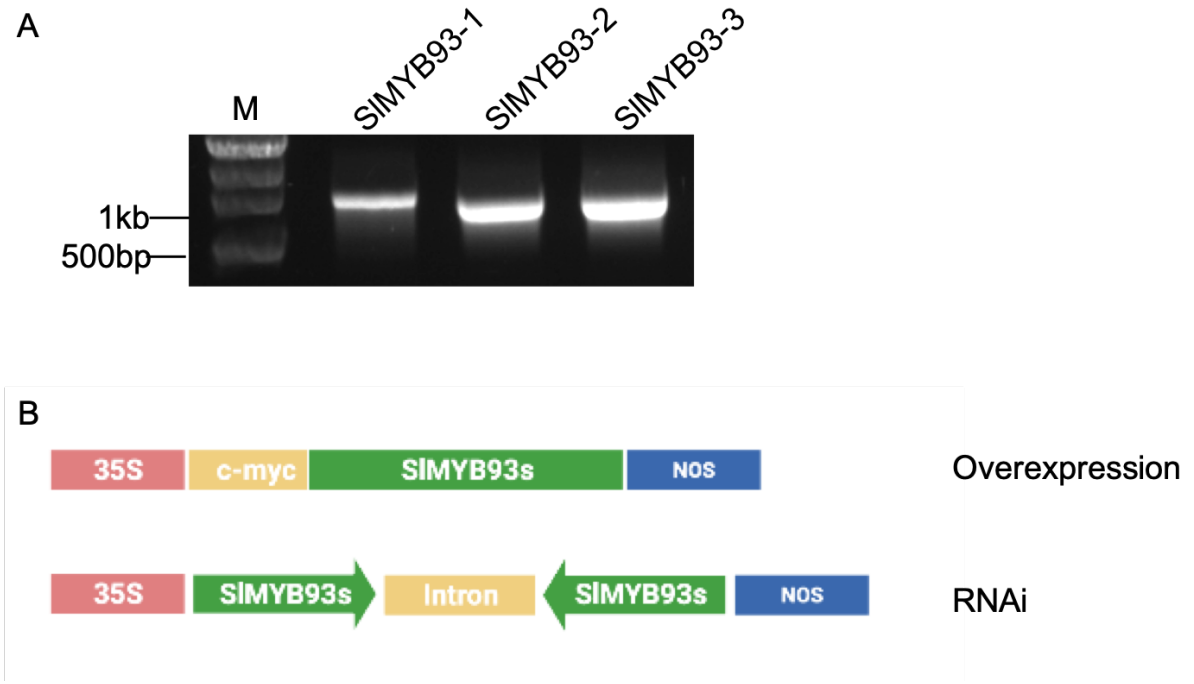

Figure 3.4 cloning of SlMYB93s.

(A) Amplification of full-length CDS of three SlMYB93s. cDNA library synthesised from Micro Tom root RNA was used as templates for PCR amplification of *SlMYB93-1*, *SlMYB93-2* and *SlMYB93-3*. (B) Schematic diagram of *SlMYB93*s overexpression and RNAi constructs. The modified pBI121 was used as plant binary vector for both constructs. The arrow in diagram of RNAi constructs indicated the direction of the same cDNA fragment selected from *SlMYB93*s, which then formed double-stranded RNA (dsRNA). Within the plant, dsRNAs become diced into 21nt small interfering RNAs, which silence the target genes by interfering their transcription.

3.7 Subcellular localisation of *Sl*MYB93s in tobacco leaves

Yellow fluorescent protein (YFP) was used as the marker of *Sl*MYB93-1 and *Sl*MYB93-2 in tobacco leaves. *Sl*MYB93-1 and -2::YFP fusion proteins were expressed in tobacco leaves by agroinfiltration. The fusion proteins of both *Sl*MYB93-1 and *Sl*MYB93-2 were only detected in the nucleus compared to the YFP control sample, which showed a YFP signal in both the nucleus and the cytosol (Figure 3.5 A-I). Western blot analysis of *Sl*MYB93-1 and -2::YFP fusion proteins confirmed their expression in tobacco leaves (Figure 3.5 J).

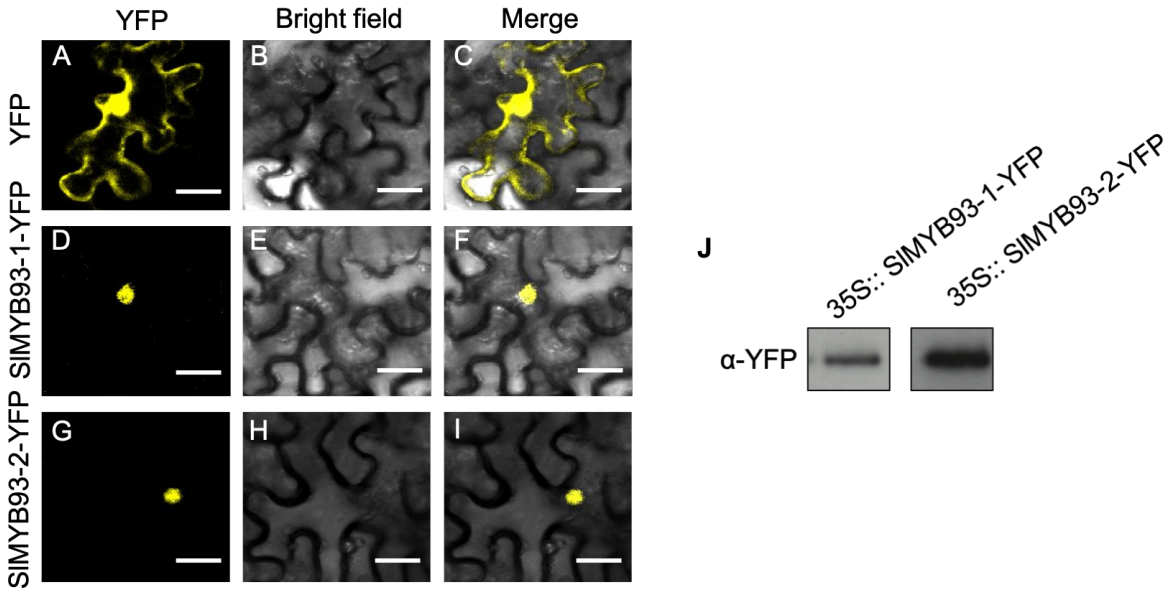

Figure 3.5 Subcellular localization of *Sl*MYB93-1-YFP and *Sl*MYB93-2-YFP in *N. benthamiana* leaves.
YFP, *Sl*MYB93-1-YFP and *Sl*MYB93-2-YFP are transiently expressed in infiltrated tobacco leaves (A-I). Yellow fluorescence channels (A, D, G), bright field channels (B, E, H) and merged channels (C, F, I) are shown. Bar=25μm. J, western blot analysis of *Sl*MYB93-1-YFP and *Sl*MYB93-2-YFP proteins.

3.8 Transformation of plants

3.8.1 Generation of heterologous expression lines of *Sl*MYB93s in Arabidopsis and analysis of their lateral root phenotype.

Due to the time-consuming tomato tissue culture transformation protocol, *Sl*MYB93-1 and -2 overexpressing constructs were introduced into *Arabidopsis thaliana* by *Agrobacterium tumefaciens* mediated transformation using the floral dip method (Section 2.7.1). Three independent *Arabidopsis* homozygous T-DNA insertion overexpressing lines of each *Sl*MYB93 were identified after three generations of selection on ½ MS agar plates with kanamycin. (Appendix.1) The overexpression of *Sl*MYB93s in those homozygous lines was confirmed by RT-PCR using RNA extracted from *Arabidopsis* whole seedlings (Figure 3.6A and Figure3.7A). The root parameters of homozygous seedlings were measured and analysed, and showed that *Arabidopsis* with overexpression of *Sl*MYB93-1 had significantly shortened primary root length compared to Col-0 in two out of three independent lines (Figure 3.6B), while overexpressing *Sl*MYB93-2 in *Arabidopsis* did not affect primary root length (Figure 3.7B). The lateral root assay was then applied, and we found that the LR density was significantly decreased in both *Sl*MYB93s overexpressing lines comparing to Col-0, in each case in two out of the three independent lines (Figure 3.6C and Figure 3.7C), which showed their similar function on lateral root development with *At*MYB93.

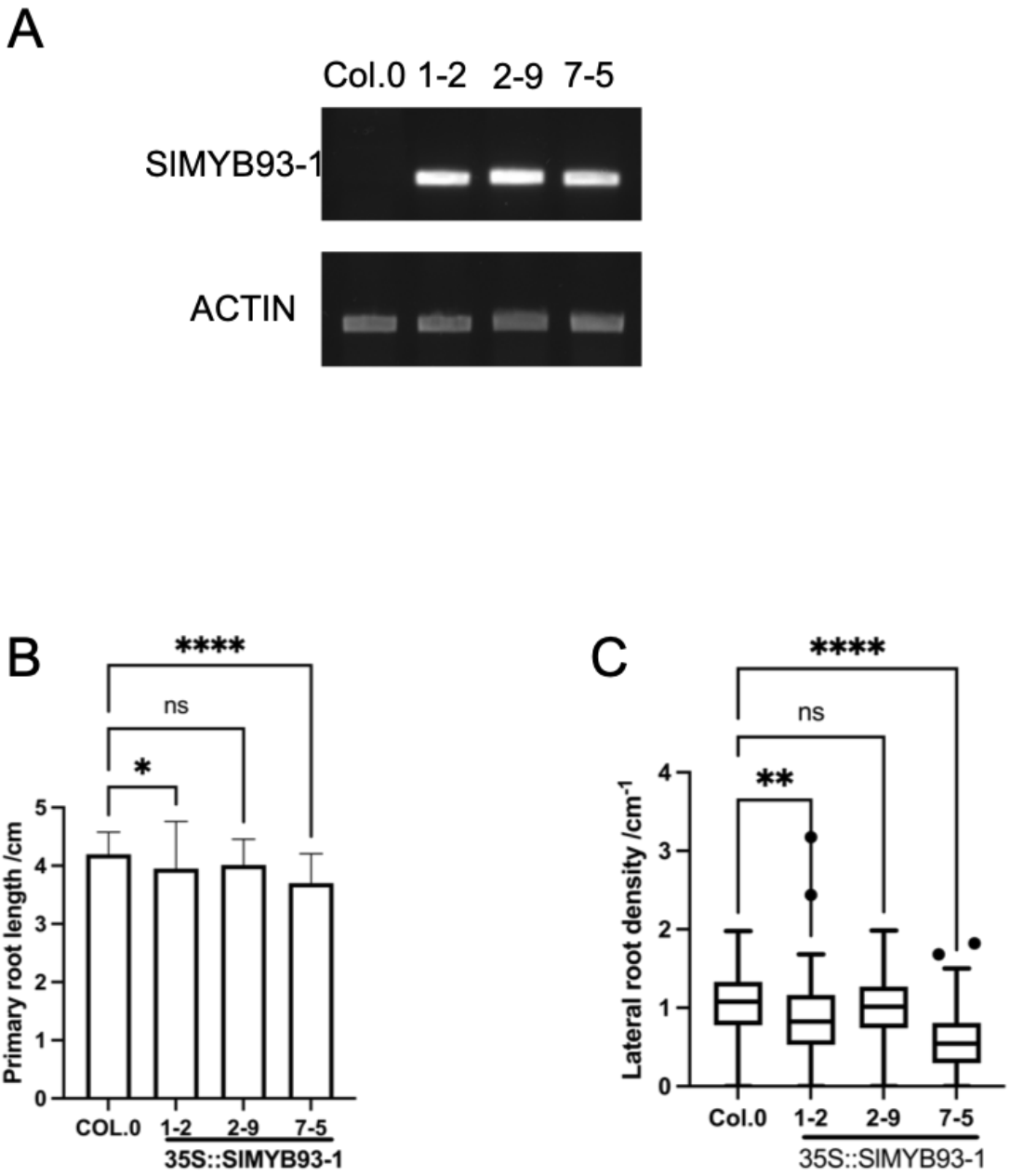

Figure 3.6 Heterologous expression of *Sl*MYB93-1 in *Arabidopsis.*

(A) Expression of *SlMYB93-1* in *Arabidopsis* detected by RT-PCR. RNA extracted from *Arabidopsis* whole seedlings was used as templates for RT PCR. *SlMYB93-1* was detected in all three lines. (B) Primary root length is significantly decreased in two out of three *Sl*MYB93-1 overexpressing lines (n>120). (B) Emerged lateral root (LR) densities in 8-day-old seedlings of wild type and *Sl*MYB93-1 overexpressing lines. Two overexpression lines showed significantly reduced lateral root density, compared to Col-0. Error bars (B), mean of standard deviation, Sidak's multiple comparisons test: *, P<0.05; **, P<0.01; ***, P<0.001; ****, P<0.0001. Whiskers (C), maximum and minimum values. Dunn's multiple comparisons test: *, P<0.05; **, P<0.01; ***, P<0.001; ****, P<0.0001.

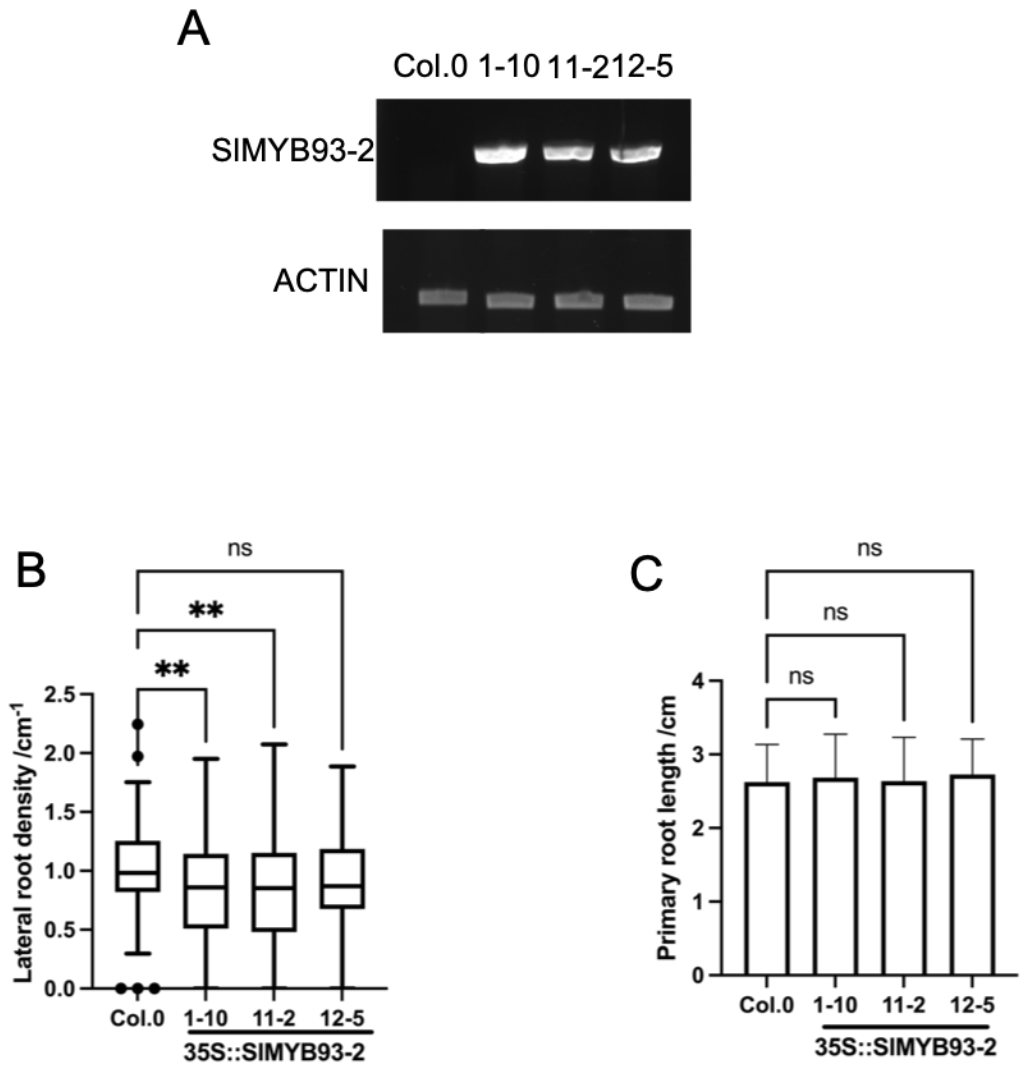

Figure 3.7 Heterologous expression of *Sl*MYB93-2 in *Arabidopsis.*

(A) Expression of *SlMYB93-2* in *Arabidopsis* detected by RT-PCR. RNA extracted from *Arabidopsis* whole seedlings was used as a template for RT PCR. *SlMYB93-2* was detected in all three lines. (B) primary root length is significantly decreased in *Sl*MYB93-2 overexpressing lines (n>120). (B) Emerged lateral root (LR) densities in 8-day-old seedlings of wild type and *Sl*MYB93-2 overexpressing lines. Two out of three overexpression lines showed significantly reduced lateral root density, compared to Col-0. Error bars (B), mean of standard deviation, Sidak's multiple comparisons test: *, P<0.05; **, P<0.01; ***, P<0.001; ****, P<0.0001. Whiskers (C), maximum and minimum values. Dunn's multiple comparisons test: *, P<0.05 ; **, P<0.01; ***, P<0.001; ****, P<0.0001.

3.8.2 Generation of tomato *Sl*MYB93s overexpression and RNAi lines.

To study the function of *Sl*MYB93s in tomato, both *Sl*MYB93s were overexpressed or silenced in *Solanum lycopersicum cv. Micro-Tom* by *Agrobacterium tumefaciens* mediated transformation using tissue culture method (Section 2.7.3). The seeds from the first generation of transformation were sowed in soil and seedlings were genotyped with primers annealing to the kanamycin resistance gene (*NPTII*) as an indicator of the presence of T-DNA insertions. Three independent homozygous overexpressing lines of both *Sl*MYB93s were identified after several rounds of screening, and three independent homozygous RNAi lines of only *Sl*MYB93-1 were acquired from tomato tissue culture (Figure 3.8A). The expression of *SlMYB93*s in those homozygous lines were confirmed by RT PCR using gene-specific primers and RNA extracted from tomato roots. Both *SlMYB93-1* and *SlMYB93-2* were highly expressed in roots of these overexpressing lines compared to the wild type. The expression level of *SlMYB93-1* was decreased in the RNAi lines (Figure 3.8B). Those transgenic tomato lines will be used for appropriate lateral root assay to study if SlMYB93s have similar phenotype on lateral root development in tomato. Previous study recognised apple MYB93 orthologue (MDP0000320772, MdMYB93) as a positive regulator of suberin deposition in apple fruit skin, which indicated that SlMYB93s may play a role in suberin deposition in tomato fruit skin. Thus, the composition and structure of those transgenic tomato fruit skin will be analysed to further study the function of SlMYB93s in suberin deposition.

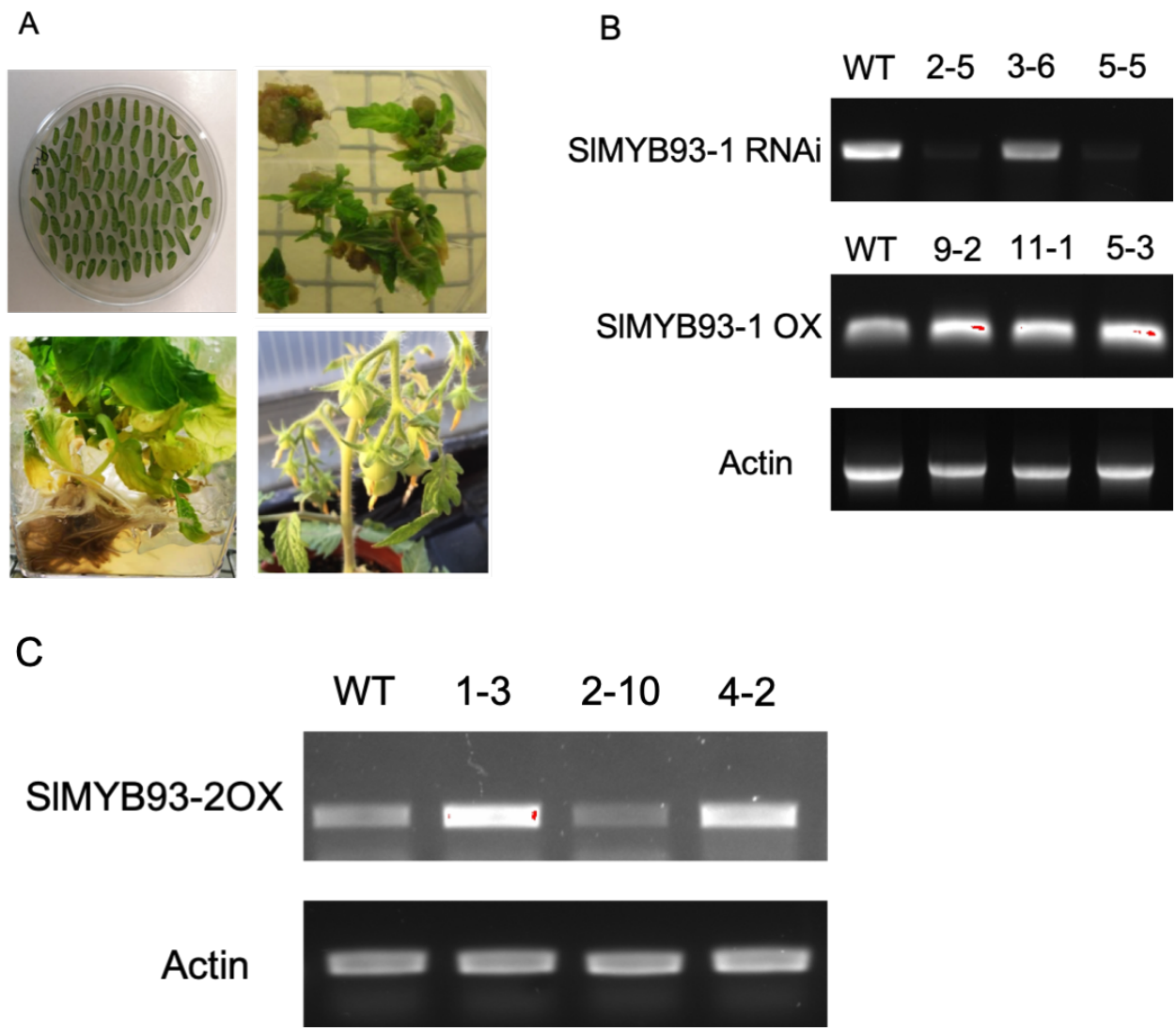

Figure 3.8 Acquisition of overexpressing and RNAi lines in tomato by tissue culture.
(A) *Agrobacterium*-mediated transformation of tomato by tissue culture. Cotyledons were immersed in *Agrobacterium tumefaciens* containing constructs of interest. Callus was grown from cotyledons and differentiated into plants, which were then induced to grow roots and transferred to soil. (B) Testing for expression of *SlMYB93-1* in transgenic tomatoes by RT-PCR. RNA extracted from tomato root was used as a template for RT PCR. RNAi lines showed decreased expression of SlMYB93-1, while overexpression lines showed increased expression of SlMYB93-1 compared to that in wild type. (C) Testing for overexpression of *Sl*MYB93-2 in tomatoes overexpressing lines by RT-PCR. RNA extracted from tomato root was used as a template for RT PCR. Overexpression lines showed increased expression of SlMYB93-2 comparing to that in wild type, except for *Sl*MYB93-2OX line 2-10. OX, overexpression. Actin Ⅱ, a globally expressed housekeeping gene in tomato, used as a loading control.

3.9 Hairy root transformation of tomato

3.9.1 Cloning for *Sl*MYB93 CRISPR constructs

Agrobacterium rhizogenes was identified as being able to transform plant genomes and induce the production of hairy roots upon wounding in both monocot and eudicot plants. (Lima et al., 2009). *A. rhizogenes* has been widely used in different species to rapidly study gene localisation, expression and function. It was also reported that this method can be used to obtain CRISPR-mediated mutation hairy root tissues in tomato (Ron et al., 2014). In order to obtain CRISPR-mediated mutation of tomato hairy root tissues for both *SlMYB93*s, the CRISPR/Cas9 system being used in Siobhan Brady's lab was applied to clone *SlMYB93* CRISPR constructs, which were then introduced into *A. rhizogenes* to generate transgenic roots.

Three sgRNAs of each SlMYB93s were selected in CRISPR-P V2 (http://crispr.hzau.edu.cn/cgi-bin/CRISPR2/CRISPR) based on the sequences of target genes (see Section 2.8.8). sgRNAs oligos and their reverse complementary oligos were synthesised and annealed. Double strand sgRNA oligos were cloned into expression vectors separately to obtain an *AtU6-1* promoter, which was then assembled to the vector pMR278 by Golden Gate Assembly (Section 2.8.8.3) A fragment containing three sgRNAs from pMR278 was introduced into plant binary vector pMR286 for CRISPR/Cas9 system by Gateway cloning. The final vector pMR286 with sgRNAs were sequences and then introduced in *Agrobacterium rhizogenes.*

3.9.2 Acquisition of *SlMYB93-1* and *SlMYB93-2* CRISPR hairy root lines

As it was described in Section 2.7.5, the hairy root transformation shared similar method to tomato tissue culture transformation with regards to seed germination and cotyledon acquisition. Cotyledons were then immersed in *Agrobacterium rhizogenes* solution with constructs of interest, which infected plant cells and induced root growth from cotyledons.

Roots grew from cotyledons were collected and selected separately on the media with appropriate antibiotic (Figure 3.9).

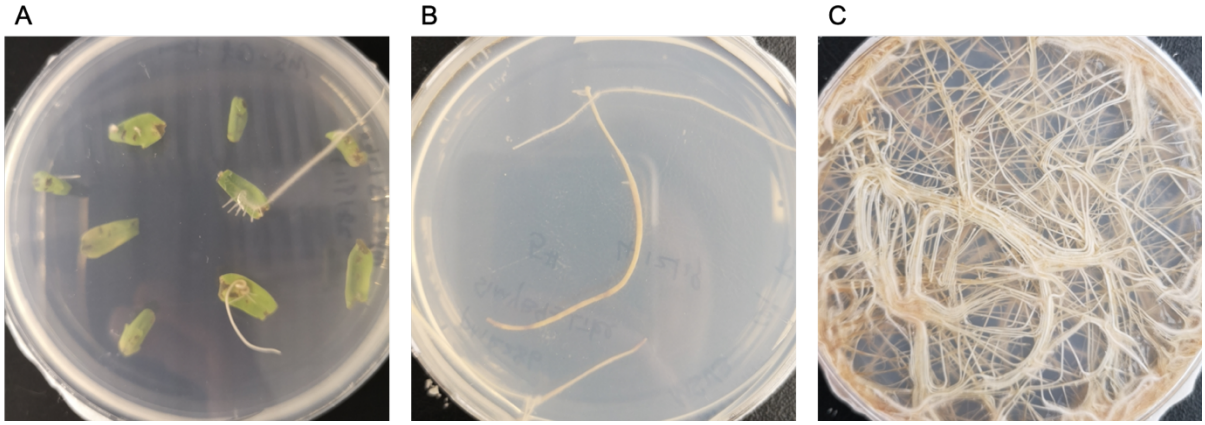

Figure 3.9 Process of hairy root transformation.
(A) Hairy roots emerged from cotyledons. Cotyledons were cultured in co-culture media after infected with *Agrobacterium rhizogenes* containing *SlMYB93*s CRISPR constructs. (B) and (C) Hairy root grown on selection media. Each root from the cotyledons was transferred and grown in selection media separately, which represented an independent transformation event.

DNA samples of selected root tissues were extracted and were then used as templates to amplify the target genes to look for CRISPR events. PCR products were purified and sequenced with the internal primers of target genes (Appendix. 3). According to the sequencing results, a 7bp-deletion was found in the target region of sgRNA in one *SlMYB93-1* CRISPR hairy root line, which shared the same result with two other independent lines (Figure 3.10 A and B). However, in an *SlMYB93-2* CRISPR hairy root line, a 279bp deletion with both sgRNA-2 and sgRNA-3 was found after alignment sequencing result with reference genome (Figure 3.11 A and B). Based on the sequencing results, the expression of *SlMYB93-1* and *SlMYB93-2* in their hairy root CRISPR lines was analysed by RT PCR. With the mutations in *SlMYB93-1* and *SlMYB93-2*, no expression of either *SlMYB93* was detected (Figure 3.10C and Figure 3.11C).

Taken together, by using hairy root transformation, CRISPR lines of *SlMYB93-1* and *SlMYB93-2* were generated and the mutations of these *SlMYB93*s in hairy root tissues was confirmed. And The cross-section and suberin dyeing will be applied to those SlMYB93s CRISPR hairy root lines to study the potential function of SlMYB93s on suberin deposition in tomato roots.

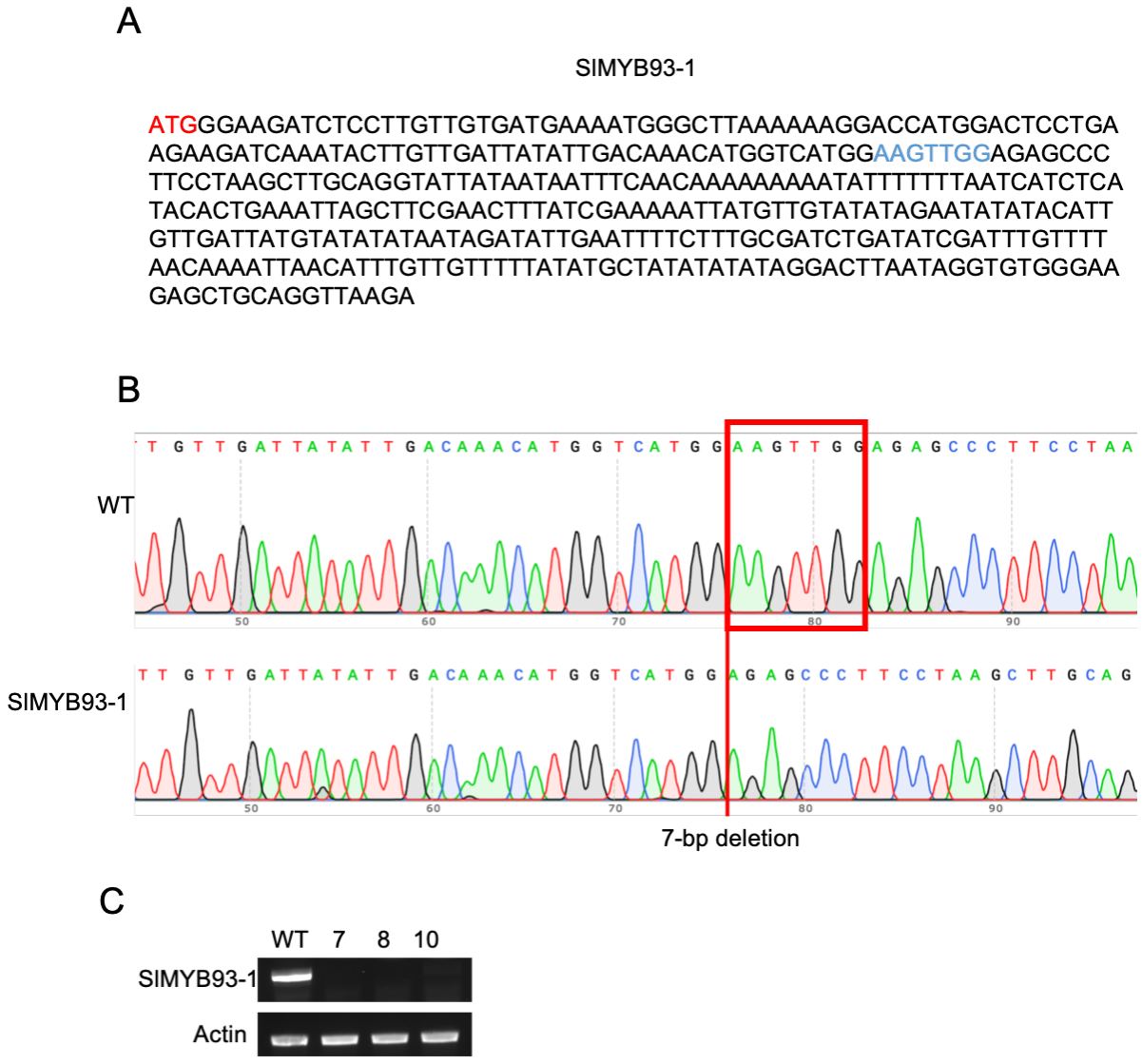

Figure 3.10 Analysis of CRISPR-mediated mutation of *SlMYB93-1* in tomato by hairy root transformation.

(A) Genomic DNA sequence of *SlMYB93-1*. The genomic DNA sequence of SlMYB93-1 (nucleotides 1-379) is shown. The expected deletion region was highlighted in blue. (B) Sequencing of PCR products of *SlMYB93-1* from a CRISPR line showed the expected 7bp deletion in *SlMYB93-1*, comparing to the wild type sequence. (C) testing for expression of *SlMYB93-1* in CRISPR lines by RT-PCR. RNA extracted from tomato hairy root tissues was used as templates for RT-PCR. All three CRISPR lines showed no expression of *SlMYB93-1*. Actin Ⅱ, a globally expressed housekeeping gene in tomato, was used as a loading control.

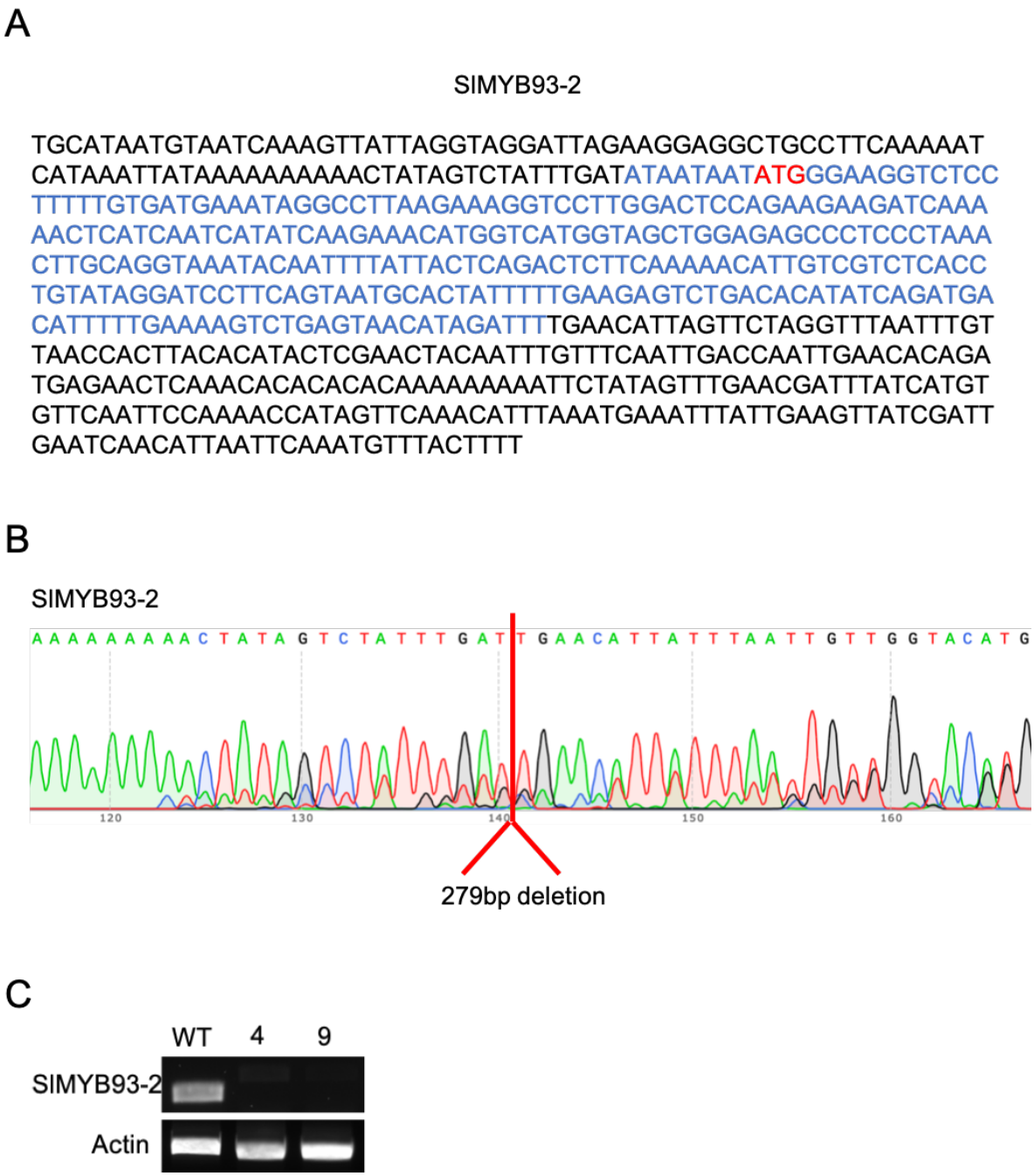

Figure 3.11 Analysis of CRISPR-mediated mutation of *SlMYB93-2* in tomato by hairy root transformation.

(A) Genomic DNA sequence of *SlMYB93-2*. 600 bp genomic DNA sequence of SlMYB93-1 (-100 to 500) was shown. The start codon of SlMYB93-2 was highlighted in red and the deletion region was highlighted in blue. (B) sequencing of PCR products of *SlMYB93-2* from CRISPR line showed a 279bp deletion in *SlMYB93-2*, compared to the wild type sequence. (C) testing for expression of *SlMYB93-2* CRISPR lines by RT-PCR. RNA extracted from tomato hairy root tissues was used as a template for RT-PCR. All three CRISPR lines showed no expression of *SlMYB93-2*. Actin Ⅱ, a globally expressed housekeeping gene in tomato, used as a loading control.

3.10 Discussion

3.10.1 Expression pattern of *SlMYB93*s

Previous expression data of R2R3 MYB genes only found that *Solyc04g056310.2.1* was highly expressed in root comparing to expression in other tissues, while no significant change among different tissues was found in *Solyc05g051550.1.1* and *SlMYB93* (Li *et al*., 2014), which is different from result in this thesis, in which *SlMYB93-1* (*SlMYB93*), *SlMYB93-2* (*Solyc04g056310.2.1*) and *SlMYB93-3* (*Solyc05g051550.1.1*) are highly expressed in root and *SlMYB93-1* is also found in early stage of fruit. This difference may be that Li *et al*., (2014) normalised relative expression level of each gene with the mean value of the gene expression in all tissues, which may exhibit no difference in some low expressed genes, such as *SlMYB44*, *SlMYB93-1* (*SlMYB93*), *SlMYB93-3* (*Solyc05g051550.1.1*) and *SlMYB100*. This hypothesis also matches with the expression data from TOMEXPRESS (http://tomexpress.toulouse.inra.fr), in which all three SlMYB93s mainly expresses in root and *SlMYB93-1* (*SlMYB93*), *SlMYB93-3* (*Solyc05g051550.1.1*) were also detected in early stage of fruit (Figure 3.3 B and D) (Zouine *et al*., 2017).

3.10.2 *SlMYB93-1* and *SlMYB93-2* overexpressing phenotype in *Arabidopsis*

To study the function of *SlMYB93-1* and *SlMYB93-2*, these two genes were overexpressed in *Arabidopsis* and three independent homozygous lines were generated for each gene. A double-blind lateral root assay was performed on these transgenic *Arabidopsis*. As it is shown in Figure3.6 and Figure3.7, overexpression of *SlMYB93-1* and *SlMYB93-2* significantly inhibited lateral root development in two out of three lines for each gene in *Arabidopsis*.

For lateral root assays of each gene, three independent experiments were conducted. Due to the potential variation of the conditions in each experiment, the lateral root phenotype of

these *SlMYB93-1* and *SlMYB93-2* overexpression lines slightly changed between biological replicates. For example, *SlMYB93-1* overexpression line 2-9 showed significantly decreased lateral root density in first and third repeat of experiment, while no significance was found in the second repeat (data not shown). Thus, to normalise the variation, data from all three biological replicate experiments were analysed and plotted together, which exhibited similar trends with each repeat, displaying decreased lateral root density in overexpression lines.

3.10.3 Large deletion in hairy root CRISPR lines

To generate hairy root CRISPR lines of *SlMYB93-1* and *SlMYB93-2*, three sgRNAs were selected and applied to guide Cas9 nuclease to the target DNA sequences to be edited. Normally, Cas9 nuclease deletes several nucleotides close to a protospacer-associated motif (PAM) NGG. Ron et al., (2014) established that Cas9-induced mutants of SHOOT ROOT (*SHR*) exhibited 1-, 2- and 7bp-deletions, respectively. In this thesis, a *SlMYB93-1* CRISPR line has been demonstrated to have a 7bp-deletion in its target region, leading to mutation of *SlMYB93-1*. A *SlMYB93-2* CRISPR line showed a large deletion in the target region, which also exhibited no expression of *SlMYB93-2* in hairy roots. Previous studies reported that large deletions were frequently generated in the CRISPR-Cas9 system in other organisms such as mouse and mammalian cells (Adikusuma *et al*., 2018; Kosicki *et al*., 2018), similar to the large deletion that occurred in this thesis. In order to confirm the function of *SlMYB93*s in hairy roots, more independent lines were generated. Another two independent lines of *SlMYB93-1* exhibited deletions in target regions with 4bp and 5bp-deletions (data not shown). In contrast, another independent line of *SlMYB93-2* still had a large deletion of 146bp in the similar region of the first line, which may be caused by choice of sgRNAs (data not shown).

3.11 Conclusion

The bioinformatic analysis and expression pattern reported at the beginning of this chapter demonstrated that the protein sequences of *Sl*MYB93-1, *Sl*MYB93-2, *Sl*MYB93-3 are highly similar to *At*MYB93 and all three *SlMYB93*s are highly expressed in roots, which indicated that they are orthologues of *AtMYB93* in tomato. Further studies showed the nuclear-localisation of *Sl*MYB93-1 and *Sl*MYB93-2 proteins as transcriptional factors, and overexpression of these two *Sl*MYB93s inhibited lateral root development in *Arabidopsis*. Hairy root CRISPR mutants and overexpression tomato lines of *SlMYB93-1* and *SlMYB93-2*, together with the RNAi lines of *SlMYB93-1* were generated and sulphur content in overexpression and RNAi lines of SlMYB93-1 were measured and analysed in Chapter 5. To study the function of these two *Sl*MYB93s in tomato in the next phase of this project, the RSA of overexpression and RNAi tomato lines of SlMYB93s will be analysed to confirm their function on lateral root development in tomato. In addition, composition analysis and suberin dyeing of transgenic (fruit skin and root) and CRISPR (hairy root) tomato lines will be conducted and analysed to study function of SlMYB93s on suberin deposition in tomato.

Chapter Ⅳ: Transcriptome analysis of the *Atmyb93* mutant

4.1 Introduction

RNA sequencing (RNAseq) is a whole transcriptome profiling method used in studies of biological mechanisms and functions (Wang *et al*., 2009). In the last decade, the cost of RNA sequencing has decreased dramatically because of advances in technology. RNA sequencing technology has been widely used in flowering plants for a variety of analyses, such as, the effects of mutations, the responses of abiotic and biotic stresses, the mechanism of chemical biosynthesis and interactions between plants and pathogens (Zhang *et al*., 2020; Song *et al*., 2020; van Weringh *et al*., 2021).

Previous studies reported that *At*MYB93, a R2R3 MYB transcription factor, expresses specifically in several endodermal cells overlapping LRPs, was identified as a negative regulator of lateral root development in *Arabidopsis* (Gibbs *et al*. 2014). One hypothesis is that *At*MYB93 may transcriptionally control expression of its downstream genes by binding to their promoters, which in turn may directly or indirectly control lateral root development. To investigate the function and potential downstream target genes of *At*MYB93, the transcriptome of the *Atmyb93* mutant and endodermis specific AtMYB93 overexpression driven by CASP1 (CASPARIAN STRIP 1) promoter were compared to wild type by using high throughput RNAseq and downstream analysis. However, transcriptome data of CASP1:: AtMYB93 lines showed no significant difference comparing to wild type, so it was not further analysed in this Chapter

This chapter describes the identification and analysis of genes that are differentially expressed between *Atmyb93* mutant and wild type Arabidopsis roots via RNA sequencing. 255 differentially expressed genes were identified and used for further GO term, KEGG pathway and network analysis to find the relevant biological processes or pathways these genes may be involved in (Kanehisa *et al*., 2007; Sherman *et al*., 2009). Another comparison

analysis between the 245 identified genes and genes upregulated at the same time as *AtMYB93* during lateral root initiation (Voss *et al*., 2015) was conducted and identified 14 genes that may be potential transcriptional targets of *At*MYB93.

4.2 RNA preparation and quality control

Whole roots of 7-day old Col-0 and *Atmyb93* mutant seedlings were harvested for RNA extraction (section 2.5.3) and the experiment was performed three times independently. The concentration and purity of the RNA samples were then measured by using a Nanodrop analyser as ~2µg RNA with an OD260/280 of ~2.0 was required for RNAseq: the results are shown in Table 4.1. To test RNA degradation and contamination, RNA samples were run on a 1% agarose gel and all RNA samples showed two clear bands (28S rRNA and 18S rRNA), which indicated qualification of the RNA samples (Fig. 4.1). RNA samples were sent to Novogene for quality control testing and sequencing. RNA samples were qualified for sequencing after the sample integrity was tested by using Agilent 2100 analysis by Novogene.

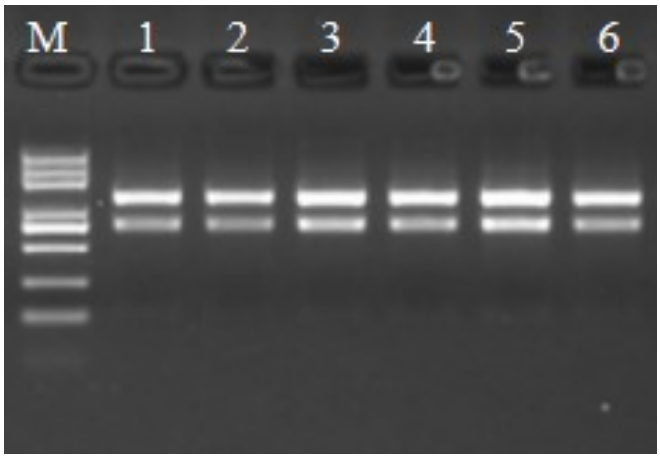

Figure 4.1 Quality control of samples for RNAseq using RNA gel electrophoresis.
~0.15 µg per lane of different RNA samples were run on a 1% agarose gel for 16 min at 180V. DNA ladder (M), Col-0 RNA samples (1-3), *Atmyb93* mutant RNA samples (4-6).

Sample name	Conc. (ng/μl)	Amount(μg)	OD260/280	OD260/230
Col-0-1	122	1.952	1.91	1.97
Col-0-2	258	3.612	2.15	2.3
Col-0-3	204	3.468	2.08	2.27
myb93-1	100	1.4	2.00	2.27
myb93-2	182	2.548	2.12	2.6
myb93-3	170	2.72	2.18	2.58

Table 4.1 Quality control summary of RNA samples.
Data from Nanodrop of all RNA samples were listed, including concentration, total amount and RNA purity indicators (Ratio of OD260/280 and OD260/230).

4.3 Library preparation and sequencing

RNA samples were then processed at Novogene via the workflow shown (Fig.4.2A). mRNA from the samples was enriched by using beads coupled with oligo(dT) and fragmented with fragmentation buffer containing 0.1mM RNA cleavage $ZnCl_2$. mRNA fragments were then used to synthesise cDNA using random hexamers and reverse transcriptase, followed by second-strand cDNA synthesis using RNase H, dNTPs and Escherichia coli polymerase I. The cDNA library was ready for sequencing after a round of end repair, A-tailing, adaptor ligation, size selection and PCR amplification. The cDNA library concentration and insert size was checked before it was loaded onto an Illumina machine for sequencing. The workflow chart was shown in Fig.4.2B

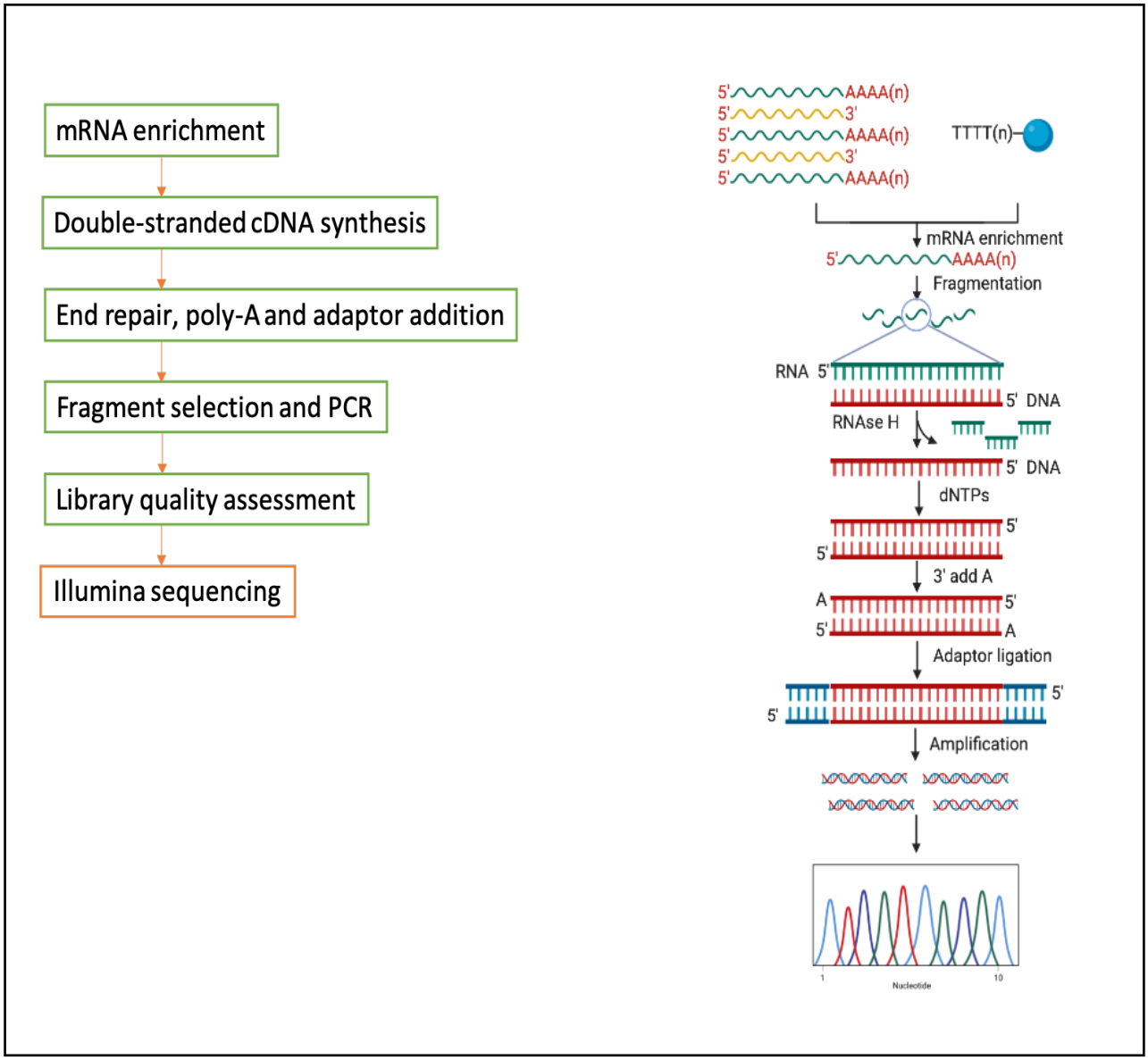

Figure 4.2 Workflow of library preparation and sequencing.
mRNAs were first enriched with beads and fragmented, to then use as templates for double-stranded cDNA synthesis. cDNAs were assembled with adaptors after a round of end repair and poly-A addition. The cDNA library was applied for sequencing after size selection and amplification. workflow was plotted in Biorender

4.4 Analysis of differentially expressed genes.

The original raw data from Illumina sequencing were first analysed by Novogene to extract differentially expressed genes (DEG). The DEGs were further analysed by GO, KEGG and comparing with other databases to screen downstream targets of *At*MYB93. The analysis workflow chart is as follow (Fig.4.3):

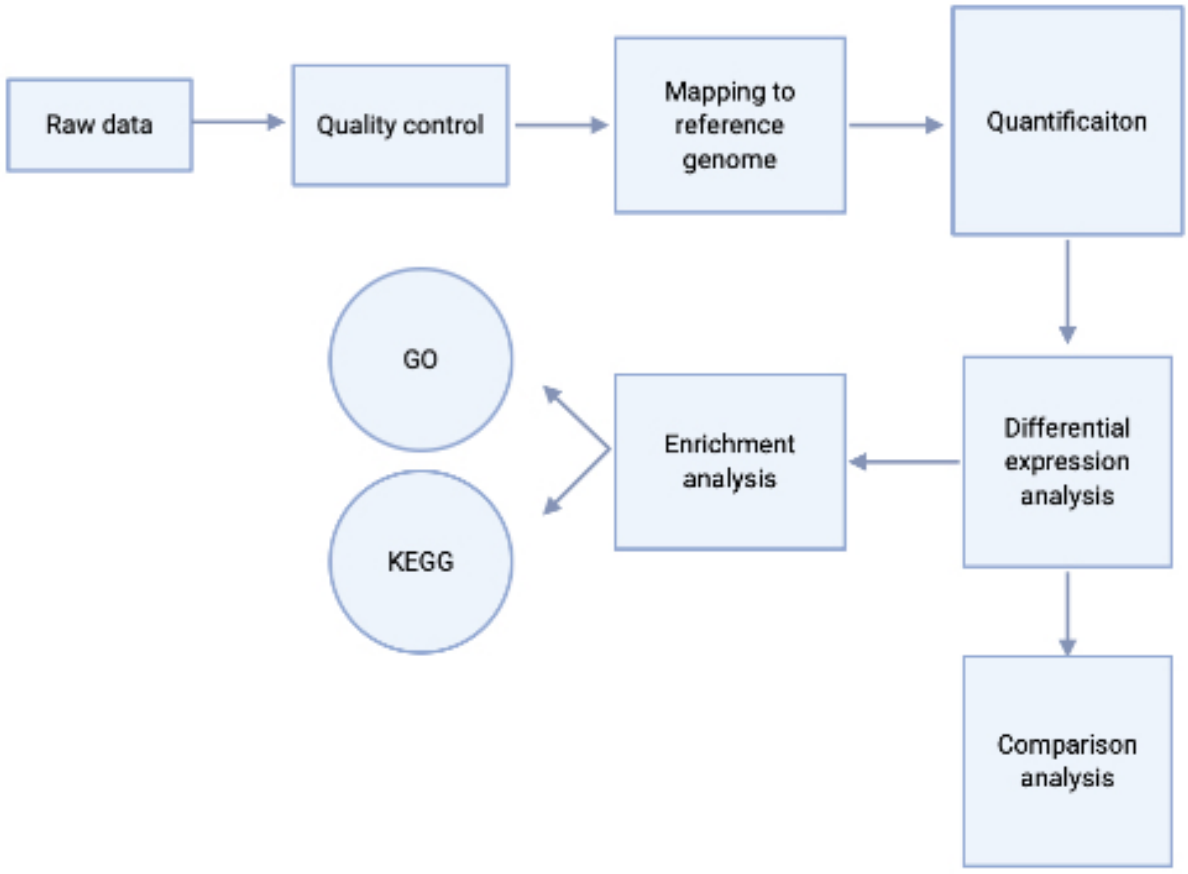

Figure 4.3 Workflow of RNAseq data analysis.
Quality of the sequencing raw data was checked before the raw data was annotated based on the *Arabidopsis thaliana* reference genome. Transcript abundance was then quantified, which were used for differential expression analysis. The differentially expressed genes (DEGs) were further analysed using enrichment and comparison methods.

4.4.1 Quality Control

The raw data were transformed to sequenced reads by base calling, which exported data in FASTQ format. This included sequence information and sequencing quality information. Phred scores in FASTQ format were used to estimate the error rate of sequenced reads for quality control. The expected base quality score is often between 30 to 40, which results in an error rate of 0.001 to 0.0001 (Sheng et al., 2017). All samples in this RNAseq experiment were considered high quality with an error rate of 0.0004 (Table 4.2). The GC content of sequenced reads was also used as an indicator of contamination. The average of GC content of coding DNA sequences was reported to be 44.9% in *Arabidopsis thaliana* (DeRose-Wilson et al., 2007), so raw reads were qualified and cleaned by removing reads with adapters and reads of low quality (Table 4.2). The filtered data were then ready for further analysis.

4.4.2 Mapping to reference genome

The clean FASTQ data was aligned to reference genome with HISAT2 (hierarchical indexing for spiced alignment for transcripts 2), which is an accurate and sensitive alignment software for both DNA and RNA sequences (Kim et al., 2019). Sequenced reads were firstly mapped to a large global Ferragina Manzini (gFM) index representing the whole reference genome and then to thousands of small indexes covering the whole reference genome. Repeat mapped reads were then aligned with the local repeat sequences rather than with corresponding locations of genome, which ensures the efficiency and accuracy of HISAT2 (Kim et al., 2019). The overview of mapping status was shown in Table 4.3. Over 98% of mapped region for each sample was classified as exons, and less than 2% of mapped sequences were from either introns or intergenic regions (Figure 4.4).

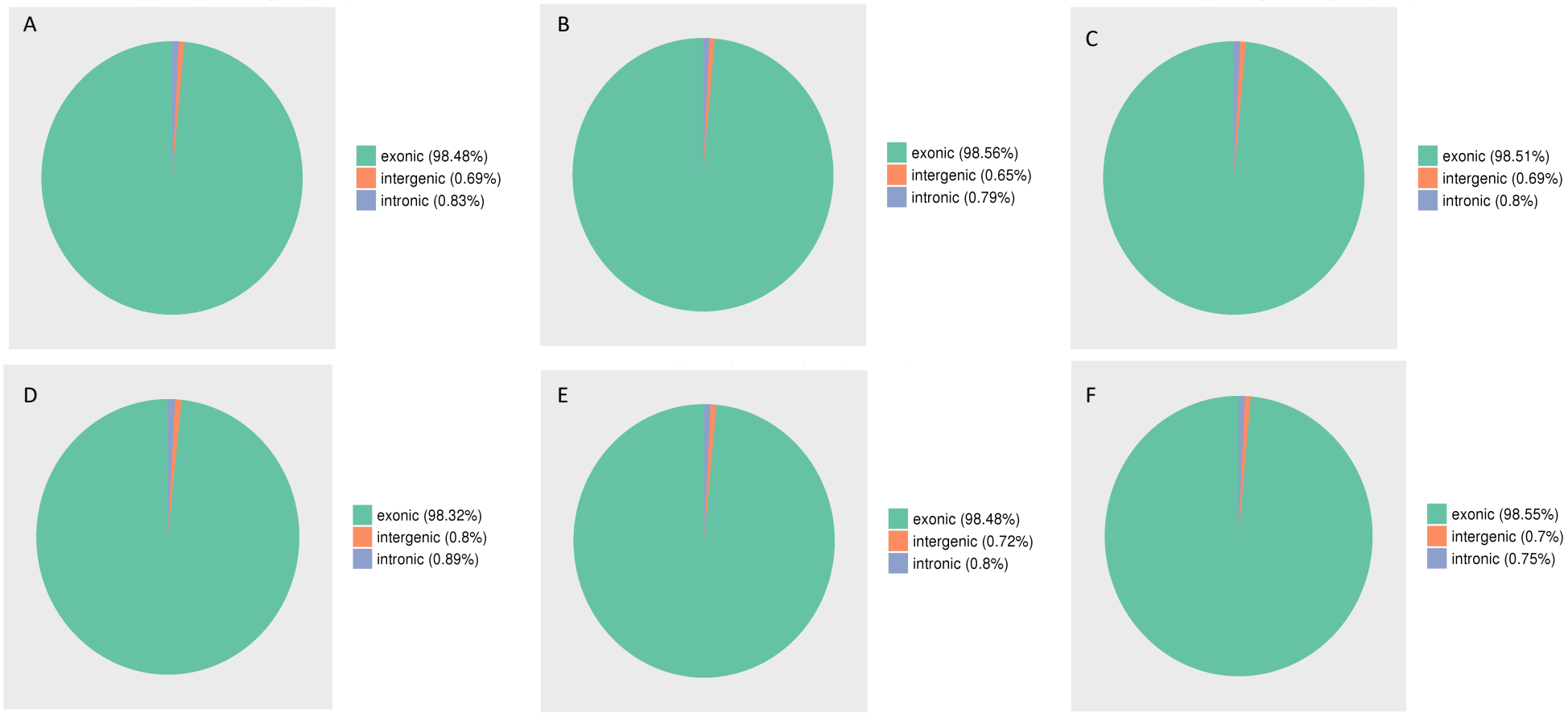

Figure 4.4 Percent of reads mapped to genome regions.
raw reads were mapped to reference genome, which were classified into three categories, exon-mapped reads (green), intron-mapped reads (red) and intergenic regions (blue).

4.5 Quantification and differential expression analysis

Clean mapped fragments that represented transcript abundance were used to estimate gene expression level. In order to compare expression of different genes between wild type (Col-0) and the *Atmyb93* mutant, the FPKM (fragments per kilobase of transcript sequence per million fragments paired sequenced) value was used. FPKM is commonly used for paired-end RNAseq, which normalises the effect of sequencing depth and gene length (Guttman et al., 2010). The analysis of gene expression level was performed in HTSeq software with the union mode, which presented the number of genes with different expression level and FPKM values of different genes (Anders et al., 2015). A total of 18241 genes were annotated in this study. By using the Pearson's correlation analysis with the normalised FPKM data, the correlation coefficient value was calculated to estimate both similarity between samples and reliability of the experiments. In general, samples with the Pearson correlation coefficient value over 0.9 were required for biological repeats. A heat map was plotted to provide an overview of the variation between samples and the biological repeat samples were then clustered together by using Pearson correlation coefficient value (Figure 4.5). All the Col-0 samples clustered together and all the *Atmyb93* samples clustered together. Thus, the experiment was estimated to be repeatable and expression data between samples were different.

In order to identify differentially expressed genes (DEGs), DEseq2 software was used with DEseq normalisation method. A total of 255 genes were identified after a threshold of false discovery rate (FDR)$\leq$ 0.05 was used as standard to screen for the DEGs. A volcano plot (Fig.4.6) and hierarchical clustering (Fig.4.7) were constructed using normalised FPKM values to provide a global view of those DEGs. Apart from *AtMYB93*, the most downregulated gene in the *Atmyb93* mutant compared to wild-type was *Trichome birefringence-like 4* (*TBL4*, -2.6-fold), a bridging protein that was predicted to involve in stabilisation of cell wall polymers by

O-acetylation. And the most upregulated gene was At3g18535 encoding a tubulin-tyrosin ligase.

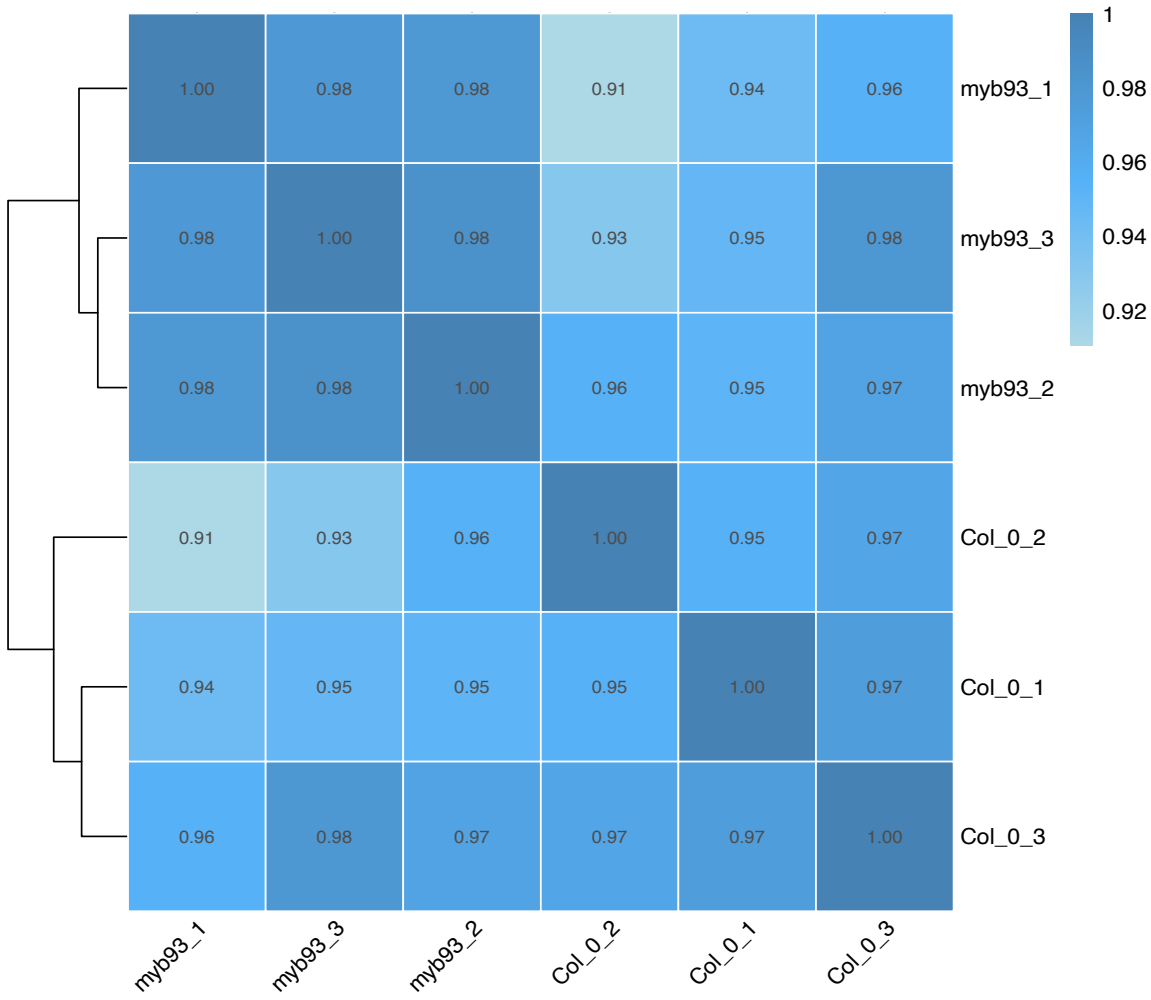

Figure 4.5 variability assessing of RNAseq samples.
Pearson's correlation heatmap was plot to estimate the similarity between samples. The correlation coefficient values (r) were calculated with the normalised FPKM values. Scale bar represents the range of correlation coefficients (r) displayed.

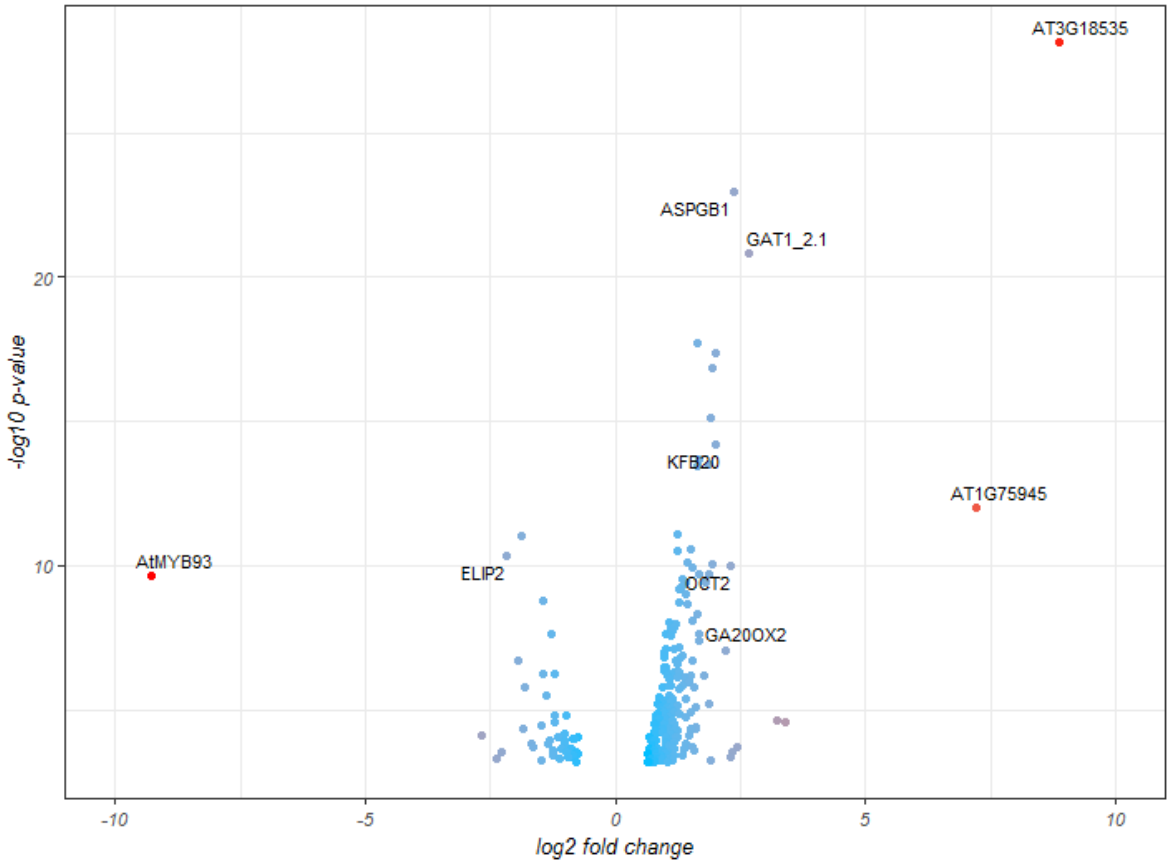

Figure 4.6 Volcano plot showing significantly DEGs between Col-0 and *the Atmyb93* mutant. Dots on the left side of log2 fold change =0 indicated downregulated genes and dots on the right side of log2 fold change=0 indicated upregulated genes. Red dots, highly differential expressed genes, blue dots, moderately differential expressed genes. As it shown above, the most downregulated gene is AtMYB93 and the most upregulated gene is At3g18535.

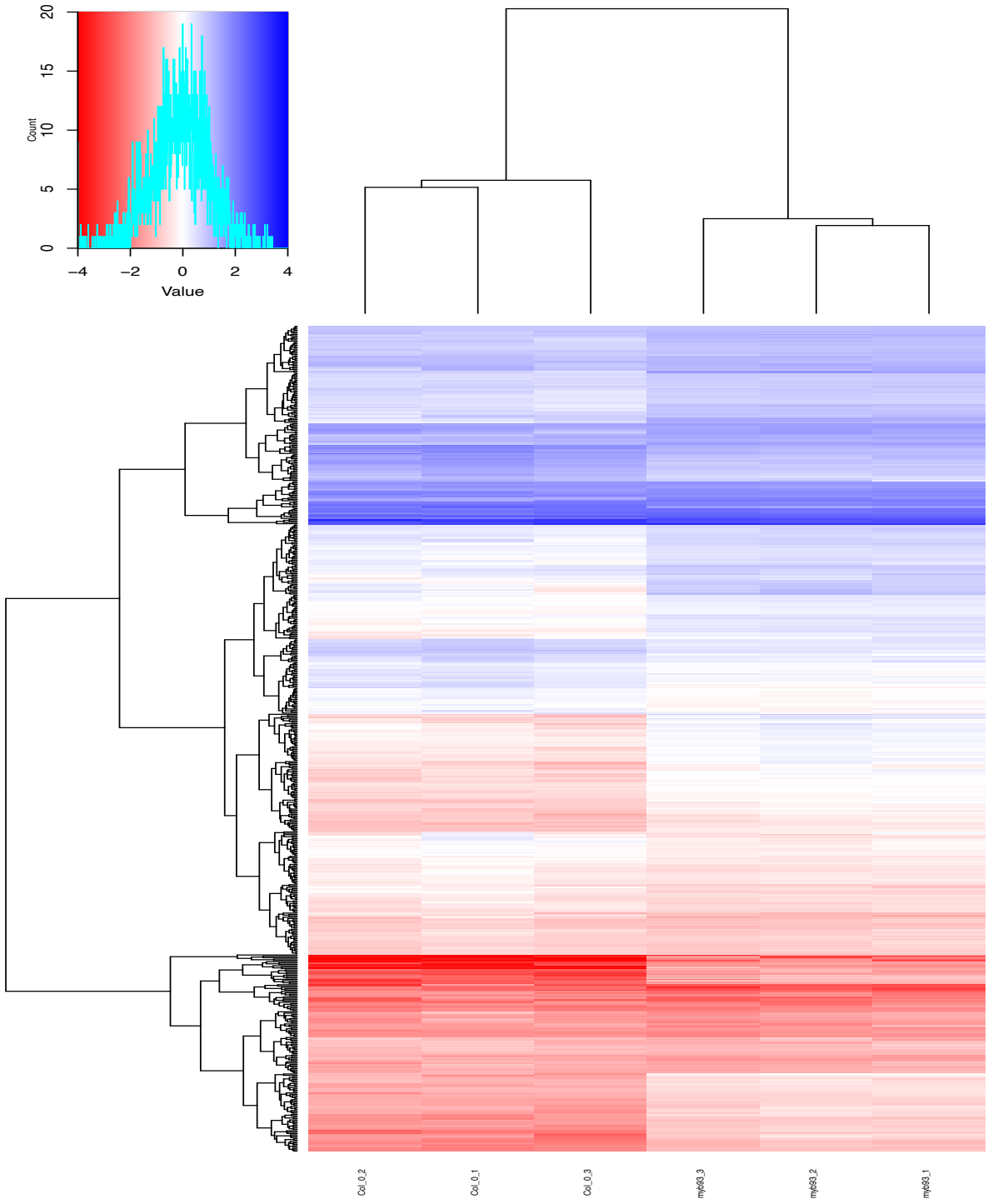

Figure 4.7 Global changes of DEGs between Col-0 and the *Atmyb93* mutant.
Hierarchical clustering of DEGs was generated between Col-0 and the *Atmyb93* mutant based on normalised FPKM values. Genes with different expression levels were labeled from red (high expression level) to blue (low expression level). The phylogenetic relationship among different genes were shown on the lefthand tree based on genes expression profile. The cluster relationship between samples was shown on the top tree.

4.6 Differentially expressed genes in the *Atmyb93* mutant root

As outlined previously, a total of 255 differentially expressed genes (DEGs) were identified in the *Atmyb93* mutant when compared to wild-type, using a threshold of false discovery rate (FDR)≤ 0.05 (Figure 4.7). Among the DEGs, a big group of genes were classified to relate or involve in sugar metabolism from GO term analysis and most of them are upregulated in Atmyb93 mutant. *SUGAR TRANSPORT PROTEINS* (*STP*) genes, *STP14*, *STP1*, *STP4* were highly enriched in the *Atmyb93* mutant. Another sugar transporters AtSWEET2, POLYOL/MONOSACCHARIDE TRANSPORTER 6 (PMT6) and TONOPLAST MONOSACCHARIDE TRANSPORTER1 (TMT1) are upregulated in Atmyb93 mutant.

Trehalose , a sugar consists of two glucose functions as a regulator of signalling pathway and sugar homeostasis in plants (Fichtner et al., 2021). Trehalose metabolism genes were also differentially expressed in *Atmyb93* mutant. *TREHALOSE-6-PHOSPHATE SYNTHASE* (*TPS*), *TPS8*, *TPS9*, *TPS10* and *TPS11* were highly upregulated and *TREHALOSE-6-PHOSPHATE PHOSPHATASE I* (*TPPI*) was strongly down-regulated in *Atmyb93* mutant (Table 4.2). Additional genes in Table 4.5 are either related to sugar indirectly or responsive to sugar stress.

Accession #	Gene name	Log_2foldchange	Details
AT1G77210	SUGAR TRANSPORT PROTEIN 14 (STP14)	2.338	Galactose transport
AT5G20250	DARK INDUCIBLE 10 (DIN10)	1.949	Response to light stimulus, response to oxidative stress
AT5G22920	RING ZINC-FINGER PROTEIN 34 (RZPF34)	1.909	Regulation of stomatal opening, ubiquitin protein ligase activity
AT3G48360	BTB AND TAZ DOMAIN PROTEIN 2 (BT2)	1.867	Involved in TAC1-mediated telomerase activation pathway
AT1G11260	SUGAR TRANSPORT PROTEIN 1 (STP1)	1.653	Glucose import
AT2G18700	TREHALOSE-6-PHOSPHATE SYNTHASE 11 (TPS11)	1.545	Trehalose biosynthesis
AT1G70290	TREHALOSE-6-PHOSPHATE SYNTHASE 8 (TPS8)	1.529	Trehalose biosynthesis
AT2G25900	TANDEM ZINC FINGER 1 (TZF1)	1.505	Regulation of transcription
AT5G49450	BASIC LEUCINE-ZIPPER 1 (BZIP1)	1.504	Response to salt stress, response to osmotic stress, response to drought stress
AT4G36670	POLYOL/MONOSACCHARIDE TRANSPORTER 6 (PMT6)	1.351	Glucose import
AT1G80920	TRANSLOCON AT THE OUTER ENVELOPE MEMBRANE OF CHLOROPLASTS 12 (TOC12)	1.278	Response to light stimulus
AT3G14770	SWEET2	1.257	Carbohydrate transport
AT1G23870	TREHALOSE-6-PHOSPHATE SYNTHASE 9 (TPS9)	1.254	Trehalose biosynthesis
AT4G38390	ROOT HAIR SPECIFIC 17 (RHS17)	1.241	
AT5G21170	Subunit of the sucrose non-fermenting-1-related protein kinase (KINβ1)	1.214	Involved in carbon, lipid and nitrogen metabolism
AT1G67070	DARK INDUCIBLE 9 (DIN9)	1.174	Phosphomannose isomerase activity, response to light stimulus
AT1G28330	DORMANCY-ASSOCIATED PROTEIN 1 (DRM1)	1.105	Response to sugar

AT3G19930	SUGAR TRANSPORT PROTEIN 4 (STP4)	1.013	Response to wound stimulus, sugar transport
AT5G28770	BASIC LEUCINE-ZIPPER 63 (BZIP63)	1.000	Response to ABA
AT1G60140	TREHALOSE-6-PHOSPHATE SYNTHASE 10 (TPS10)	0.986	Trehalose biosynthesis
AT1G20840	TONOPLAST MONOSACCHARIDE TRANSPORTER1 (TMT1)	0.797	Glucose import
AT5G06800	myb-like HTH transcriptional regulator family protein	0.785	Regulation of transcription
AT1G75220	EARLY RESPONSE TO DEHYDRATION LIKE 6 (ERDL6)	0.726	Vacuolar glucose exporter
AT5G02270	ATP-BINDING CASSETTE I20 (ABCI20)	-0.748	Response to karrikin, ATPase activity
AT5G44110	ATP-BINDING CASSETTE I21 (ABCI21)	-0.977	Response to light stimulus, ATPase activity
AT5G10100	TREHALOSE-6-PHOSPHATE PHOSPHATASE I (TPPI)	-1.809	Trehalose biosynthesis, regulation of stomatal opening

Table 4.2 DEGs between wild-type and the *Atmyb93* mutant involved in sugar metabolism.

4.7 GO and KEGG enrichment analysis

4.7.1 GO term enrichment

The Gene Ontology (GO) term enrichment was firstly performed to interpret these DEGs. Genes were analysed under three categories of biological process (BP), cellular component (CC) and molecular function (MF) at a gene functional interpretation website—DAVID (https://david.ncifcrf.gov/home.jsp) (Sherman *et al*., 2009). All the significantly enriched terms (P<0.05) in each category were presented in Fig.4.8A.

According to this analysis, the most enriched term in by Biological Process was “trehalose metabolism in response to stress”, which included some trehalose biosynthesis related genes such as *TREHALOSE PHOSPHATE SYNTHASE 8* (*TPS8*; AT1G70290), *TPS9* (AT1G23870), *TPS10* (AT1G60140), *TPS11* (AT2G18700) and *TREHALOSE-6-PHOSPHATE PHOSPHATASE I* (*TPPI*; AT5G10100) (Aubourg *et al*., 2002). In Molecular Function, genes were concentrated in “carbohydrate transmembrane transporter activity”, which was concluded from some sugar transport related genes, *SUGAR TRANSPORT PROTEIN STP1* (At1g11260), *STP4* (AT3G19930) and *STP14* (AT1G77210) (Poschet *et al*., 2010; Flütsch *et al*., 2021). The most represented term within Cellular Component was “integral component of plasma membrane”. Another interesting term in cellular component was “plant-type cell wall”, which was also spotted in most down-regulated DEG.

4.7.2 KEGG pathway analysis

To identify potential signalling pathways *At*MYB93 may be involved in, Kyoto Encyclopedia Genes and Genomes (KEGG) pathway analysis was applied to the 255 DEGs (Kanehisa *et al*., 2007; Sherman *et al*., 2009). All the enriched KEGG pathways present in the *Atmyb93* mutant are shown in Figure 4.8B. The top 3 pathways are significantly clustered, which include

"Metabolic pathway", "Biosynthesis of secondary metabolites" and "Flavone and flavonol biosynthesis".

Within the "Flavone and flavonol biosynthesis" pathway category, 2 DEGs (flavonoid 3'-hydroxylase, TT7 and UDP-dependent glycosyltransferase, UGT78D2), which play a key role in flavonoid biosynthesis, were enriched. The loss-of-function mutant of UGT78D2 was reported to exhibit dwarf phenotype and loss of apical dominance after bolting, which was due to the accumulation of kaempferol 3-O-rhamnoside-7-O- rhamnoside, accompanied with the reduced Polar auxin transport in *ugt78d2* mutant shoots. (Yin *et al*., 2014)

"Phenylpropanoid biosynthesis" was the fourth enriched pathway from KEGG, which does not show in Figure 4.8. Within the "Phenylpropanoid biosynthesis" pathway category, 6 DEGs (β-glucosidase, *BGLUC46*, UDP- glucosyltransferase *UGT84A2* and four peroxidase superfamily genes, PERs) were enriched. Furthermore, those DEGs were predicted in KEGG to be required for lignin biosynthesis, which was also associated with cell wall structure shown in the GO term analysis.

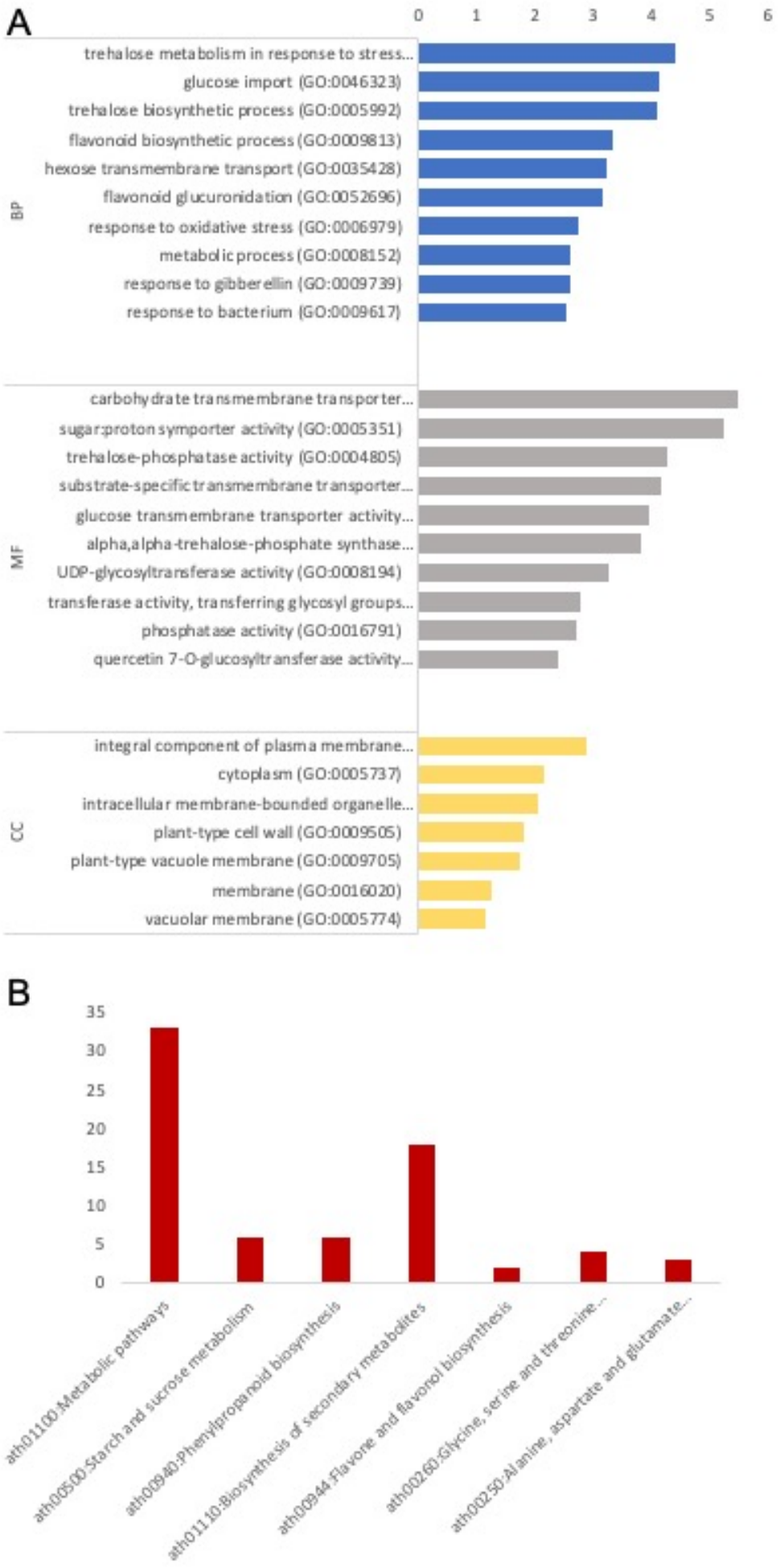
A
0
1
2
3
4
5
6
BP
trehalose metabolism in response to stress...
glucose import (GO:0046323)
trehalose biosynthetic process (GO:0005992)
flavonoid biosynthetic process (GO:0009813)
hexose transmembrane transport (GO:0035428)
flavonoid glucuronidation (GO:0052696)
response to oxidative stress (GO:0006979)
metabolic process (GO:0008152)
response to gibberellin (GO:0009739)
response to bacterium (GO:0009617)
MF
carbohydrate transmembrane transporter...
sugar:proton symporter activity (GO:0005351)
trehalose-phosphatase activity (GO:0004805)
substrate-specific transmembrane transporter...
glucose transmembrane transporter activity...
alpha,alpha-trehalose-phosphate synthase...
UDP-glycosyltransferase activity (GO:0008194)
transferase activity, transferring glycosyl groups...
phosphatase activity (GO:0016791)
quercetin 7-O-glucosyltransferase activity...
CC
integral component of plasma membrane...
cytoplasm (GO:0005737)
intracellular membrane-bounded organelle...
plant-type cell wall (GO:0009505)
plant-type vacuole membrane (GO:0009705)
membrane (GO:0016020)
vacuolar membrane (GO:0005774)
B
35
30
25
20
15
10
5
0
ath01100:Metabolic pathways
ath00500:Starch and sucrose metabolism
ath00940:Phenylpropanoid biosynthesis
ath01110:Biosynthesis of secondary metabolites
ath00944:Flavone and flavonol biosynthesis
ath00260:Glycine, serine and threonine...
ath00250:Alanine, aspartate and glutamate...

Figure 4.8 Gene ontology (GO) and KEGG pathway enrichment analysis of differentially expressed genes (DEGs).
All enriched GO terms (A) and KEGG pathways (B) analysis of DEGs are displayed based on the numbers of genes enriched. Different colours represent molecular function (MF, grey), cellular components (CC, yellow) and biological process (BP, blue) for GO term enrichment. Results of KEGG analysis are displayed in red bars.

4.8 Comparison analysis

*At*MYB93 was previously described as a negative regulator of lateral root development in *Arabidopsis* (Gibbs *et al*., 2014) whose expression increased significantly between 12hr and 15 hr after lateral root induction (Voß *et al*., 2015). An overlapping of DEGs from the *Atmyb93* mutant RNAseq data with genes significantly changed during lateral root initiation data (12-15h) (Voß *et al*., 2015) was performed to identify 14 genes present in both datasets (Figure 4.9). Among those 14 genes, 4 genes were down regulated in the *Atmyb93* mutant and rest were upregulated in the *Atmyb93* mutant. 13 of the 14 overlapping genes showed negatively correlative expression, which were identified as the potential transcriptional target genes of *At*MYB93 (Figure 4.9).

The potential *At*MYB93 target genes are involved in a variety of processes during plant development, especially during root development. *CASPL1D2* (At3g06390) was the only gene upregulated in both lateral root initiation transcriptome and *Atmyb93* mutant RNAseq results and upregulation of its expression was the largest among the 14 genes. Four more other genes (*GH9C3*, *CYP86A4*, AT3G07320 and AT1G63530) were also upregulated (Figure 4.9) during lateral root initiation, but expressions of these genes were decreased (Figure 4.9) in the *Atmyb93* knockout. Among them, *CYP86A4* was the most significantly downregulated in the *Atmyb93* mutant. The rest of the putative targets were upregulated in the *Atmyb93* knockout and showed opposing expression pattern in the lateral root initiation dataset. *GLUTAMINE AMIDOTRANSFERASE 1_2.1* (*GAT1_2.1*) was most upregulated (Figure 4.9) when *AtMYB93* was knocked out in *Arabidopsis* and also most downregulated in wild type lateral root initiation dataset. Expression of eight genes including *RZPF34*(*RING ZINC-FINGER PROTEIN 34*), *POX1*(*PROLINE OXIDASE1*), *PMI2*(*PHOSPHOMANNOSE ISOMERASE 2*), *DIN10*(*DARK INDUCIBLE 10*), *CTPS1*(*CYTIDINE TRIPHOSPHATE SYNTHASE1*),

GDPD2(GLYCEROPHOSPHODIESTER PHOSPHODIESTERASE 2) and *NUDX8*(NUDIX HYDROLASE HOMOLOG 8) were also increased in the *Atmyb93* mutant and reduced in lateral root initiation. (Figure 4.9)

With the help of Dr Alex Mason (Prof Siobhan Brady's lab, University of California, Davis), the promoters of the 14 potential target genes were analysed in the MEME Suite (http://meme-suite.org) with predicted *At*MYB93 binding motifs "GGTNGGTG" or "CACCNACC" (Niwa et al., 2018). The promoters of *CASPL1D2* and *GH9C3* were predicted to have the highest probability of being bound by *At*MYB93 among those 14 promoters ($p<0.05$).

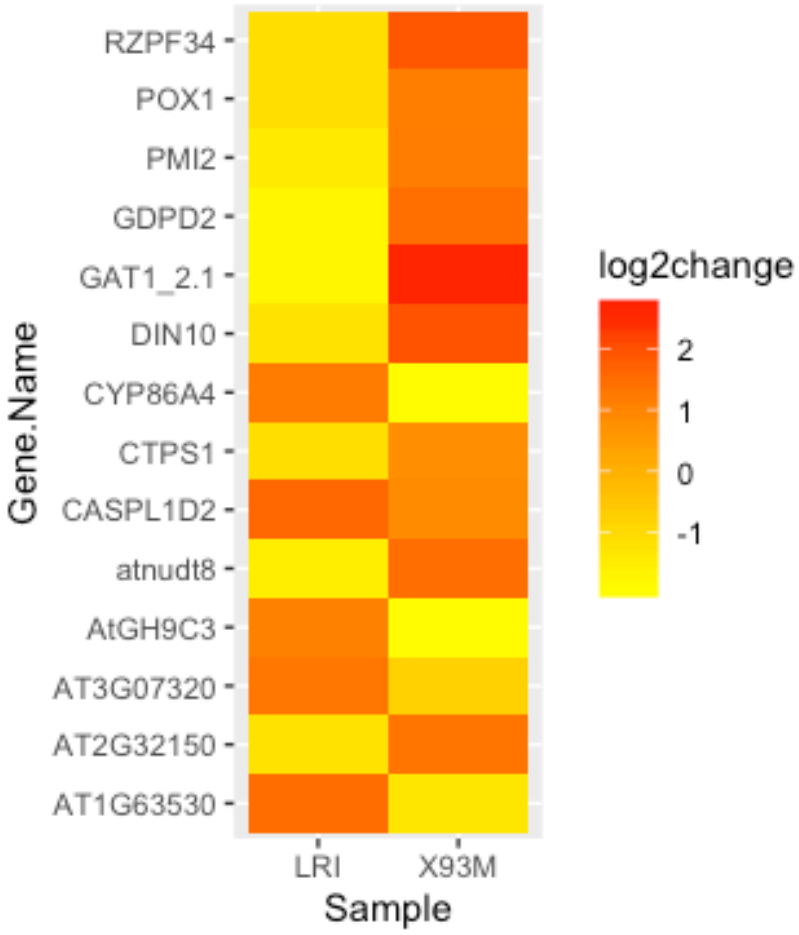

Figure 4.9 Comparison of potential *At*MYB93 target gene expression levels.
14 genes were identified by overlapping significantly DEGs from both *Atmyb93* mutant RNAseq data (X93M) and lateral root initiation transcriptome data (LRI). Log_2 fold change values were applied to visualize expression changes of those genes. Red, upregulated. Yellow, downregulated.

4.9 Network analysis of DEGs

All downregulated DEGs were analysed in STRING (https://string-db.org) by using all active interaction sources, including Textmining, Experiments, Databases, Co-expression, Neighbourhood, Gene fusion and Co-occurrence. These genes were clustered into four groups. Most of the genes were grouped in the flavonoid and phenylpropanoid metabolism group including *TT7*, *MYB12*, *UGT78D2*, *UGT84A1* and *UGT84A2*. In addition, *GLYCOSYL HYDROLASE GH9C3*, *XYLOGLUCAN ENDOTRANSGLUCOSYLASE/HYDROLASE XTH19* and *CELLULOSE SYNTHASE LIKE CSLA9* were linked in cell wall development group. A sulphur metabolism group contained *S-ADENOSYLMETHIONINE SYNTHETASE MTO3*, *5'ADENYLYLPHOSPHOSULFATE REDUCTASE APR2* and *SULPHATE TRANSPORTER SULTR1;3*. Oddly, there was one group of genes involved in a variety of different developmental or metabolic processes. These genes either showed root specific expression like *AtMYB93* or were highly expressed in root compared to their expression in other tissues, which indicated that they may function in *Arabidopsis* root development.

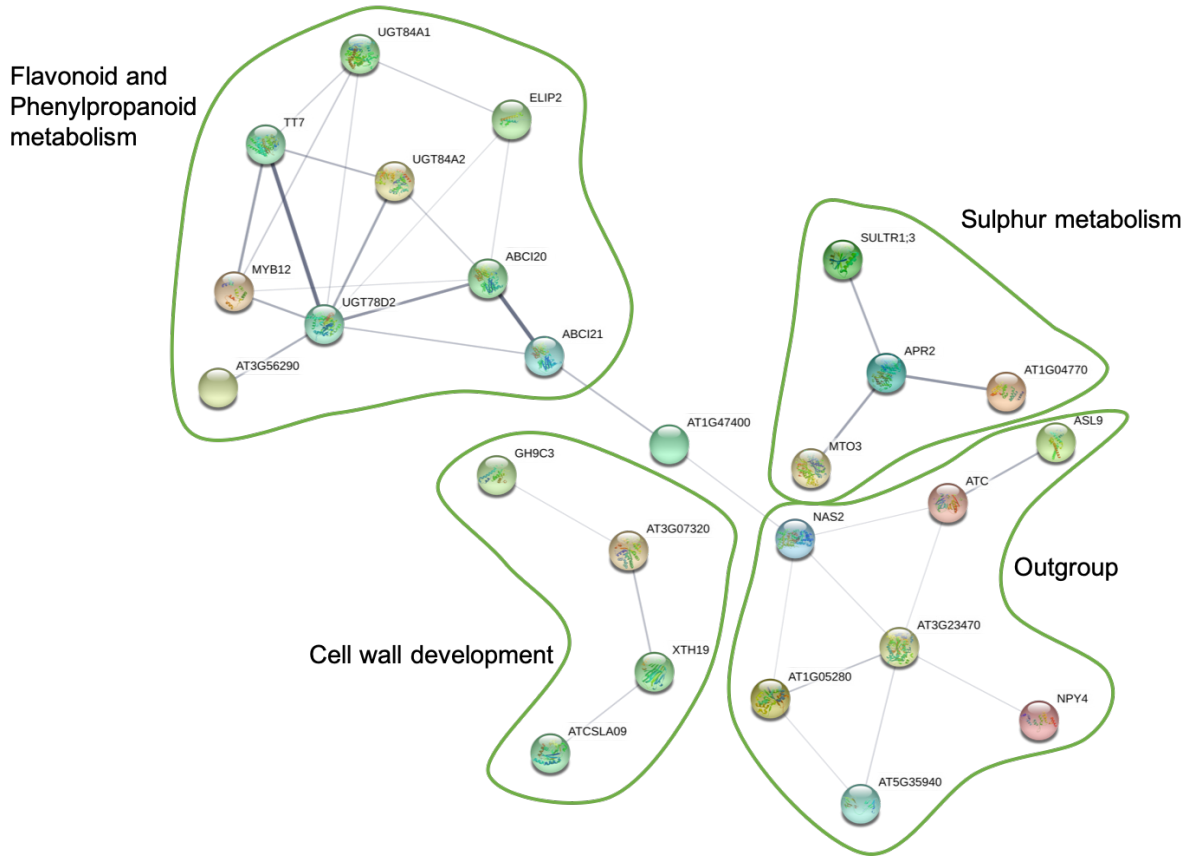

Figure 4.10 Network matrix performed using String from the significantly down-regulated genes in the *Atmyb93* mutant.

Grey lines display the confidence of associations between two genes, which shared a role in some biological processes. The thickness of the line corresponds to the significance of the interaction with a minimum cutoff value of 0.4. Genes that displayed lower than this cutoff value are not represented. Coloured nodes do not display any biological meanings.

4.10 Potential interactors of AtMYB93

Dinesh-Kumar lab identified substrates of 10 activate MPKs in Arabidopsis by using the protein microarray, in which AtMYB93 was predicted as interactor with both AtMPK3 and AtMPK6. To test the interaction between AtMYB93 and AtMPKs and identify which region of AtMYB93 is crucial to the binding with AtMPKs, both AtMPKs and three different versions of *AtMYB93* were amplified by PCR and cloned into yeast two-hybrid vectors (Fig 4.11). The full length CDS of *AtMYB93* in pGADT7 was constructed by Prof Daniel Gibbs, which was then used as the templates for three truncated *AtMYB93*s cloning (R2R3 domain (*AtMYB93* R2R3; amino acids 2-365), N-terminal (*AtMYB93*-N345; amino acids 115-365) and N-terminal without conserved domain (*AtMYB93*-N468; amino acids 156-365)) and AtMPKs were introduced into pGBKT7.

The yeast two-hybrid assays described in Chapter 2.6.5 was performed to test interaction between AtMYB93 and AtMPKs. The yeast colonies containing Full length CDS of AtMYB93 and AtMYB93 R2R3 domain with AtMPK3 grows on -AWLT agar plate and no growth can be observed in transformants containing other regions of AtMYB93 with AtMPK3 (Fig.4.11). It indicates that AtMYB93, especially R2R3 domain interacts with AtMPK3 were found to interact with AtMPK3. Inconsistent results were observed in yeast two hybrid assay between Full length CDS of AtMYB93 and AtMPK6 (data not shown), so no further experiment has been done for this combination.

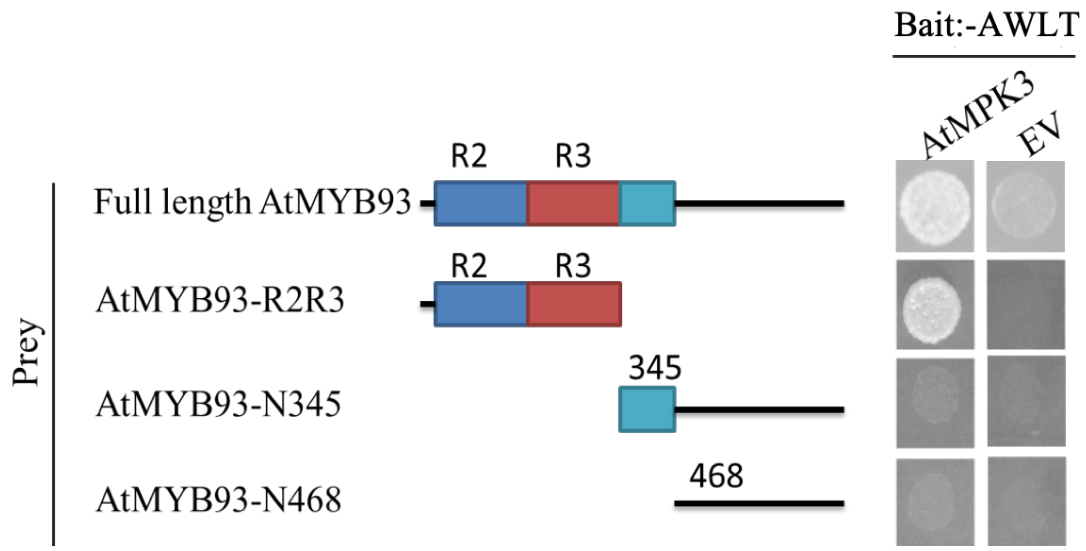

Figure4. 11Yeast two-hybrid interaction of AtMYB93s and AtMPK3
Different domain and amino acids range of AtMYB93 were shown on the left (R2 domain (blue bar), R3 domain (red bar) and conserved domain (turquoise bar)). Different truncated AtMYB93s and AtMPK3 were introduced into pGADT7 (activation domain) and pGBKT7 (binding domain) separately. Growth on the AWLT(Adenine-Histidine-Leucine-Tryptophan) drop out medium indicated the interaction between AtMPK3 and truncated AtMYB93.

4.11 Discussion

RNA sequencing technology is a powerful tool for whole transcriptome profiling. This chapter describes RNAseq analysis of *Arabidopsis* roots from 7-day-old wild type and *Atmyb93* mutant seedlings. The aim of RNAseq is to study the effects of the *AtMYB93* knock out in *Arabidopsis* roots and to identify putative transcriptional targets of *At*MYB93.

4.11.1 Potential false positive or negative DEGs in RNA sequencing

255 DEGs were identified by differential expression analysis of RNAseq data in this chapter. Some false positive DEGs may come from RNA sequencing techniques or analysis methods, which are inevitable (González *et al*., 2013). Some false positives may develop from the effect of the phenotype, rather than mutations of the gene. Previously, *Atmyb93* mutant was identified to have more lateral roots compared to wild type, possibly leading to increased water and nutrients uptake or other developmental processes, which may affect some related genes' expression in turn.

Not only should false positives be taken into account, false negatives also happen frequently. In this study, the RNA was extracted from the whole roots of wild type and *Atmyb93* mutants, while *AtMYB93* expression was previously reported to be restricted to several endodermal cells overlapping the lateral root primordium. It is plausible to hypothesise that the expression change of the potential *At*MYB93 target genes in *Atmyb93* mutant may be normalised or masked by these genes' expression in other cells, in which no expression of *AtMYB93* was detected. However, AtMYB93 was the most downregulated gene in RNAseq data, which makes false negatives less likely to be presented in our data.

4.11.2 Sugar metabolism related genes are changed in the *Atmyb93* mutant.

A big group of sugar metabolism related genes was identified from the RNAseq data. Three *STP*s were upregulated in *Atmyb93* mutant, which belong to a group of monosaccharide transporters unique to plants (Schneidereit *et al*., 2003). *STP1* and *STP4* were reported to play major roles in monosaccharide uptake under normal conditions (Yamada et al., 2011). In contrast, *STP14* showed low expression in the wild-type root and was identified as a galactose-specific transporter (Poschet *et al*., 2010). *STP1*, *STP4* have higher expression level than other *STP*s in the wild-type *Arabidopsis* root such as *STP2*, *STP3*, *STP5*, indicating their function in monosaccharides uptake in root (Yamada *et al*., 2011).

It is reported that *AtSWEET2* (Tao *et al*., 2015) is highly expressed in the *Arabidopsis* root and localised on the vacuolar membrane to function as a sugar importer to vacuoles. *AtSWEET2* is also involved in sugar secretion to the rhizosphere and contributes to pathogen resistance in *Arabidopsis* (Chen *et al*., 2015). *EDRL6* and *TMT1* encode glucose transporters to regulate glucose homeostasis in the cell, (Poschet *et al*., 2011; Wingenter *et al*., 2010) while the function of *PMT6* is uncharacterised: *PMT6* is predicted to encode a glucose importer from the PMT family, in which PMT1 and PMT2 were reported as transporters for xylitol and fructose, respectively, in *Arabidopsis* (Klepek *et al*.,2010).

TPS proteins convert UDP-glucose and glucose 6-phosphate into trehalose-6-phosphate, which is then dephosphorylated by TPP proteins to produce trehalose (Lunn *et al*., 2014). Trehalose-6-phosphate is a signalling regulator of sucrose status in plant, which is involved in many developmental and metabolic processes, such as the photoperiod pathway, embryogenesis and stomatal conductance (Figueroa *et al*., 2016). Taken together, these data shows that *AtMYB93* may involve in sugar transport and metabolism in *Arabidopsis*.

4.11.3 MPK3 involves in lateral root development

Mitogen-Activated Protein Kinase (MAPK) cascades are highly conserved signalling modules in all eukaryotes. In plant, MAPK cascades play important roles in transduction of extracellular stimuli into cellular responses by phosphorylating substrates, which affect plant growth and development (Taj *et al*., 2010; Huang *et al*., 2019). In this Chapter, we demonstrated the interaction between AtMPK3 and AtMYB93, specially R2R3 domain of AtMYB93 by yeast two hybrid. Previous reports showed that both WRKY33 and ETHYLENE RESPONSE FACTOR6 (ERF6) were phosphorylated by AtMPK3/AtMPK6 leading to activate and stabilise these substrates respectively, which were important for plant defense against pathogens (Meng *et al*., 2013; Mao *et al*., 2011). Li *et al*. (2017) reported that ICE1 (Inducer of C-repeat-binding factor expression 1) was phosphorylated and destabilised by AtMPK3/AtMPK6 in response to cold stress to decrease freezing tolerance in Arabidopsis. In addition, it is reported that AtMPK3 and AtMPK6 are also involving in lateral root development by regulating cell division in response to auxin signalling in Arabidopsis (Huang *et al*., 2019; Zhu *et al*., 2019). And potential phosphorylated sites of AtMYB93 were analysed in PhosPhAT (https://phosphat.uni-hohenheim.de), which predicted highly potential phosphorylated sites in R2R3 region (data not shown). Thus, it is plausible to hypothesis that AtMYB93 may be deactivated or degraded by phosphorylation of AtMPK3, leading to increased lateral root density, which matches with the lateral root density phenotype in mpk3/mpk6 double mutant (Zhu *et al*., 2019).

4.12 Conclusion

RNAseq data of *Atmyb93* mutant was generated by NOVEGENE. By analysing the RNAseq data, 255 DEGs were identified, which were further found to function in a wide area, such as flavonoid metabolism, sugar transport, glucosinolate biosynthesis and sulphur metabolism. Sulphur metabolism related genes will be further analysed and discussed in Chapter 5. By comparative analysis with lateral root initiation data (Voß *et al*., 2015), 14 genes were identified as the potential transcriptional target genes of *At*MYB93. Further promoter analysis confirmed promoters of two genes (*AtG9H3*, *AtCASPL1D1*) possess *At*MYB93 binding motifs, which made them highly possible to be *At*MYB93 downstream targets. These potential downstream target genes will be test by Protein-DNA interaction assay, such as Yeast one Hybrid. And mutant lines of these genes will be ordered to study if they have similar phenotype on lateral root development or suberin deposition with *AtMYB93* in *Arabidopsis*.

Chapter Ⅴ： Investigation of sulphur-related phenotype in *Atmyb93* mutant

5.1 Introduction

Sulphur (S) is an essential macronutrient for plant growth, which is involved in many metabolic processes in plants (Gigolashvili *et al*., 2014). S is taken up from soil by the plant in the form of sulphate, which is used for biosynthesis of essential metabolites, such as cysteine, methionine, glutathione and glucosinolate (Davidian *et al*.,2010). These metabolites are involved in responses to both biotic and abiotic stress. For example, glutathione was identified as an antioxidant in plants that is in charge of preventing oxidative damage of important compounds caused by reactive oxygen species (ROS) such as carbohydrates, lipids, proteins and DNA (Hasanuzzaman *et al*., 2017). Sulphur also plays vital roles in the biosynthesis and structure formation of proteins, coenzymes, vitamins and prosthetic groups. Previous studies on sulphur assimilation (Figure 5.1) described that sulphur was taken up by roots in the form of sulphate, which was then used for sulphurisation of Adenosine triphphosphate (ATP) to adenosine 5'-phosphosulphate (APS). APS was reduced to sulphide by two rounds of reduction with APS reductase (APR) and Sulphite reductase (SiR) separately. Sulphide was then involved in synthesis of cysteine with O-acetylserine (OAS) catalysed by OAS (thiol)lyase (OASTL), in which OAS was from the acetylation of serine by serine acetyltransferase (SAT) (Kopriva 2006; Leustel et al., 1999; Tabe et al., 2010). Cysteine as a sulphur containing metabolite is involved in synthesis of other metabolites and sulphur compounds. APS can also be phosphorylated by APS kinase (APK) to phosphoadenosine 5'-phosphosulphate (PAPS) (Mugford et al., 2009). By using PAPS as a donor of active sulphate groups, Sulphotransferase (SOT) participated in transferring the active sulphate group onto its acceptors in plant secondary metabolism, such as glucosinolate, flavonoids, jasmonate, brassinosteriods (Mugford *et al*., 2009).

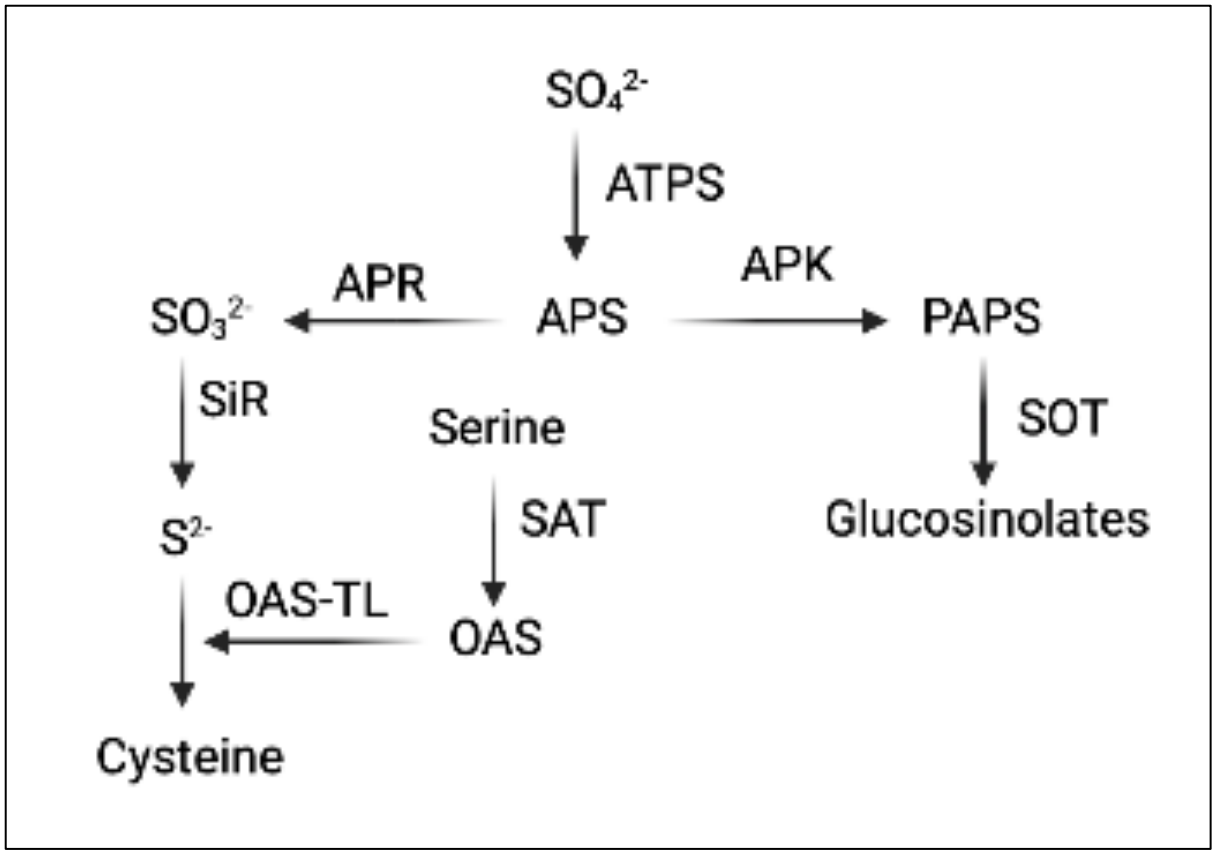

Figure 5.1 Schematic representation of sulphur assimilation in Arabidopsis.
Sulphate was taken up and activated by ATPS to APS, which was then reduced by APR to sulphite. With catalyzing by SiR, sulphite was further reduced to sulphide, which was used for synthesis of cysteine with OAS (Acetylation of serine) by OAS-TL. APS can also be phosphorylated to PAPS, which act as a donor of active sulphate group for synthesis of secondary metabolites in plant, catalysed by SOT.

Previous studies showed that sulphur affects root growth in plant. In *Arabidopsis*, sulphur depletion weakly increased root length and significantly inhibited lateral root development (Dan *et al*., 2007; Gruber et al., 2013; Dong *et al*., 2019). In *Medicago*, the root morphological parameters such as root length, root surface area and lateral root numbers were all significantly decreased treatment with sulphur deficient medium compared to sulphur sufficient medium (Gao *et al*., 2016). Transcriptome data from Bielecka *et al*., (2015) showed that the relative expression level of *AtMYB93* was up-regulated under sulphur starvation. Combining these data with the knowledge that *At*MYB93 negatively regulates lateral root development in *Arabidopsis* (Gibbs *et al*., 2014), we hypothesised that *AtMYB93* was involved in sulphur assimilation in *Arabidopsis* and other plants.

In this chapter, sulphur metabolism related DEGs from Chapter 4 were analysed and identified as putative transcriptional targets of *At*MYB93. To determine the function of *AtMYB93* in sulphur assimilation, sulphur element content in shoots of the *Atmyb93* mutant and leaves of transgenic tomatoes with overexpression or knockdown of *SlMYB93* were analysed by using Inductively coupled plasma mass spectrometry (ICP-MS). Root development parameters were also collected and analysed to determine the effect of sulphur depletion and OAS treatment on the *Atmyb93* mutant.

5.2 Analysis of sulphur related genes from the *Atmyb93* differential transcriptome

Based on the transcriptome data from Chapter 4, loss of function of *AtMYB93* significantly altered the expression of genes involved in sulphur metabolism. (Table 5.1) SULPHATE TRANSPORTERs (*SULT1;3* and *SULTR3;5*) are downregulated in Atmyb93 mutant. In addition, *5'ADENYLYLPHOSPHOSULFATE REDUCTASE2* (APR2) also showed significant decreased expression in *Atmyb93* mutant, indicated that sulphur assimilation may be inhibited in *Atmyb93* mutant.

Interestingly, expression glucosinolate biosynthesis related genes were also affected by mutation of AtMYB93. *INDOLE GLUCOSINOLATE O-METHYLTRANSFERASE 1* and *4* (*IGMT1* and *IGMT4*) are both upregulated in *Atmyb93* mutant, in which downregulation of *SULFUR DEFICIENCY INDUCED2* (SDI2) was found, which suggests the potential accumulation of glucosinolates in *Atmyb93* mutant.

Other genes involving in downstream of sulphur assimilation also exhibits significantly differential expression in *Atmyb93* mutant. S-adenosylmethionine synthetase 3 (SAMS3) and Cyclopropane-fatty-acyl-phospholipid synthase are both downregulated in Atmyb93 mutant, while AT3G61210 (S-adenosyl-L-methionine-dependent methyltransferases superfamily protein), which was in the downstream of S-adenosylmethionine, showed significantly increased expression in the *Atmyb93* mutant. Additional genes in Table 5.1 are either related to sugar indirectly or responsive to sulphur stress.

Accession	Gene name	Log2foldchange	Details
AT3G48360	BTB AND TAZ DOMAIN PROTEIN 2 (BT2)	1.867	Involved in TAC1-mediated telomerase activation pathway
AT3G61210	S-adenosyl-L-methionine-dependent methyltransferases superfamily protein	1.861	Protein methylation
AT3G01175	Unknown protein	1.535	
AT1G21130	INDOLE GLUCOSINOLATE O-METHYLTRANSFERASE 4 (IGMT4)	1.288	Glucosinolate metabolism
AT1G21100	INDOLE GLUCOSINOLATE O-METHYLTRANSFERASE 1 (IGMT1)	1.026	Glucosinolate metabolism
AT1G61740	Sulfite exporter TauE/SafE family protein	1.024	
AT3G28740	CYTOCHROME P450, FAMILY 81, SUBFAMILY D, POLYPEPTIDE 11 (CYP81D11)	0.666	Defense response
AT3G17390	S-adenosylmethionine synthetase 3 (SAMS3)	-0.767	S-adenosylmethionine synthetase activity
AT3G23470	Cyclopropane-fatty-acyl-phospholipid synthase	-0.780	Lipid metabolism
AT5G19600	SULFATE TRANSPORTER 3;5 (SULTR3;5)	-0.793	Sulfate transport activity
AT1G62180	5'ADENYLYLPHOSPHOSULFATE REDUCTASE 2 (APR2)	-1.217	Sulfur assimilation
AT1G04770	SULFUR DEFICIENCY INDUCED 2 (SDI2)	-1.339	Response to sulfur stress, involve in glucosinolate biosynthesis
AT1G22150	SULFATE TRANSPORTER 1;3 (SULTR1;3)	-2.272	Sulfate transport activity

Table 5.1DEGs from *Atmyb93* RNAseq involved in sulphur metabolism.

5.3 Effect on sulphate assimilation in model plants with knockout or knockdown of their *MYB93* genes

According to the transcriptome data, APR2 was significantly down regulated in *Atmyb93* mutant, which may negatively affect reduction of sulphate to sulphite in root, and more sulphate may be transported from root to shoot. To establish if loss function of *MYB93* affected transport of sulphate from root to shoot in both *Arabidopsis* and tomato, tissue was harvested from wild type plants and those with perturbed *MYB93* function. Collaborators from Dr Neil Graham's lab (University of Nottingham) used inductively coupled plasma-mass spectrometry (ICP-MS; Thermo Fisher Scientific iCAPQ, Thermo Fisher Scientific, Bremen, Germany) to measure the concentrations of different elements in wild type and the *Atmyb93* mutant *Arabidopsis* shoots. My analysis of two repeat experiments set up by Helen Wilkinson showed that shoots of the *Atmyb93* mutant had more sulphur than wild type shoots (Figure 5.2A).

Dry leaf tissues of different tomato lines were also analysed by ICP-MS, which showed a similar result to *Arabidopsis*. Two independent tomato SlMYB93 RNAi lines showed increased accumulation of sulphur in leaves comparing to that of both wild type and SlMYB93 overexpression lines (Figure 5.2B). In order to further confirm these results, more repeat experiments will be needed for statistical analysis.

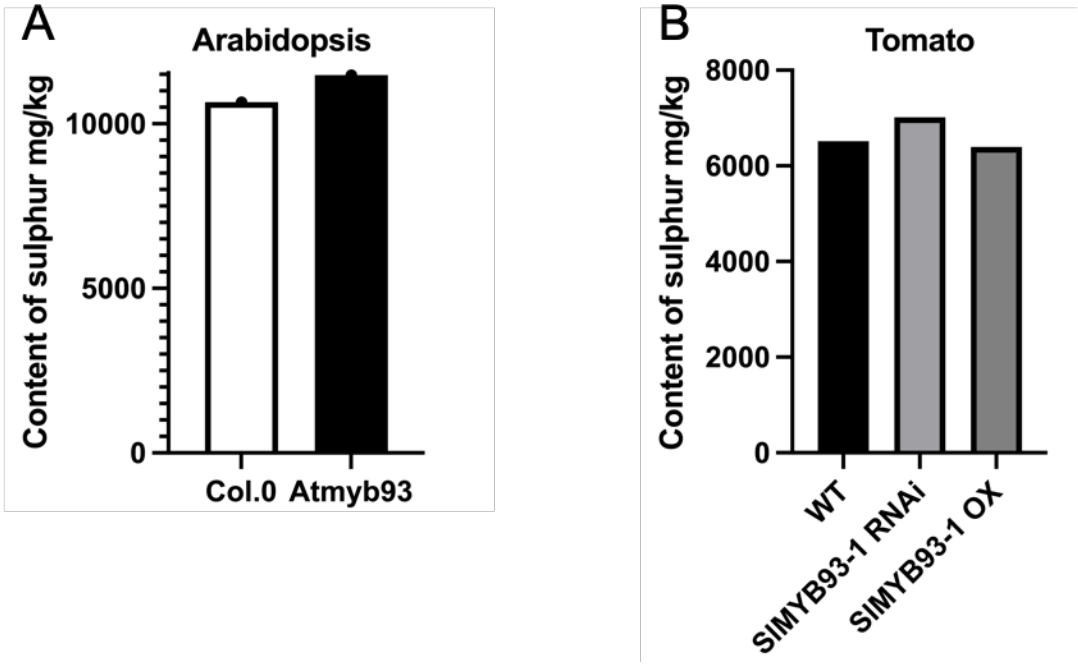

Figure 5.2 Total shoot sulphur in wild type and MYB93 loss/reduction of function in *Arabidopsis* and tomato.

(A) Total sulphur in shoots of Col-0 and *Atmyb93* mutant plants, 21 days after sowing and before flowering. *Arabidopsis* was grown in ½ MS medium in magenta pots. (B) Total sulphur in leaves of 8-week-old WT, *SlMYB93-1* overexpressing line and *SlMYB93-RNAi* lines grown in soil. Shoots and leaves were harvested and dried for ICP-MS.

5.4 Phenotype of *Atmyb93* mutants grown with and without sulphur

Previous studies showed that AtMYB93 was induced in sulphur starvation, which also led to decreased lateral root density (Zheng et al., 2007; Gruber et al., 2013). This result was similar with the phenotype AtMYB93 overexpressing lines in Arabidopsis (Gibbs et al., 2014). So, loss function of AtMYB93 may less sensitive to sulphur starvation.

In order to further study effect of sulphur deprivation on the *Atmyb93* mutant, lateral root assays were performed on wild type and *Atmyb93* mutant plants grown in ½ MS media with or without sulphur (Section 2.7.2). The results indicated that *Atmyb93* mutants have longer primary roots than wild-type under both conditions (with or without sulphur stress) and that sulphur stress does not affect root length in either genotype (Figure 5.3A). The lateral root (LR) density of both Col-0 and *Atmyb93* mutant plants was calculated: this showed that LR density was significantly reduced in wild type plants with sulphur stress, whereas the LR density of *Atmyb93* mutants showed no significant difference under sulphur stress compared to normal conditions. This suggested that the *Atmyb93* mutant is somewhat insensitive to sulphur stress. (Figure 5.3B)

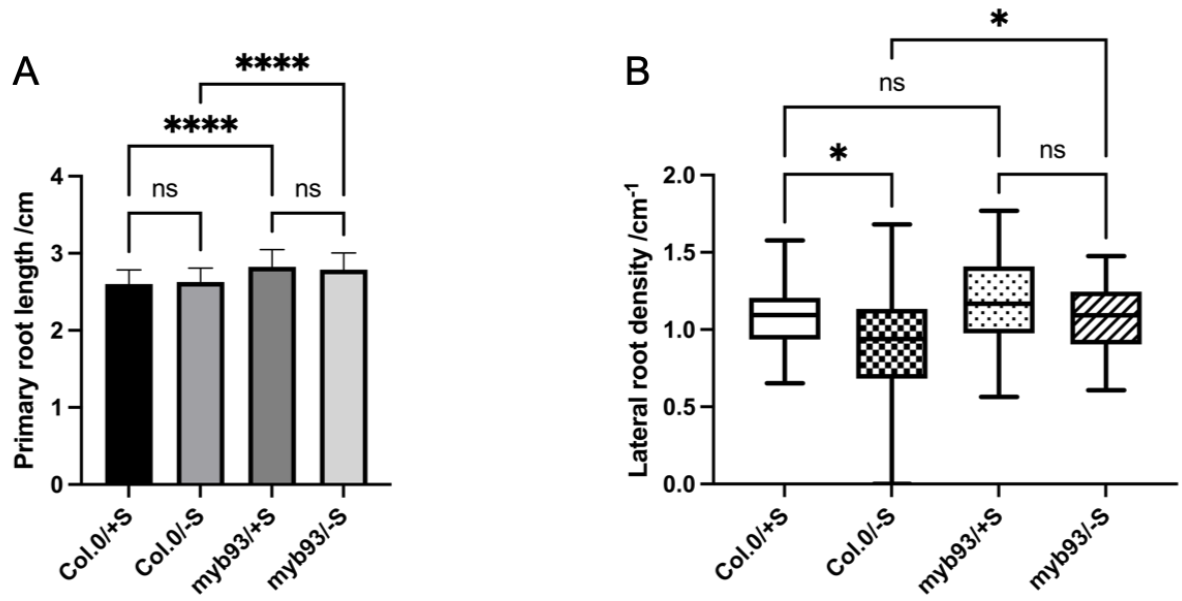

Figure 5.3 Root phenotypes of *Atmyb93* mutant under sulphur stress.
(A) primary root length is significantly increased in *Atmyb93* mutants compared to wild type, with or without sulphur stress (n>150 over 3 biological repeats). (B) Emerged lateral root (LR) densities in 8-day-old seedlings of wild type and *Atmyb93* mutants. Col-0 has significantly reduced LR density in sulphur stress compared with in normal conditions. The *Atmyb93* mutant has significantly greater LR density compared with Col-0 in sulphur stress (n>150 over 3 biological repeats). Error bars (A), mean of standard deviation, Sidak's multiple comparisons test: *, P<0.05 ; **, P<0.01; ***, P<0.001; ****, P<0.0001. Whiskers (B), maximum and minimum values. Dunn's multiple comparisons test: : *, P<0.05 ; **, P<0.01; ***, P<0.001; ****, P<0.0001.

5.5 Effect of OAS treatment on WT and Atmyb93 mutants.

OAS as a carbon backbone of cysteine synthesis, also was identified as a signalling indicator of sulphur starvation (Bogdanova *et al*., 1997). OAS was accumulated in plant under sulphur starvation and plants treatment with OAS also showed similar regulation of sulphur assimilation-related genes with that in sulphur starvation, such as SULTRs and APRs (Koprivova *et al*.,2000; Hirai *et al*., 2003; Hubberten *et al*., 2012;).

To determine effect of OAS treatment on *Atmyb93* mutant, root parameters (root length and lateral root density) were collected and analysed from lateral root assays of Col-0 and *Atmyb93* mutants with or without addition of 0.1mM OAS. *Atmyb93* mutants showed significantly increased primary root length with or without 0.1mM OAS compared to Col-0, however there was no difference in root length caused by OAS treatment in either genotype (Figure 5.4A). The lateral root density of *Atmyb93* mutants treated with 0.1mM OAS was significantly increased compared to Col-0, while the *Atmyb93* mutant without OAS treatment did not show a significant increase in lateral root density compared to Col-0 in the same growth conditions (Figure 5.4B).

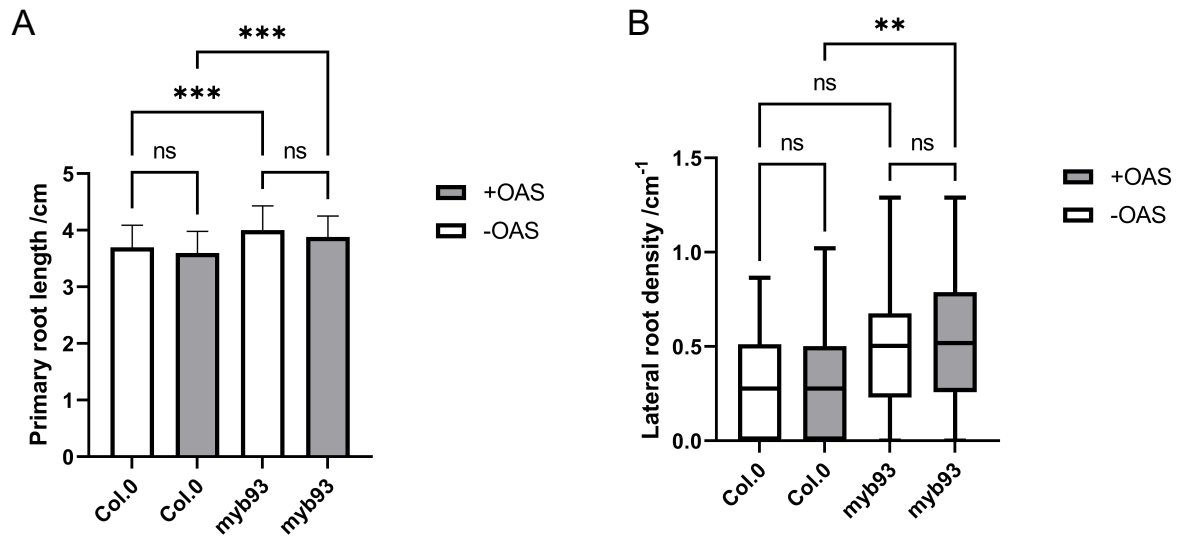

Figure 5.4 Comparing root development between Col-0 and *Atmyb93* mutants with or without 0.1mM OAS.

(A) primary root length is significantly increased in the *Atmyb93* mutant with or without 0.1mM OAS with no effect of OAS treatment in either genotype (n>50 over 2 biological repeats). (B) Emerged lateral root (LR) densities in 8-day-old seedlings of wild type and *Atmyb93* mutant seedlings with or without 0.1mM OAS. *Atmyb93* mutants have significantly greater LR density compared to Col-0 supplemented with 0.1mM OAS (n>50 over 2 biological repeats). Error bars (A), mean of standard deviation, Sidak's multiple comparisons test: *, P<0.05 ; **, P<0.01; ***, P<0.001; ****, P<0.0001. Whiskers (B), maximum and minimum values. Dunn's multiple comparisons test: *, P<0.05 ; **, P<0.01; ***, P<0.001; ****, P<0.0001.

5.6 Discussion

5.6.1 Sulphur metabolism related genes in *Atmyb93* mutant

According to RNAseq analysis in Chapter 4, a group of genes involving in sulphur metabolism has been identified. *SULPHATE TRANSPORTERs* (*SULTR1;3* and *SULTR3;5*) play a vital role in sulphate transport in vascular tissues (Yoshimoto *et al*.,2003; Tohge *et al*.,2005). *SULTR3;5* also functions as an enhancer of sulphur nutrient transport from root to shoot (Tohge *et al*.,2005). *APR2* is involved in reduction of 5' adenosineohosphosulphate during sulphur assimilation (Loudet *et al*., 2007). Interestingly, *SULFUR DEFICIENCY INDUCED 2* (*SDI2*) has been identified as a negative regulator of GSL synthesis, while *INDOLE GLUCOSINOLATE O-METHYLTRANSFERASE 1* and *4* (*IGMT1* and *IGMT4*) have been demonstrated to facilitate formation of different types of indole glucosinolates (Aarabi *et al*., 2016; Pfalz *et al*., 2011). Thus, *At*MYB93 may be involved in sulphur metabolism in *Arabidopsis*, and those sulphur related DEGs are likely to be potential downstream transcriptional targets of *At*MYB93, especially those that are downregulated in the *Atmyb93* mutant.

5.6.2 Sulphur assimilation in *Atmyb93* mutant

Previously, it was shown that *AtMYB53*, *AtMYB92* and *AtMYB93* are all induced by sulphur deficiency (Nikiforova *et al*.,2003; Bielecka *et al*., 2015). Moreover, *Arabidopsis* wild type plants make fewer lateral roots in response to S deficiency, which is similar to the phenotype of *AtMYB93* overexpressing lines. Thus, it was hypothesised that *At*MYB93 may be involved in response to S stress and overexpression of *AtMYB93* may limit S uptake from roots. Sulphur contents in shoots of the *Atmyb93* mutant and leaves of the *SlMYB93* RNAi tomato line were analysed and increased S content in these samples were observed compared to wild type,

which supports the hypothesis that *At*MYB93 involved in regulating S assimilation and affects S uptake.

The expression of sulphur metabolism related genes in *Atmyb93* mutant were analysed. *SULTR1;3* and *SULTR3;5* encoding sulphate efflux transporters are downregulated in the *Atmyb93* mutant. *SULTR3;5* was identified as a low-affinity transporter, which functions to enhance the activity of SULTR2;1, and a *sultr3;5* mutant showed no effect on shoot sulphate content (Kataoka *et al*., 2004). Yoshimoto *et al*., (2003) reported that SULTR1;3 plays a role in transporting sulphur nutrients from cotyledons to roots in *Arabidopsis*. Thus, downregulation of *SULTR1;3* expression may lead to less sulphur nutrients being transported to the roots and more S therefore being retained in the shoot, in the *Atmyb93* mutant.

5.6.3 lateral root development in S deficiency

Lateral root assays of Col-0 and the *Atmyb93* mutant were performed in 1/2MS medium with or without sulphur. In these assays, the *Atmyb93* mutant exhibited insignificantly increased in lateral root density in normal conditions, which may be caused by using different Murashige & Skoog media. However, the *Atmyb93* mutant exhibited no significant difference in lateral root density in response to S stress, while Col-0 showed a significant reduction in lateral root density, which suggests that *Atmyb93* mutant is insensitive to S deficiency compared to Col-0. It is therefore hypothesised that the inhibition in lateral root development under S stress seen in wild type plants may be caused by upregulation of *AtMYB93* gene expression under S-deficient conditions.

It was reported that accumulation of OAS was induced by S deficiency in *Arabidopsis*, and treatment with OAS also exhibited similar effects on the activity of sulphate assimilation related genes, such as *APR*s, *ATPS*, *CS* (Koprivova *et al*., 2000). Thus, lateral root assays of Col-

0 and *Atmyb93* mutants were performed in 1/2MS medium with or without 0.1mM OAS. These assays exhibited similar results to those with S deficiency, in which the *Atmyb93* mutant showed an increase in lateral root density upon OAS treatment compared to Col-0. Loss function of *AtMYB93* mutant may lose the ability to inhibit lateral root development in response to S deficiency. OAS accumulated in S deficiency may act as an indicator of S stress, which also cannot trigger reduction in lateral root density in *Atmyb93* mutant. Taken together, the results presented here supported the hypothesis that *AtMYB93* plays a role in sulphur assimilation and inhibits lateral root development in response to S starvation.

Chapter Ⅵ: General discussion

6.1 Introduction

Root systems are essential for plant growth and survival. Modulation of root system architecture enables plants' adaption in the continuously changing environment. The lateral root emerging from a primary root is an important component in root system, it not only enables plant access to water and nutrient in wider area, but also enhances plant anchorage in the soil. Thus, understanding molecular mechanisms underlying this process is vital for crop improvement in agriculture production and food security.

Previously, *At*MYB93 was identified as a negative regulator of lateral root development in *Arabidopsis* and *Md*MYB93 was identified in regulating suberin deposition in russeted apple fruit skin (Gibbs *et al*., 2014; Legay *et al*). The focus of this study was to identify MYB93 orthologues in tomato (*Solanum lycoperscium*) and characterise their function in both *Arabidopsis* and tomato. In addition, this study tried to further understand the molecular mechanism(s) by which *At*MYB93 inhibited LR development. As a result of transcriptome analysis, this study also sought to determine the effect of *MYB93* on sulphur metabolism in *Arabidopsis* and tomato. The general findings of this study are discussed below.

6.2 R2R3 type MYBs in tomato

Bioinformatic analysis and expression data presented in this thesis characterise three orthologues of *At*MYB93 in tomato, which are *Sl*MYB93-1, *Sl*MYB93-2 and *Sl*MYB93-3. Previous studies on tomato R2R3 MYB family analysed the phylogenetic relationship of each MYB gene based on the alignment analysis among all R2R3 MYBs (Li *et al*., 2014; Gates *et al*., 2016). The phylogenetic analysis presented in this thesis is focused on the evolutionary differences of MYB93s from different plant species. Together with the expression pattern data, this analysis of *Sl*MYB93s further suggests that these three SlMYB93s are likely to be

orthologues of AtMYB93, rather than of *At*MYB53 and *At*MYB92. In a similar study, Davis *et al*., (2021) identified two MYB17s (*Sl*MYB17-1 and *Sl*MYB17-2) in tomato by phylogenetic analysis of MYB17 orthologues from different plant species, which were demonstrated to control the anther trichome development.

Some R2R3 MYBs have been identified to have similar functions to their orthologues in *Arabidopsis*. Previous studies reported that overexpression of *Sl*MYB75 induced accumulation of anthocyanin in the whole plant (Jian *et al*., 2019), which was similar to the phenotype of *At*MYB75 overexpressing lines (Borevitz *et al*., 2000). Thus, it was hypothesised that *Sl*MYB93s may have similar functions to *At*MYB93 in lateral root development.

6.3 MYBs and lateral root development.

Some R2R3 MYB transcription factors have been implicated in playing roles in lateral root development. Previously, *At*MYB96 was shown to be induced by both drought and ABA. An activation-tagged *Atmyb96-ox* mutant, in which *AtMYB96* expression was upregulated compared to in Col-0, exhibited enhanced drought resistance and hypersensitivity to ABA (Seo *et al*., 2009). Furthermore, overexpression of *AtMYB96* inhibited lateral root formation by inducing expression of *GH3*s (*GH3.3*, *GH3.5* and *GH3.6*), which encode auxin-conjugating enzymes, leading to decreased levels of free active IAA (Seo *et al*., 2009; Ludwig-Müller *et al*., 2011). This suggests that *At*MYB96 acts as a negative regulator of lateral root development mediated by crosstalk of ABA and auxin signalling in response to drought stress.

*At*MYB93 was found to negatively modulate lateral root development in *Arabidopsis*, and *AtMYB93* gene expression can be induced by both IAA and ABA (Gibbs *et al*., 2014). The mechanism of lateral root development regulation by *At*MYB93 is yet to be found. It may be that *At*MYB93 regulates lateral root development in response to external conditions, like

*At*MYB96 inhibited formation of lateral roots in response to drought stress. Interestingly, *GH3.3* was identified to be upregulated in *Atmyb93* mutant (Section 4), which was supposed to produce more conjugated IAA, leading to a reduction in lateral root formation. However, *Atmyb93* mutant was found to have more lateral roots compared to Col-0, which indicates that *At*MYB93 may participate in another molecular pathway, by which AtMYB93 still significantly modulated lateral root development independently to any interference with *GH3.3* expression. In BioGRID interactome database, AtMYB93 protein was identified to interact with MITOGEN-ACTIVATED PROTEIN KINASE 3 and 6 (MPK3 and MPK6) as their phosphorylation substrate, and mpk3mpk6 double mutant exhibited significant reduction in latera root density (Popescu *et al*., 2009; Oughtred *et al*., 2021). Interaction between MPK3 and AtMYB93 was confirmed by Yeast two hybrid, while no interaction was found between AtMYB93 and AtMPK6 (data not shown).

6.4 Does *At*MYB93 function in suberin biosynthesis affect LR development?

Suberin lamellae form on endodermis cell walls, acting as a protective secondary cell wall for controlling water loss, nutrient leakage and for protecting plants from pathogens (Ursache *et al*.,2020). Previous studies also reported that degradation of suberin overlapping LRP was required for lateral root emergence, as an *abcg2*/*abcg6*/*abcg20* triple mutant was found to have decreased lateral root formation, displaying higher levels of suberin in *Arabidopsis* roots (Yadav *et al*., 2014). In addition, promoter of ABCG2, identified as potential target of AtMYB93 by Dr Clare Clayton has been demonstrated to be bound by AtMYB93 using agroinfiltration in tobacco leaves (data not shown). Moreover, another two R2R3 MYB transcription factors *At*MYB9 and *At*MYB107 were identified to be involved in suberin deposition in *Arabidopsis* seed coats, which regulated the permeability of the seed coat (Lashbrooke *et al*., 2016). A

recent study found that *At*MYB93 together with *At*MYB53, *At*MYB92 and *At*MYB41 participated in suberin lamellae formation in the *Arabidopsis* root, as overexpressing each of the four MYBs in the endodermis increased numbers of suberised cells in primary root (Shukla *et al*., 2021). An *Atmyb41*/*Atmyb53*/*Atmyb92* /*Atmyb93* quadruple mutant was reported to have no suberised cell, which suggested that *At*MYB93 was involved in suberin deposition in root but may work redundantly with the other three MYBs (Shukla *et al*., 2021). It may be hypothesised that the reduction of LRs observed in *At*MYB93 overexpression lines may depend on enhanced suberisation of endodermis cells overlapping lateral root primordium, leading to inhibition of lateral root emergence. However, given that the *Atmyb93* mutant shows an increase in LR density whilst the quadruple mutant does not (Shukla *et al*., 2021), nor does the *Atmyb53*/*Atmyb92* /*Atmyb93* triple mutant (Clare Clayton, unpublished data), it seems likely that *At*MYB93 has additional, unique functions during lateral root development independently of its role in suberin deposition. This was explored further in the RNAseq analysis of the *Atmyb93* mutant as described in the next section.

6.5 *At*MYB93 target genes

RNAseq analysis of *Atmyb93* mutant roots identified 14 potential direct transcriptional target genes of *At*MYB93 by comparing with a lateral root initiation expression profile (Voss *et al*., 2015), in which *AtMYB93* expression was upregulated at a specific time point. Among these, *AtGH9C3* and *AtCASPL1D2* were further identified as potential target genes, as putative *At*MYB93 binding motifs were present in their promoters. Subsequent qRT-PCR of these genes could be done to confirm their differences, along with LR assays in appropriate mutants and promoter binding assays between *At*MYB93 and the *At*GH9C3 and *At*CASPL1D2 promoters.

Previous studies revealed that *Arabidopsis AtGH9C1* was expressed mainly in roots and siliques and produced an endo β-1, 4 glucanase, which participated in the development of root hairs and endosperm (del Campillo *et al*., 2012). Tomato *SlGH9C1* was reported to bind to crystalline cellulose, suggest its potential ability to modulate cell walls (Urbanowicz *et al*., 2007). *AtGH9C3* encodes a glycosyl hydrolase may be involved in degradation of cellulose, leading to cell wall loosening or separation in *Arabidopsis.* and its expression was downregulated in *Atmyb93* mutant, which match with the increased lateral root density of *Atmyb93* mutant (Gibbs *et al*., 2014).

*At*CASPL1D2 from the CASPARIAN STRIP MEMBRANE DOMAIN Like family was also found to express in endodermis cells overlapping lateral root primordia throughout the lateral root development process, which is similar to the expression pattern of *At*MYB93 in *Arabidopsis* (Roppolo *et al*., 2014), which suggests that *At*CASPL1D2 expression may be partially upregulated by *At*MYB93, as its expression was induced more when AtMYB93 overexpressed during lateral root initiation than in the *Atmyb93* mutant. Thus, if *AtCASPL1D2* are *At*MYB93 target genes, it is likely that its expression is also regulated by other transcription factors.

To further study the relationship between *At*MYB93 and its potential target genes, Yeast one hybrid (Y1H) was applied to test interaction of *At*MYB93 and promoters of target genes, but has been so far unsuccessful. T-DNA mutants for *At*GH9C3 and *At*CASPL1D2 were ordered from NASC, but *Atcaspl1d2* mutant seeds cannot germinate in either soil or ½ MS, which suggests this T-DNA mutant line is lethal. The *Atgh9c3* mutant was genotyped (data not shown) and grown for harvesting more homozygous seeds for testing its lateral root development.

6.6 MYBs and sulphur metabolism

Within the RNAseq data, many genes involved in sulphur metabolism showed altered expression in *Atmyb93* mutant roots. In *Arabidopsis*, some R2R3 transcription factors have previously been reported to participate in sulphur metabolism. For example, six R2R3 MYBs (MYB28, MYB29, MYB76, MYB34, MYB51 and MYB122) were reported to activate expression of genes involving in sulphur assimilation, such as *ATP-SULFURYLASEs ATPS*s (*ATPS1* and *ATPS3*), *ADENOSIN 5'-PHOSPHOSUPHATE REDUCTASE*s APRs (*APR1*, *APR2* and *APR3*) and *APS KINASEs APK*s (*APK1* and *APK2*) by binding to their promoters respectively (Yatusevich *et al*., 2010). Interestingly, these MYBs, which were divided into two groups according to their function, were also found to regulate the biosynthesis of glucosinolates. MYB28, MYB29 and MYB76 participated in the biosynthesis of aliphatic glucosinolate, while MYB34, MYB51 and MYB122 were involved in indole glucosinolate biosynthesis (Frerigmann *et al*., 2016). This provides a theory on the function of *At*MYB93 in sulphur metabolism, where *At*MYB93 may bind to the promoter of *APR2* and activate its expression, which matches with the downregulation of APR2 in *Atmyb93* mutant. it is plausible to hypothesise that mutation of *At*MYB93 may increase glucosinolate in Arabidopsis root.

Since the expression of sulphate efflux transporters (SULTR1;3 and SULTR3;5) were down regulated, it is hypothesised that there would be increased sulphate content in root cells in the *Atmyb93* mutant, although only the shoot S content was tested in this study. One prediction is that more APS would then accumulate and be used for biosynthesis of glucosinolate, due to the downregulation of APR2, which aligns well with expression data of the other glucosinolate synthesis related genes *SDI2* (downregulated), *IGMT1* and *IGMT4* (upregulated). An accumulation of glucosinolate in the *Atmyb93* mutant would help plants to grow and survive in response to abiotic and biotic stress. It was reported that SULTR1;3 also

regulated flux of sulphate from cotyledons to roots. Thus, downregulation of SULTR1;3 in *Atmyb93* mutant may inhibit sulphate efflux from shoots, leading to accumulation of sulphate in shoots.

6.7 Conclusion and Future prospects

This project analysed the molecular mechanisms of lateral root development via MYB93 in both tomato and *Arabidopsis*. Three orthologues of *At*MYB93 in tomato have been identified, which share a similar root specific expression pattern with *At*MYB93 tomato. Stable homozygous transgenic tomato lines were generated to study their function, in which two *Sl*MYB93s (*SlMYB93-1*, *SlMYB93-2*) were overexpressed or silenced, respectively. The hairy root CRISPR lines of *SlMYB93-1* and *SlMYB93-2* have also been generated to study their function in a specific cell type, namely roots.

To further study *At*MYB93, RNAseq analysis was performed by NOVOGENE, which identified 255 Differentially Expressed Genes, covering a wide range of functions such as sugar transport, flavonoid synthesis, sulphur metabolism. By analysing this expression data, 14 genes were recognised as potential target genes of *At*MYB93, which were further screened by analysing promoters. MYB binding motifs were present in two genes, *AtGH9C3* and *AtCASPL1D2*, so it is hypothesised that *AtGH9C3* and *AtCASPL1D2* are direct transcriptional targets of AtMYB93. As a group of sulphur metabolism related genes has been identified from transcriptome data of the *Atmyb93* mutant, it is hypothesised that *At*MYB93 plays a role in sulphur metabolism. Both the *Atmyb93* mutant and *SlMYB93-1* RNAi line showed increased sulphur accumulation in shoots and leaves, respectively. In *Arabidopsi*s, the Atmyb93 mutant exhibited more sensitivity to both sulphur stress and O-acetyl serine treatment.

A great deal of research still needs to be done to further understand the function of MYB93s in lateral root development and sulphur metabolism. For *Sl*MYB93s, a suitable protocol of phenotyping transgenic plants or tissues should be applied to study their function. In *Arabidopsis*, ChIP-seq of *At*MYB93 (or targeted ChIP-PCR) should be conducted to construct the molecular network of *At*MYB93, which may be applied for crop improvement. For example, crops with much branching root system, which may enhance their tolerance in response to the dynamic changing environment and increase the yields, ultimately help with the challenge we are facing on food security.

Chapter Ⅶ: Reference

Aarabi, F., Kusajima, M., Tohge, T., Konishi, T., Gigolashvili, T., Takamune, M., Sasazaki, Y., Watanabe, M., Nakashita, H., Fernie, A.R. and Saito, K., 2016. Sulfur deficiency–induced repressor proteins optimize glucosinolate biosynthesis in plants. *Science advances*, *2*(10), p.e1601087.

Abe, H., Urao, T., Ito, T., Seki, M., Shinozaki, K. and Yamaguchi-Shinozaki, K., 2003. Arabidopsis AtMYC2 (bHLH) and AtMYB2 (MYB) function as transcriptional activators in abscisic acid signaling. *The Plant Cell*, *15*(1), pp.63-78.

"About FAO". Food and Agriculture Organization of the United Nations. Retrieved 31 December 2019. (website)

AbuQamar, S., Luo, H., Laluk, K., Mickelbart, M.V. and Mengiste, T., 2009. Crosstalk between biotic and abiotic stress responses in tomato is mediated by the AIM1 transcription factor. *The Plant Journal*, *58*(2), pp.347-360.

Aday, S. and Aday, M.S., 2020. Impact of COVID-19 on the food supply chain. *Food Quality and Safety*, *4*(4), pp.167-180.

Adetan, D.A., Adekoya, L.O. and Aluko, O.B., 2003. Characterisation of some properties of cassava root tubers. *Journal of Food Engineering*, *59*(4), pp.349-353.

Adikusuma, F., Piltz, S., Corbett, M.A., Turvey, M., McColl, S.R., Helbig, K.J., Beard, M.R., Hughes, J., Pomerantz, R.T. and Thomas, P.Q., 2018. Large deletions induced by Cas9 cleavage. *Nature*, *560*(7717), pp.E8-E9.

Agarwal, M., Hao, Y., Kapoor, A., Dong, C.H., Fujii, H., Zheng, X. and Zhu, J.K., 2006. A R2R3 type MYB transcription factor is involved in the cold regulation of CBF genes and in acquired freezing tolerance. *Journal of Biological Chemistry*, *281*(49), pp.37636-37645.

Akukwe, T.I., Oluoko-Odingo, A.A. and Krhoda, G.O., 2020. Do floods affect food security? A before-and-after comparative study of flood-affected households' food security status in South-Eastern Nigeria. *Bulletin of Geography. Socio-economic Series*, *47*(47), pp.115-131.

Alaguero-Cordovilla A, Gran-Gómez FJ, Tormos-Moltó S, Pérez-Pérez JM. Morphological characterization of root system architecture in diverse tomato genotypes during early growth. International journal of molecular sciences. 2018 Dec;19(12):3888.

An, J.P., Li, R., Qu, F.J., You, C.X., Wang, X.F. and Hao, Y.J., 2018. R2R3-MYB transcription factor Md MYB 23 is involved in the cold tolerance and proanthocyanidin accumulation in apple. *The Plant Journal*, *96*(3), pp.562-577.

An, J.P., Wang, X.F., Zhang, X.W., Xu, H.F., Bi, S.Q., You, C.X. and Hao, Y.J., 2020. An apple MYB transcription factor regulates cold tolerance and anthocyanin accumulation and undergoes MIEL1-mediated degradation. *Plant biotechnology journal*, *18*(2), pp.337-353.

Anders, S., Pyl, P.T. and Huber, W., 2015. HTSeq—a Python framework to work with high-throughput sequencing data. *Bioinformatics*, *31*(2), pp.166-169.

Araya, T., Miyamoto, M., Wibowo, J., Suzuki, A., Kojima, S., Tsuchiya, Y.N., Sawa, S., Fukuda, H., Von Wirén, N. and Takahashi, H., 2014. CLE-CLAVATA1 peptide-receptor signaling module regulates the expansion of plant root systems in a nitrogen-dependent manner. *Proceedings of the National Academy of Sciences*, *111*(5), pp.2029-2034.

Aubourg, S., Lecharny, A. and Bohlmann, J., 2002. Genomic analysis of the terpenoid synthase (AtTPS) gene family of Arabidopsis thaliana. *Molecular Genetics and Genomics*, *267*(6), pp.730-745.

Bajguz, A., Chmur, M. and Gruszka, D., 2020. Comprehensive overview of the brassinosteroid biosynthesis pathways: substrates, products, inhibitors, and connections. *Frontiers in plant science*, *11*, p.1034.

Balasubramanian, A., 2017. Soil erosion–causes and effects. *Centre forAdvanced Studies in Earth Science, University of Mysore, Mysore*.

Ballester, A.R., Molthoff, J., de Vos, R., Hekkert, B.T.L., Orzaez, D., Fernaŭndez-Moreno, J.P., Tripodi, P., Grandillo, S., Martin, C., Heldens, J. and Ykema, M., 2010. Biochemical and molecular analysis of pink tomatoes: deregulated expression of the gene encoding

transcription factor SlMYB12 leads to pink tomato fruit color. *Plant physiology*, *152*(1), pp.71-84.

Battat, M., Eitan, A., Rogachev, I., Hanhineva, K., Fernie, A., Tohge, T., Beekwilder, J. and Aharoni, A., 2019. A MYB triad controls primary and phenylpropanoid metabolites for pollen coat patterning. *Plant physiology*, *180*(1), pp.87-108.

Baud, S. and Lepiniec, L., 2009. Regulation of de novo fatty acid synthesis in maturing oilseeds of Arabidopsis. *Plant Physiology and Biochemistry*, *47*(6), pp.448-455.

Bellini, C., Pacurar, D.I. and Perrone, I., 2014. Adventitious roots and lateral roots: similarities and differences. *Annual review of plant biology*, *65*, pp.639-666.

Benfey, P.N. and Scheres, B., 2000. Root development. *Current Biology*, *10*(22), pp.R813-R815.

Berry, P.M., Baker, C.J., Hatley, D., Dong, R., Wang, X., Blackburn, G.A., Miao, Y., Sterling, M. and Whyatt, J.D., 2021. Development and application of a model for calculating the risk of stem and root lodging in maize. *Field Crops Research*, *262*, p.108037.

Bielecka, M., Watanabe, M., Morcuende, R., Scheible, W.R., Hawkesford, M.J., Hesse, H. and Hoefgen, R., 2015. Transcriptome and metabolome analysis of plant sulfate starvation and resupply provides novel information on transcriptional regulation of metabolism associated

with sulfur, nitrogen and phosphorus nutritional responses in Arabidopsis. *Frontiers in Plant Science*, *5*, p.805.

Bishop, G.J., Nomura, T., Yokota, T., Harrison, K., Noguchi, T., Fujioka, S., Takatsuto, S., Jones, J.D. and Kamiya, Y., 1999. The tomato DWARF enzyme catalyses C-6 oxidation in brassinosteroid biosynthesis. *Proceedings of the National Academy of Sciences*, *96*(4), pp.1761-1766.

Bogdanova, N. and Hell, R., 1997. Cysteine synthesis in plants: protein-protein interactions of serine acetyltransferase from Arabidopsis thaliana. *The Plant Journal*, *11*(2), pp.251-262.

Boyer, L.A., Latek, R.R. and Peterson, C.L., 2004. The SANT domain: a unique histone-tail-binding module?. *Nature reviews Molecular cell biology*, *5*(2), pp.158-163.

Brady, S.M., Orlando, D.A., Lee, J.Y., Wang, J.Y., Koch, J., Dinneny, J.R., Mace, D., Ohler, U. and Benfey, P.N., 2007. A high-resolution root spatiotemporal map reveals dominant expression patterns. *Science*, *318*(5851), pp.801-806.

Byrne, M.E., Barley, R., Curtis, M., Arroyo, J.M., Dunham, M., Hudson, A. and Martienssen, R.A., 2000. Asymmetric leaves1 mediates leaf patterning and stem cell function in Arabidopsis. *Nature*, *408*(6815), pp.967-971.

Cao, Y., Tang, X., Giovannoni, J., Xiao, F. and Liu, Y., 2012. Functional characterization of a tomato COBRA-like gene functioning in fruit development and ripening. *BMC plant biology*, *12*(1), pp.1-15.

Cao, H., Chen, J., Yue, M., Xu, C., Jian, W., Liu, Y., Song, B., Gao, Y., Cheng, Y. and Li, Z., 2020. Tomato transcriptional repressor MYB70 directly regulates ethylene-dependent fruit ripening. *Plant J*, *104*, pp.1568-1581.

Casimiro, I., Beeckman, T., Graham, N., Bhalerao, R., Zhang, H., Casero, P., Sandberg, G. and Bennett, M.J., 2003. Dissecting Arabidopsis lateral root development. *Trends in plant science*, *8*(4), pp.165-171.

Castaneda, R., Doan, D., Newhouse, D.L., Nguyen, M., Uematsu, H. and Azevedo, J.P., 2016. Who are the poor in the developing world?. *World Bank Policy Research Working Paper*, (7844).

Chen, H.Y., Huh, J.H., Yu, Y.C., Ho, L.H., Chen, L.Q., Tholl, D., Frommer, W.B. and Guo, W.J., 2015. The Arabidopsis vacuolar sugar transporter SWEET 2 limits carbon sequestration from roots and restricts Pythium infection. *The Plant Journal*, *83*(6), pp.1046-1058.

Cheng, H., Song, S., Xiao, L., Soo, H.M., Cheng, Z., Xie, D. and Peng, J., 2009. Gibberellin acts through jasmonate to control the expression of MYB21, MYB24, and MYB57 to promote stamen filament growth in Arabidopsis. *PLoS genetics*, *5*(3), p.e1000440.

Chezem, W.R., Memon, A., Li, F.S., Weng, J.K. and Clay, N.K., 2017. SG2-type R2R3-MYB transcription factor MYB15 controls defense-induced lignification and basal immunity in Arabidopsis. *The Plant Cell*, *29*(8), pp.1907-1926.

Cole, M.B., Augustin, M.A., Robertson, M.J. and Manners, J.M., 2018. The science of food security. *npj Science of Food*, *2*(1), pp.1-8.

Coates, J.C., Laplaze, L. and Haseloff, J., 2006. Armadillo-related proteins promote lateral root development in Arabidopsis. *Proceedings of the National Academy of Sciences*, *103*(5), pp.1621-1626.

Crandall, S.G., Gold, K.M., Jiménez-Gasco, M.D.M., Filgueiras, C.C. and Willett, D.S., 2020. A multi-omics approach to solving problems in plant disease ecology. *Plos one*, *15*(9), p.e0237975.

Crooks, G.E., Hon, G., Chandonia, J.M. and Brenner, S.E., 2004. WebLogo: a sequence logo generator. *Genome research*, *14*(6), pp.1188-1190.

Cui, M.H., Yoo, K.S., Hyoung, S., Nguyen, H.T.K., Kim, Y.Y., Kim, H.J., Ok, S.H., Yoo, S.D. and Shin, J.S., 2013. An Arabidopsis R2R3-MYB transcription factor, AtMYB20, negatively regulates type 2C serine/threonine protein phosphatases to enhance salt tolerance. *Febs Letters*, *587*(12), pp.1773-1778.

Dan, H., Yang, G. and Zheng, Z.L., 2007. A negative regulatory role for auxin in sulphate deficiency response in Arabidopsis thaliana. *Plant molecular biology*, *63*(2), pp.221-235.

Davidian, J.C. and Kopriva, S., 2010. Regulation of sulfate uptake and assimilation—the same or not the same?. *Molecular plant*, *3*(2), pp.314-325.

del Campillo, E., Gaddam, S., Mettle-Amuah, D. and Heneks, J., 2012. A tale of two tissues: AtGH9C1 is an endo-β-1, 4-glucanase involved in root hair and endosperm development in Arabidopsis. *PLoS One*, *7*(11), p.e49363.

DeRose-Wilson, L.J. and Gaut, B.S., 2007. Transcription-related mutations and GC content drive variation in nucleotide substitution rates across the genomes of Arabidopsis thaliana and Arabidopsis lyrata. *BMC Evolutionary Biology*, *7*(1), pp.1-12.

De Smet, I., Vanneste, S., Inzé, D. and Beeckman, T., 2006. Lateral root initiation or the birth of a new meristem. *Plant molecular biology*, *60*(6), pp.871-887.

Devereux, S., 2007. The impact of droughts and floods on food security and policy options to alleviate negative effects. *Agricultural Economics*, *37*, pp.47-58.

Dolan, L., Janmaat, K., Willemsen, V., Linstead, P., Poethig, S., Roberts, K. and Scheres, B., 1993. Cellular organisation of the Arabidopsis thaliana root. *Development*, *119*(1), pp.71-84.

Dong, W., Wang, Y. and Takahashi, H., 2019. CLE-CLAVATA1 signaling pathway modulates lateral root development under sulfur deficiency. *Plants*, *8*(4), p.103.

Dreher, K. and Callis, J., 2007. Ubiquitin, hormones and biotic stress in plants. *Annals of botany*, *99*(5), pp.787-822.

Du, H., Zhang, L., Liu, L., Tang, X.F., Yang, W.J., Wu, Y.M., Huang, Y.B. and Tang, Y.X., 2009. Biochemical and molecular characterization of plant MYB transcription factor family. *Biochemistry (Moscow)*, *74*(1), pp.1-11.

Du, H., Liang, Z., Zhao, S., Nan, M.G., Tran, L.S.P., Lu, K., Huang, Y.B. and Li, J.N., 2015. The evolutionary history of R2R3-MYB proteins across 50 eukaryotes: new insights into subfamily classification and expansion. Scientific reports, 5(1), pp.1-16.

Du, Y. and Scheres, B., 2018. Lateral root formation and the multiple roles of auxin. *Journal of Experimental Botany*, *69*(2), pp.155-167.

Dubos, C., Stracke, R., Grotewold, E., Weisshaar, B., Martin, C. and Lepiniec, L., 2010. MYB transcription factors in Arabidopsis. *Trends in plant science*, *15*(10), pp.573-581.

Engler, C., Kandzia, R. and Marillonnet, S., 2008. A one pot, one step, precision cloning method with high throughput capability. *PloS one*, *3*(11), p.e3647.

Ezura, H., 2009. Tomato is a next-generation model plant for research and development. *Journal of the Japanese Society for Horticultural Science*, *78*(1), pp.1-2.

Feller, A., Machemer, K., Braun, E.L. and Grotewold, E., 2011. Evolutionary and comparative analysis of MYB and bHLH plant transcription factors. *The Plant Journal*, *66*(1), pp.94-116.

Feng, C.Z., Luo, Y.X., Wang, P.D., Gilliham, M. and Long, Y., 2021. MYB77 regulates high-affinity potassium uptake by promoting expression of HAK5. *New Phytologist*.

Fraanje, W., & Lee-Gammage, S. (2018). What is food security? (Foodsource: building blocks). Food Climate Research Network, University of Oxford.

FAO. The state of food security and nutrition in the world. (2020)

FAO. Trade Reforms and Food Security: Conceptualizing the Linkages. (Food and Agriculture Organization of the United Nations, 2003)

FAO. Healthy soil are the basis for healthy food production. (2015), viewed 22nd July, 2021, < http://www.fao.org/3/i4405e/i4405e.pdf >

FAO and ITPS*. Status of the World's Soils. Food and Agriculture Organization of the United Nations and Intergovernmental Technical Panel on Soils, Rome, Italy (2015)*

Fichtner, F. and Lunn, J.E., 2021. The role of trehalose 6-phosphate (Tre6P) in plant metabolism and development. *Annual Review of Plant Biology*, *72*.

Figueroa, C.M., Feil, R., Ishihara, H., Watanabe, M., Kölling, K., Krause, U., Höhne, M., Encke, B., Plaxton, W.C., Zeeman, S.C. and Li, Z., 2016. Trehalose 6–phosphate coordinates organic and amino acid metabolism with carbon availability. *The Plant Journal*, *85*(3), pp.410-423.

Flütsch, S. and Santelia, D., 2021. Mesophyll-derived sugars are positive regulators of light-driven stomatal opening. *New Phytologist*, *230*(5), pp.1754-1760.

Foodlist News 2015, *Myanmar Floods – 1 Million Affected, 100 Dead – Crop Damage Increases Fear of Food Shortages*, Foodlist, viewed 2 March 2021, < http://floodlist.com/asia/myanmar-floods-1-million-affected-100-dead-food-shortages>

Forde, B. and Lorenzo, H., 2001. The nutritional control of root development. *Plant and soil*, *232*(1), pp.51-68.

Frerigmann, H., Piślewska-Bednarek, M., Sánchez-Vallet, A., Molina, A., Glawischnig, E., Gigolashvili, T. and Bednarek, P., 2016. Regulation of pathogen-triggered tryptophan metabolism in Arabidopsis thaliana by MYB transcription factors and indole glucosinolate conversion products. *Molecular Plant*, *9*(5), pp.682-695.

Fujiishi, M., Maejima, E. and Watanabe, T., 2019. Effect of mixed cropping with lupin (Lupinus albus L.) on growth and nitrogen uptake in pasture grasses grown under manure application. *Archives of agronomy and soil science*.

Gabrielsen, O.S., Sentenac, A. and Fromageot, P., 1991. Specific DNA binding by c-Myb: evidence for a double helix-turn-helix-related motif. *Science*, *253*(5024), pp.1140-1143.

Gan, Y., Filleur, S., Rahman, A., Gotensparre, S. and Forde, B.G., 2005. Nutritional regulation of ANR1 and other root-expressed MADS-box genes in Arabidopsis thaliana. *Planta*, *222*(4), pp.730-742.

Gan, Y., Bernreiter, A., Filleur, S., Abram, B. and Forde, B.G., 2012. Overexpressing the ANR1 MADS-box gene in transgenic plants provides new insights into its role in the nitrate regulation of root development. *Plant and Cell Physiology*, *53*(6), pp.1003-1016.

Gao, R., Gruber, M.Y., Amyot, L. and Hannoufa, A., 2018. SPL13 regulates shoot branching and flowering time in Medicago sativa. *Plant molecular biology*, *96*(1), pp.119-133.

Gao, Y., Li, X., Tian, Q.Y., Wang, B.L. and Zhang, W.H., 2016. Sulfur deficiency had different effects on Medicago truncatula ecotypes A17 and R108 in terms of growth, root morphology and nutrient contents. *Journal of Plant Nutrition*, *39*(3), pp.301-314.

Gates, D.J., Strickler, S.R., Mueller, L.A., Olson, B.J. and Smith, S.D., 2016. Diversification of R2R3-MYB transcription factors in the tomato family Solanaceae. *Journal of molecular evolution*, *83*(1), pp.26-37.

Giaquinta, R.T., 1979. Sucrose translocation and storage in the sugar beet. *Plant Physiology*, *63*(5), pp.828-832.

Gigolashvili, T. and Kopriva, S., 2014. Transporters in plant sulfur metabolism. *Frontiers in Plant Science*, *5*, p.442.

Gläser, K., Kanawati, B., Kubo, T., Schmitt-Kopplin, P. and Grill, E., 2014. Exploring the A rabidopsis sulfur metabolome. *The Plant Journal*, *77*(1), pp.31-45.

González, E. and Joly, S., 2013. Impact of RNA-seq attributes on false positive rates in differential expression analysis of de novo assembled transcriptomes. *BMC Research Notes*, *6*(1), pp.1-8.

Gregory, P.J., Ingram, J.S. and Brklacich, M., 2005. Climate change and food security. *Philosophical Transactions of the Royal Society B: Biological Sciences*, *360*(1463), pp.2139-2148.

Gross, M., 2014. Plant science called up to provide food security.

Gruber, B.D., Giehl, R.F., Friedel, S. and von Wirén, N., 2013. Plasticity of the Arabidopsis root system under nutrient deficiencies. *Plant physiology*, *163*(1), pp.161-179.

Gubler, F., Chandler, P.M., White, R.G., Llewellyn, D.J. and Jacobsen, J.V., 2002. Gibberellin signaling in barley aleurone cells. Control of SLN1 and GAMYB expression. *Plant Physiology*, *129*(1), pp.191-200.

Gubler, F., Kalla, R., Roberts, J.K. and Jacobsen, J.V., 1995. Gibberellin-regulated expression of a myb gene in barley aleurone cells: evidence for Myb transactivation of a high-pI alpha-amylase gene promoter. *The Plant Cell*, *7*(11), pp.1879-1891.

Guo, H.S., Fei, J.F., Xie, Q. and Chua, N.H., 2003. A chemical-regulated inducible RNAi system in plants. *The Plant Journal*, *34*(3), pp.383-392.

Gutierrez, L., Mongelard, G., Floková, K., Păcurar, D.I., Novák, O., Staswick, P., Kowalczyk, M., Păcurar, M., Demailly, H., Geiss, G. and Bellini, C., 2012. Auxin controls Arabidopsis adventitious root initiation by regulating jasmonic acid homeostasis. *The Plant Cell*, *24*(6), pp.2515-2527.

Guttman, M., Garber, M., Levin, J.Z., Donaghey, J., Robinson, J., Adiconis, X., Fan, L., Koziol, M.J., Gnirke, A., Nusbaum, C. and Rinn, J.L., 2010. Ab initio reconstruction of cell type–specific transcriptomes in mouse reveals the conserved multi-exonic structure of lincRNAs. *Nature biotechnology*, *28*(5), pp.503-510.

Hall, C., Dawson, T.P., Macdiarmid, J.I., Matthews, R.B. and Smith, P., 2017. The impact of population growth and climate change on food security in Africa: looking ahead to 2050. *International Journal of Agricultural Sustainability*, *15*(2), pp.124-135.

Harvey, C.A., Medina, A., Sánchez, D.M., Vílchez, S., Hernández, B., Saenz, J.C., Maes, J.M., Casanoves, F. and Sinclair, F.L., 2006. Patterns of animal diversity in different forms of tree cover in agricultural landscapes. *Ecological applications*, *16*(5), pp.1986-1999.

Hasanuzzaman, M., Nahar, K., Anee, T.I. and Fujita, M., 2017. Glutathione in plants: biosynthesis and physiological role in environmental stress tolerance. *Physiology and Molecular Biology of Plants*, *23*(2), pp.249-268.

Heldt, H.W. and Piechulla, B., 2021. *Plant biochemistry*. Academic Press.

Taiz, L., Zeiger, E., Møller, I.M. and Murphy, A., 2015. *Plant physiology and development* (No. Ed. 6). Sinauer Associates Incorporated.

Hellens, R., Mullineaux, P. and Klee, H., 2000. Technical focus: a guide to Agrobacterium binary Ti vectors. *Trends in plant science*, *5*(10), pp.446-451.

Hirai, M.Y., Fujiwara, T., Awazuhara, M., Kimura, T., Noji, M. and Saito, K., 2003. Global expression profiling of sulfur-starved Arabidopsis by DNA macroarray reveals the role of O-

acetyl-l-serine as a general regulator of gene expression in response to sulfur nutrition. *The Plant Journal*, *33*(4), pp.651-663.

Hirai, M.Y., Sugiyama, K., Sawada, Y., Tohge, T., Obayashi, T., Suzuki, A., Araki, R., Sakurai, N., Suzuki, H., Aoki, K. and Goda, H., 2007. Omics-based identification of Arabidopsis Myb transcription factors regulating aliphatic glucosinolate biosynthesis. *Proceedings of the National Academy of Sciences*, *104*(15), pp.6478-6483.

Hose, E., Clarkson, D.T., Steudle, E., Schreiber, L. and Hartung, W., 2001. The exodermis: a variable apoplastic barrier. *Journal of Experimental Botany*, *52*(365), pp.2245-2264.

Hu, S., Yu, Y., Chen, Q., Mu, G., Shen, Z. and Zheng, L., 2017. OsMYB45 plays an important role in rice resistance to cadmium stress. *Plant Science*, *264*, pp.1-8.

Huang, H., Gong, Y., Liu, B., Wu, D., Zhang, M., Xie, D. and Song, S., 2020. The DELLA proteins interact with MYB21 and MYB24 to regulate filament elongation in Arabidopsis. *BMC plant biology*, *20*(1), pp.1-9.

Huang, K.L., Ma, G.J., Zhang, M.L., Xiong, H., Wu, H., Zhao, C.Z., Liu, C.S., Jia, H.X., Chen, L., Kjorven, J.O. and Li, X.B., 2018. The ARF7 and ARF19 transcription factors positively regulate PHOSPHATE STARVATION RESPONSE1 in Arabidopsis roots. *Plant Physiology*, *178*(1), pp.413-427.

Hubberten, H.M., Klie, S., Caldana, C., Degenkolbe, T., Willmitzer, L. and Hoefgen, R., 2012. Additional role of O-acetylserine as a sulfur status-independent regulator during plant growth. *The Plant Journal*, *70*(4), pp.666-677.

IEA (2020), *Global Energy Review 2020*, IEA, Paris https://www.iea.org/reports/global-energy-review-2020

Iorizzo, M., Ellison, S., Senalik, D., Zeng, P., Satapoomin, P., Huang, J., Bowman, M., Iovene, M., Sanseverino, W., Cavagnaro, P. and Yildiz, M., 2016. A high-quality carrot genome assembly provides new insights into carotenoid accumulation and asterid genome evolution. *Nature genetics*, *48*(6), pp.657-666.

James, P., Halladay, J. and Craig, E.A., 1996. Genomic libraries and a host strain designed for highly efficient two-hybrid selection in yeast. *Genetics*, *144*(4), pp.1425-1436.

Jia, L., Clegg, M.T. and Jiang, T., 2004. Evolutionary dynamics of the DNA-binding domains in putative R2R3-MYB genes identified from rice subspecies indica and japonica genomes. *Plant Physiology*, *134*(2), pp.575-585.

Jia, Y.B., Yang, X.E., Feng, Y. and Jilani, G., 2008. Differential response of root morphology to potassium deficient stress among rice genotypes varying in potassium efficiency. *Journal of Zhejiang University Science B*, *9*(5), pp.427-434.

Jia, X., Liu, P. and Lynch, J.P., 2018. Greater lateral root branching density in maize improves phosphorus acquisition from low phosphorus soil. *Journal of Experimental Botany*, *69*(20), pp.4961-4970.

Jian, W., Cao, H., Yuan, S., Liu, Y., Lu, J., Lu, W., Li, N., Wang, J., Zou, J., Tang, N. and Xu, C., 2019. SlMYB75, an MYB-type transcription factor, promotes anthocyanin accumulation and enhances volatile aroma production in tomato fruits. *Horticulture research*, *6*(1), pp.1-15.

Jin, H. and Martin, C., 1999. Multifunctionality and diversity within the plant MYB-gene family. *Plant molecular biology*, *41*(5), pp.577-585.

Jung, C., Seo, J.S., Han, S.W., Koo, Y.J., Kim, C.H., Song, S.I., Nahm, B.H., Do Choi, Y. and Cheong, J.J., 2008. Overexpression of AtMYB44 enhances stomatal closure to confer abiotic stress tolerance in transgenic Arabidopsis. *Plant physiology*, *146*(2), pp.623-635.

Kacjan Maršić, N., Može, K.S., Mihelič, R., Nečemer, M., Hudina, M. and Jakopič, J., 2021. Nitrogen and Sulphur Fertilisation for Marketable Yields of Cabbage (Brassica oleracea L. var. Capitata), Leaf Nitrate and Glucosinolates and Nitrogen Losses Studied in a Field Experiment in Central Slovenia. *Plants*, *10*(7), p.1304.

Kajala, K., Gouran, M., Shaar-Moshe, L., Mason, G.A., Rodriguez-Medina, J., Kawa, D., Pauluzzi, G., Reynoso, M., Canto-Pastor, A., Manzano, C. and Lau, V., 2021. Innovation,

conservation, and repurposing of gene function in root cell type development. *Cell*, *184*(12), pp.3333-3348.

Kanehisa, M., Araki, M., Goto, S., Hattori, M., Hirakawa, M., Itoh, M., Katayama, T., Kawashima, S., Okuda, S., Tokimatsu, T. and Yamanishi, Y., 2007. KEGG for linking genomes to life and the environment. *Nucleic acids research*, *36*(suppl_1), pp.D480-D484.

Kang, Y.H., Kirik, V., Hulskamp, M., Nam, K.H., Hagely, K., Lee, M.M. and Schiefelbein, J., 2009. The MYB23 gene provides a positive feedback loop for cell fate specification in the Arabidopsis root epidermis. *The Plant Cell*, *21*(4), pp.1080-1094.

Kaul, S., Koo, H.L., Jenkins, J., Rizzo, M., Rooney, T., Tallon, L.J., Feldblyum, T., Nierman, W., Benito, M.I., Lin, X. and Town, C.D., 2000. Analysis of the genome sequence of the flowering plant Arabidopsis thaliana. *nature*, *408*(6814), pp.796-815.

Kataoka, T., Hayashi, N., Yamaya, T. and Takahashi, H., 2004. Root-to-shoot transport of sulfate in Arabidopsis. Evidence for the role of SULTR3; 5 as a component of low-affinity sulfate transport system in the root vasculature. *Plant physiology*, *136*(4), pp.4198-4204.

Kessler, D., 2006. Enzymatic activation of sulfur for incorporation into biomolecules in prokaryotes. *FEMS microbiology reviews*, *30*(6), pp.825-840.

Kim, D., Paggi, J.M., Park, C., Bennett, C. and Salzberg, S.L., 2019. Graph-based genome alignment and genotyping with HISAT2 and HISAT-genotype. *Nature biotechnology*, *37*(8), pp.907-915.

Kim, M.J., Ciani, S. and Schachtman, D.P., 2010. A peroxidase contributes to ROS production during Arabidopsis root response to potassium deficiency. *Molecular plant*, *3*(2), pp.420-427.

Kim, S.H., Lam, P.Y., Lee, M.H., Jeon, H.S., Tobimatsu, Y. and Park, O.K., 2020. The Arabidopsis R2R3 MYB transcription factor MYB15 is a key regulator of lignin biosynthesis in effector-triggered immunity. *Frontiers in plant science*, *11*, p.1456.

Kimura, S. and Sinha, N., 2008. Tomato (Solanum lycopersicum): a model fruit-bearing crop. *Cold Spring Harbor Protocols*, *2008*(11), pp.pdb-emo105.

Kirik, V., Lee, M.M., Wester, K., Herrmann, U., Zheng, Z., Oppenheimer, D., Schiefelbein, J. and Hulskamp, M., 2005. Functional diversification of MYB23 and GL1 genes in trichome morphogenesis and initiation.

Kishi-Kaboshi, M., Seo, S., Takahashi, A. and Hirochika, H., 2018. The MAMP-responsive MYB transcription factors MYB30, MYB55 and MYB110 activate the HCAA synthesis pathway and enhance immunity in Rice. *Plant and Cell Physiology*, *59*(5), pp.903-915.

Klempnauer, K.H., Gonda, T.J. and Bishop, J.M., 1982. Nucleotide sequence of the retroviral leukemia gene v-myb and its cellular progenitor c-myb: the architecture of a transduced oncogene. *Cell*, *31*(2), pp.453-463.

Klepek, Y.S., Volke, M., Konrad, K.R., Wippel, K., Hoth, S., Hedrich, R. and Sauer, N., 2010. Arabidopsis thaliana POLYOL/MONOSACCHARIDE TRANSPORTERS 1 and 2: fructose and xylitol/H+ symporters in pollen and young xylem cells. *Journal of experimental botany*, *61*(2), pp.537-550.

Ko, J.H., Kim, W.C. and Han, K.H., 2009. Ectopic expression of MYB46 identifies transcriptional regulatory genes involved in secondary wall biosynthesis in Arabidopsis. *The Plant Journal*, *60*(4), pp.649-665.

Kong, X., Zhang, C., Zheng, H., Sun, M., Zhang, F., Zhang, M., Cui, F., Lv, D., Liu, L., Guo, S. and Zhang, Y., 2020. Antagonistic interaction between auxin and SA signaling pathways regulates bacterial infection through lateral root in Arabidopsis. *Cell Reports*, *32*(8), p.108060.

Koornneef, M. and Meinke, D., 2010. The development of Arabidopsis as a model plant. *The Plant Journal*, *61*(6), pp.909-921.

Kopittke, P.M., Menzies, N.W., Wang, P., McKenna, B.A. and Lombi, E., 2019. Soil and the intensification of agriculture for global food security. *Environment International*, *132*, p.105078.

Kopriva, S., 2006. Regulation of sulfate assimilation in Arabidopsis and beyond. *Annals of botany*, *97*(4), pp.479-495.

Koprivova, A., Suter, M., den Camp, R.O., Brunold, C. and Kopriva, S., 2000. Regulation of sulfate assimilation by nitrogen in Arabidopsis. *Plant Physiology*, *122*(3), pp.737-746.

Kosicki, M., Tomberg, K. and Bradley, A., 2018. Repair of double-strand breaks induced by CRISPR–Cas9 leads to large deletions and complex rearrangements. *Nature biotechnology*, *36*(8), pp.765-771.

Kranz, H.D., Denekamp, M., Greco, R., Jin, H., Leyva, A., Meissner, R.C., Petroni, K., Urzainqui, A., Bevan, M., Martin, C. and Smeekens, S., 1998. Towards functional characterisation of the members of the R2R3-MYB gene family from Arabidopsis thaliana. *The Plant Journal*, *16*(2), pp.263-276.

Kutz, A., Müller, A., Hennig, P., Kaiser, W.M., Piotrowski, M. and Weiler, E.W., 2002. A role for nitrilase 3 in the regulation of root morphology in sulphur-starving Arabidopsis thaliana. *The Plant Journal*, *30*(1), pp.95-106.

Lal, R., 2015. Restoring soil quality to mitigate soil degradation. *Sustainability*, *7*(5), pp.5875-5895.

Lashbrooke, J., Cohen, H., Levy-Samocha, D., Tzfadia, O., Panizel, I., Zeisler, V., Massalha, H., Stern, A., Trainotti, L., Schreiber, L. and Costa, F., 2016. MYB107 and MYB9 homologs regulate suberin deposition in angiosperms. *The Plant Cell*, *28*(9), pp.2097-2116.

Lau, H., Khosrawipour, V., Kocbach, P., Mikolajczyk, A., Schubert, J., Bania, J. and Khosrawipour, T., 2020. The positive impact of lockdown in Wuhan on containing the COVID-19 outbreak in China. *Journal of travel medicine*, *27*(3), p.taaa037.

Legay, S., Guerriero, G., André, C., Guignard, C., Cocco, E., Charton, S., Boutry, M., Rowland, O. and Hausman, J.F., 2016. MdMyb93 is a regulator of suberin deposition in russeted apple fruit skins. *New Phytologist*, *212*(4), pp.977-991.

Leibman-Markus, M., Pizarro, L., Schuster, S., Lin, Z.D., Gershony, O., Bar, M., Coaker, G. and Avni, A., 2018. The intracellular nucleotide-binding leucine-rich repeat receptor (SlNRC4a) enhances immune signalling elicited by extracellular perception. *Plant, cell & environment*, *41*(10), pp.2313-2327.

Leustek, T. and Saito, K., 1999. Sulfate transport and assimilation in plants. *Plant physiology*, *120*(3), pp.637-644.

Li, B., Fan, R., Guo, S., Wang, P., Zhu, X., Fan, Y., Chen, Y., He, K., Kumar, A., Shi, J. and Wang, Y., 2019. The Arabidopsis MYB transcription factor, MYB111 modulates salt responses by regulating flavonoid biosynthesis. *Environmental and Experimental Botany*, *166*, p.103807.

Li, H., Ding, Y., Shi, Y., Zhang, X., Zhang, S., Gong, Z. and Yang, S., 2017. MPK3-and MPK6-mediated ICE1 phosphorylation negatively regulates ICE1 stability and freezing tolerance in Arabidopsis. *Developmental cell*, *43*(5), pp.630-642.

Li, J., Wu, W.H. and Wang, Y., 2017. Potassium channel AKT1 is involved in the auxin-mediated root growth inhibition in Arabidopsis response to low K+ stress. *Journal of integrative plant biology*, *59*(12), pp.895-909.

Li, Q., Liu, G.B., Zhang, Z., Tuo, D.F., Bai, R.R. and Qiao, F.F., 2017. Relative contribution of root physical enlacing and biochemistrical exudates to soil erosion resistance in the Loess soil. *Catena*, *153*, pp.61-65.

Li, Z., Peng, R., Tian, Y., Han, H., Xu, J. and Yao, Q., 2016. Genome-wide identification and analysis of the MYB transcription factor superfamily in Solanum lycopersicum. *Plant and Cell Physiology*, *57*(8), pp.1657-1677.

Liberman, L.M., Sparks, E.E., Moreno-Risueno, M.A., Petricka, J.J. and Benfey, P.N., 2015. MYB36 regulates the transition from proliferation to differentiation in the Arabidopsis root. *Proceedings of the National Academy of Sciences*, *112*(39), pp.12099-12104.

Lima, J.E., Benedito, V.A., Figueira, A. and Peres, L.E.P., 2009. Callus, shoot and hairy root formation in vitro as affected by the sensitivity to auxin and ethylene in tomato mutants. *Plant cell reports*, *28*(8), pp.1169-1177.

Lima, J.E., Kojima, S., Takahashi, H. and von Wirén, N., 2010. Ammonium triggers lateral root branching in Arabidopsis in an AMMONIUM TRANSPORTER1; 3-dependent manner. *The Plant Cell*, *22*(11), pp.3621-3633.

Loudet, O., Saliba-Colombani, V., Camilleri, C., Calenge, F., Gaudon, V., Koprivova, A., North, K.A., Kopriva, S. and Daniel-Vedele, F., 2007. Natural variation for sulfate content in Arabidopsis thaliana is highly controlled by APR2. *Nature genetics*, *39*(7), pp.896-900.

Ludwig-Müller, J., 2011. Auxin conjugates: their role for plant development and in the evolution of land plants. *Journal of experimental botany*, *62*(6), pp.1757-1773.

Lunn, J.E., Delorge, I., Figueroa, C.M., Van Dijck, P. and Stitt, M., 2014. Trehalose metabolism in plants. *The Plant Journal*, *79*(4), pp.544-567.

Lux, A. and Rost, T.L., 2012. Plant root research: the past, the present and the future. *Annals of botany*, *110*(2), pp.201-204.

Malamy, J.E. and Benfey, P.N., 1997. Organization and cell differentiation in lateral roots of Arabidopsis thaliana. *Development*, *124*(1), pp.33-44.

Mallah, S.I., Ghorab, O.K., Al-Salmi, S., Abdellatif, O.S., Tharmaratnam, T., Iskandar, M.A., Sefen, J.A.N., Sidhu, P., Atallah, B., El-Lababidi, R. and Al-Qahtani, M., 2021. COVID-19: breaking down a global health crisis. *Annals of clinical microbiology and antimicrobials*, *20*(1), pp.1-36.

Mann, J. and Truswell, A.S. eds., 2017. *Essentials of human nutrition*. Oxford University Press.

Mao, G., Meng, X., Liu, Y., Zheng, Z., Chen, Z. and Zhang, S., 2011. Phosphorylation of a WRKY transcription factor by two pathogen-responsive MAPKs drives phytoalexin biosynthesis in Arabidopsis. *The Plant Cell*, *23*(4), pp.1639-1653.

Marschner, H., 2011. *Marschner's mineral nutrition of higher plants*. Academic press.

Maruyama-Nakashita, A., Nakamura, Y., Tohge, T., Saito, K. and Takahashi, H., 2006. Arabidopsis SLIM1 is a central transcriptional regulator of plant sulfur response and metabolism. *The Plant Cell*, *18*(11), pp.3235-3251.

Meng, X., Xu, J., He, Y., Yang, K.Y., Mordorski, B., Liu, Y. and Zhang, S., 2013. Phosphorylation of an ERF transcription factor by Arabidopsis MPK3/MPK6 regulates plant defense gene induction and fungal resistance. *The Plant Cell*, *25*(3), pp.1126-1142.

Meng, X., Yang, D., Li, X., Zhao, S., Sui, N. and Meng, Q., 2015. Physiological changes in fruit ripening caused by overexpression of tomato SlAN2, an R2R3-MYB factor. *Plant Physiology and Biochemistry*, *89*, pp.24-30.

Mengiste, T., Chen, X., Salmeron, J. and Dietrich, R., 2003. The BOTRYTIS SUSCEPTIBLE1 gene encodes an R2R3MYB transcription factor protein that is required for biotic and abiotic stress responses in Arabidopsis. *The Plant Cell*, *15*(11), pp.2551-2565

Meier, M., Liu, Y., Lay-Pruitt, K.S., Takahashi, H. and von Wirén, N., 2020. Auxin-mediated root branching is determined by the form of available nitrogen. *Nature Plants*, *6*(9), pp.1136-1145.

Meissner, R., Jacobson, Y., Melamed, S., Levyatuv, S. and Levy, A., 2010. A new model system for tomato genetics. *The Plant Journal, 12*(6), pp.1465-1472.

Mi, H., Muruganujan, A., Ebert, D., Huang, X. and Thomas, P.D., 2019. PANTHER version 14: more genomes, a new PANTHER GO-slim and improvements in enrichment analysis tools. *Nucleic acids research*, *47*(D1), pp.D419-D426.

Misra, P., Pandey, A., Tiwari, M., Chandrashekar, K., Sidhu, O.P., Asif, M.H., Chakrabarty, D., Singh, P.K., Trivedi, P.K., Nath, P. and Tuli, R., 2010. Modulation of transcriptome and metabolome of tobacco by Arabidopsis transcription factor, AtMYB12, leads to insect resistance. *Plant Physiology*, *152*(4), pp.2258-2268.

Morkunas, I., Woźniak, A., Mai, V.C., Rucińska-Sobkowiak, R. and Jeandet, P., 2018. The role of heavy metals in plant response to biotic stress. *Molecules*, *23*(9), p.2320.

Mu, R.L., Cao, Y.R., Liu, Y.F., Lei, G., Zou, H.F., Liao, Y., Wang, H.W., Zhang, W.K., Ma, B., Du, J.Z. and Yuan, M., 2009. An R2R3-type transcription factor gene AtMYB59 regulates root growth and cell cycle progression in Arabidopsis. *Cell research*, *19*(11), pp.1291-1304.

Mugford, S.G., Yoshimoto, N., Reichelt, M., Wirtz, M., Hill, L., Mugford, S.T., Nakazato, Y., Noji, M., Takahashi, H., Kramell, R. and Gigolashvili, T., 2009. Disruption of adenosine-5'-phosphosulfate kinase in Arabidopsis reduces levels of sulfated secondary metabolites. *The Plant Cell*, *21*(3), pp.910-927.

Müller, J., Gödde, V., Niehaus, K. and Zörb, C., 2015. Metabolic adaptations of white lupin roots and shoots under phosphorus deficiency. *Frontiers in plant science*, *6*, p.1014.

Müller, J., Toev, T., Heisters, M., Teller, J., Moore, K.L., Hause, G., Dinesh, D.C., Bürstenbinder, K. and Abel, S., 2015. Iron-dependent callose deposition adjusts root meristem maintenance to phosphate availability. *Developmental cell*, *33*(2), pp.216-230.

Muoni, T., Koomson, E., Öborn, I., Marohn, C., Watson, C.A., Bergkvist, G., Barnes, A., Cadisch, G. and Duncan, A., 2020. Reducing soil erosion in smallholder farming systems in east Africa through the introduction of different crop types. *Experimental Agriculture*, *56*(2), pp.183-195.

Naulin, P.A., Armijo, G.I., Vega, A.S., Tamayo, K.P., Gras, D.E., de la Cruz, J. and Gutiérrez, R.A., 2020. Nitrate induction of primary root growth requires cytokinin signaling in Arabidopsis thaliana. *Plant and Cell Physiology*, *61*(2), pp.342-352.

Nikiforova, V., Freitag, J., Kempa, S., Adamik, M., Hesse, H. and Hoefgen, R., 2003. Transcriptome analysis of sulfur depletion in Arabidopsis thaliana: interlacing of biosynthetic pathways provides response specificity. *The Plant Journal*, *33*(4), pp.633-650.

Niu, Y.F., Chai, R.S., Jin, G.L., Wang, H., Tang, C.X. and Zhang, Y.S., 2013. Responses of root architecture development to low phosphorus availability: a review. *Annals of botany*, *112*(2), pp.391-408.

Niwa, H., 2018. The principles that govern transcription factor network functions in stem cells. *Development*, *145*(6).

O'Brien, J.A., Vega, A., Bouguyon, E., Krouk, G., Gojon, A., Coruzzi, G. and Gutiérrez, R.A., 2016. Nitrate transport, sensing, and responses in plants. *Molecular plant*, *9*(6), pp.837-856.

Odufuwa, B.O. Adedeji, O.H. Oladesu, J.O. and Bongwa, A. (2012). Floods of Fury in Nigerian Cities. *Journal of Sustainable Development,* 5(7): 69–79.

Ogata, K., Morikawa, S., Nakamura, H., Sekikawa, A., Inoue, T., Kanai, H., Sarai, A., Ishii, S. and Nishimura, Y., 1994. Solution structure of a specific DNA complex of the Myb DNA-binding domain with cooperative recognition helices. *Cell*, *79*(4), pp.639-648.

Ojigi, M.L., Abdulkadir, F.I. and Aderoju, M.O., 2013, April. Geospatial mapping and analysis of the 2012 flood disaster in central parts of Nigeria. In *8th National GIS Symposium. Dammam. Saudi Arabia* (pp. 1067-1077).

Omary, M., Gil-Yarom, N., Yahav, C., Steiner, E. and Efroni, I., 2020. A conserved superlocus regulates above-and belowground root initiation. *bioRxiv*.

Osmont, K.S., Sibout, R. and Hardtke, C.S., 2007. Hidden branches: developments in root system architecture. *Annu. Rev. Plant Biol.*, *58*, pp.93-113.

Oughtred, R., Rust, J., Chang, C., Breitkreutz, B.J., Stark, C., Willems, A., Boucher, L., Leung, G., Kolas, N., Zhang, F. and Dolma, S., 2021. The BioGRID database: A comprehensive biomedical resource of curated protein, genetic, and chemical interactions. *Protein Science*, *30*(1), pp.187-200.

Ötvös, K., Marconi, M., Vega, A., O'Brien, J., Johnson, A., Abualia, R., Antonielli, L., Montesinos, J.C., Zhang, Y., Tan, S. and Cuesta, C., 2021. Modulation of plant root growth by nitrogen source-defined regulation of polar auxin transport. *The EMBO journal*, *40*(3), p.e106862.

Park, J.S., Kim, J.B., Cho, K.J., Cheon, C.I., Sung, M.K., Choung, M.G. and Roh, K.H., 2008. Arabidopsis R2R3-MYB transcription factor AtMYB60 functions as a transcriptional repressor of anthocyanin biosynthesis in lettuce (Lactuca sativa). *Plant cell reports*, *27*(6), pp.985-994.

Park, M.Y., Kang, J.Y. and Kim, S.Y., 2011. Overexpression of AtMYB52 confers ABA hypersensitivity and drought tolerance. *Molecules and cells*, *31*(5), pp.447-454.

Paz-Ares, J., Ghosal, D., Wienand, U., Peterson, P.A. and Saedler, H., 1987. The regulatory c1 locus of Zea mays encodes a protein with homology to myb proto-oncogene products and with structural similarities to transcriptional activators. *The EMBO journal*, *6*(12), pp.3553-3558.

Péret, B., Larrieu, A. and Bennett, M.J., 2009. Lateral root emergence: a difficult birth. *Journal of experimental botany*, *60*(13), pp.3637-3643.

Perianez-Rodriguez, J., Rodriguez, M., Marconi, M., Bustillo-Avendaño, E., Wachsman, G., Sanchez-Corrionero, A., De Gernier, H., Cabrera, J., Perez-Garcia, P., Gude, I. and Saez, A., 2021. An auxin-regulable oscillatory circuit drives the root clock in Arabidopsis. *Science advances*, *7*(1), p.eabd4722.

PERUMALLA, C.J., PETERSON, C.A. and ENSTONE, D.E., 1990. A survey of angiosperm species to detect hypodermal Casparian bands. I. Roots with a uniseriate hypodermis and epidermis. *Botanical Journal of the Linnean Society*, *103*(2), pp.93-112.

Pfalz, M., Mikkelsen, M.D., Bednarek, P., Olsen, C.E., Halkier, B.A. and Kroymann, J., 2011. Metabolic engineering in Nicotiana benthamiana reveals key enzyme functions in Arabidopsis indole glucosinolate modification. *The Plant Cell*, *23*(2), pp.716-729.

Pimentel, D. and Burgess, M., 2013. Soil erosion threatens food production. *Agriculture*, *3*(3), pp.443-463.

Planchais, S., Perennes, C., Glab, N., Mironov, V., Inzé, D. and Bergounioux, C., 2002. Characterization of cis-acting element involved in cell cycle phase-independent activation of Arath; CycB1; 1 transcription and identification of putative regulatory proteins. *Plant molecular biology*, *50*(1), pp.109-125.

Popescu, S.C., Popescu, G.V., Bachan, S., Zhang, Z., Gerstein, M., Snyder, M. and Dinesh-Kumar, S.P., 2009. MAPK target networks in Arabidopsis thaliana revealed using functional protein microarrays. *Genes & development*, *23*(1), pp.80-92.

Poschet, G., Hannich, B. and Büttner, M., 2010. Identification and characterization of AtSTP14, a novel galactose transporter from Arabidopsis. *Plant and cell physiology*, *51*(9), pp.1571-1580.

Poschet, G., Hannich, B., Raab, S., Jungkunz, I., Klemens, P.A., Krueger, S., Wic, S., Neuhaus, H.E. and Büttner, M., 2011. A novel Arabidopsis vacuolar glucose exporter is involved in cellular sugar homeostasis and affects the composition of seed storage compounds. *Plant physiology*, *157*(4), pp.1664-1676.

Postma, J.A., Dathe, A. and Lynch, J.P., 2014. The optimal lateral root branching density for maize depends on nitrogen and phosphorus availability. *Plant physiology*, *166*(2), pp.590-602.

Pu, M. and Zhong, Y., 2020. Rising concerns over agricultural production as COVID-19 spreads: Lessons from China. *Global food security*, *26*, p.100409.

Qin, H., He, L. and Huang, R., 2019. The coordination of ethylene and other hormones in primary root development. *Frontiers in plant science*, *10*, p.874.

Rabinowicz, P.D., Braun, E.L., Wolfe, A.D., Bowen, B. and Grotewold, E., 1999. Maize R2R3 Myb genes: sequence analysis reveals amplification in the higher plants. *Genetics*, *153*(1), pp.427-444.

Ranjan, A., Ichihashi, Y. and Sinha, N.R., 2012. The tomato genome: implications for plant breeding, genomics and evolution. *Genome biology*, *13*(8), pp.1-8.

Rapp, R.A. and Wendel, J.F., 2005. Epigenetics and plant evolution. *New Phytologist*, *168*(1), pp.81-91.

Rogers, E.D. and Benfey, P.N., 2015. Regulation of plant root system architecture: implications for crop advancement. *Current Opinion in Biotechnology*, *32*, pp.93-98.

Roppolo, D., Boeckmann, B., Pfister, A., Boutet, E., Rubio, M.C., Dénervaud-Tendon, V., Vermeer, J.E., Gheyselinck, J., Xenarios, I. and Geldner, N., 2014. Functional and evolutionary analysis of the CASPARIAN STRIP MEMBRANE DOMAIN PROTEIN family. *Plant physiology*, *165*(4), pp.1709-1722.

Rosinski, J.A. and Atchley, W.R., 1998. Molecular evolution of the Myb family of transcription factors: evidence for polyphyletic origin. *Journal of Molecular Evolution*, *46*(1), pp.74-83.

Ron, M., Kajala, K., Pauluzzi, G., Wang, D., Reynoso, M.A., Zumstein, K., Garcha, J., Winte, S., Masson, H., Inagaki, S. and Federici, F., 2014. Hairy root transformation using Agrobacterium rhizogenes as a tool for exploring cell type-specific gene expression and function using tomato as a model. *Plant physiology*, *166*(2), pp.455-469.

Roy, S., 2016. Function of MYB domain transcription factors in abiotic stress and epigenetic control of stress response in plant genome. *Plant signaling & behavior*, *11*(1), p.e1117723.

Sahu, S.K., Behera, P.K., Choudhury, P., Panda, S. and Rout, L., 2020. Strategy and Problems for Synthesis of Antimalaria Artemisinin (Qinghaosu). *ChemistrySelect*, *5*(40), pp.12333-12344.

Scheres, B., Wolkenfelt, H., Willemsen, V., Terlouw, M., Lawson, E., Dean, C. and Weisbeek, P., 1994. Embryonic origin of the Arabidopsis primary root and root meristem initials. *Development*, *120*(9), pp.2475-2487.

Schmitz G, Tillmann E, Carriero F, *et al*. The tomato Blind gene encodes a MYB transcription factor that controls the formation of lateral meristems[J]. Proceedings of the National Academy of Sciences of the United States of America, 2002, 99(2):1064-9.

Schneidereit, A., Scholz-Starke, J. and Büttner, M., 2003. Functional characterization and expression analyses of the glucose-specific AtSTP9 monosaccharide transporter in pollen of Arabidopsis. *Plant Physiology*, *133*(1), pp.182-190.

Seo, P.J. and Park, C.M., 2009. Auxin homeostasis during lateral root development under drought condition. *Plant signaling & behavior*, *4*(10), pp.1002-1004.

Seo, P.J., Xiang, F., Qiao, M., Park, J.Y., Lee, Y.N., Kim, S.G., Lee, Y.H., Park, W.J. and Park, C.M., 2009. The MYB96 transcription factor mediates abscisic acid signaling during drought stress response in Arabidopsis. *Plant physiology*, *151*(1), pp.275-289.

Shanks, J.V. and Morgan, J., 1999. Plant 'hairy root'culture. *Current Opinion in Biotechnology*, *10*(2), pp.151-155.

Shaw, D. John, (2007), World Food Security: A History Since 1945.

Shen, B., Li, C. and Tarczynski, M.C., 2002. High free-methionine and decreased lignin content result from a mutation in the Arabidopsis S-adenosyl-L-methionine synthetase 3 gene. *The Plant Journal*, *29*(3), pp.371-380.

Sheng, Q., Vickers, K., Zhao, S., Wang, J., Samuels, D.C., Koues, O., Shyr, Y. and Guo, Y., 2017. Multi-perspective quality control of Illumina RNA sequencing data analysis. *Briefings in functional genomics*, *16*(4), pp.194-204.

Sherman, B.T. and Lempicki, R.A., 2009. Systematic and integrative analysis of large gene lists using DAVID bioinformatics resources. *Nature protocols*, *4*(1), pp.44-57.

Shi, P., Fu, X., Shen, Q., Liu, M., Pan, Q., Tang, Y., Jiang, W., Lv, Z., Yan, T., Ma, Y. and Chen, M., 2018. The roles of Aa MIXTA 1 in regulating the initiation of glandular trichomes and cuticle biosynthesis in Artemisia annua. *New Phytologist*, *217*(1), pp.261-276.

Shin, R., Burch, A.Y., Huppert, K.A., Tiwari, S.B., Murphy, A.S., Guilfoyle, T.J. and Schachtman, D.P., 2007. The Arabidopsis transcription factor MYB77 modulates auxin signal transduction. *The Plant Cell*, *19*(8), pp.2440-2453.

Shukla, V., Han, J.P., Cléard, F., Lefebvre-Legendre, L., Gully, K., Flis, P., Berhin, A., Andersen, T.G., Salt, D.E., Nawrath, C. and Barberon, M., 2021. Suberin plasticity to developmental and exogenous cues is regulated by a set of MYB transcription factors. *bioRxiv*.

Singh, M., Gupta, A. and Laxmi, A., 2017. Striking the right chord: signaling enigma during root gravitropism. *Frontiers in plant science*, *8*, p.1304.

Sogn, T.A., Dragicevic, I., Linjordet, R., Krogstad, T., Eijsink, V.G. and Eich-Greatorex, S., 2018. Recycling of biogas digestates in plant production: NPK fertilizer value and risk of leaching. *International Journal of Recycling of Organic Waste in Agriculture*, *7*(1), pp.49-58.

Song, S., Qi, T., Huang, H., Ren, Q., Wu, D., Chang, C., Peng, W., Liu, Y., Peng, J. and Xie, D., 2011. The Jasmonate-ZIM domain proteins interact with the R2R3-MYB transcription factors MYB21 and MYB24 to affect Jasmonate-regulated stamen development in Arabidopsis. *The Plant Cell*, *23*(3), pp.1000-1013.

Song, Y., Wang, Y., Mao, W., Sui, H., Yong, L., Yang, D., Jiang, D., Zhang, L. and Gong, Y., 2017. Dietary cadmium exposure assessment among the Chinese population. *PLoS One*, *12*(5), p.e0177978.

Song, L., Pan, Z., Chen, L., Dai, Y., Wan, J., Ye, H., Nguyen, H.T., Zhang, G. and Chen, H., 2020. Analysis of whole transcriptome RNA-seq data reveals many alternative splicing events in soybean roots under drought stress conditions. *Genes*, *11*(12), p.1520.

Soumya, P.R., Sharma, S., Meena, M.K. and Pandey, R., 2021. Response of diverse bread wheat genotypes in terms of root architectural traits at seedling stage in response to low phosphorus stress. *Plant Physiology Reports*, *26*(1), pp.152-161.

Steffens, B. and Rasmussen, A., 2016. The physiology of adventitious roots. *Plant physiology*, *170*(2), pp.603-617.

Stracke, R., Jahns, O., Keck, M., Tohge, T., Niehaus, K., Fernie, A.R. and Weisshaar, B., 2010. Analysis of PRODUCTION OF FLAVONOL GLYCOSIDES-dependent flavonol glycoside accumulation in Arabidopsis thaliana plants reveals MYB11-, MYB12-and MYB111-independent flavonol glycoside accumulation. *New Phytologist*, *188*(4), pp.985-1000.

Sukumar, P., Maloney, G.S. and Muday, G.K., 2013. Localized induction of the ATP-binding cassette B19 auxin transporter enhances adventitious root formation in Arabidopsis. *Plant physiology*, *162*(3), pp.1392-1405.

Svistoonoff, S., Creff, A., Reymond, M., Sigoillot-Claude, C., Ricaud, L., Blanchet, A., Nussaume, L. and Desnos, T., 2007. Root tip contact with low-phosphate media reprograms plant root architecture. *Nature genetics*, *39*(6), pp.792-796.

Szczepanek, M., Pobereżny, J., Wszelaczyńska, E. and Gościnna, K., 2020. Effect of biostimulants and storage on discoloration potential of carrot. *Agronomy*, *10*(12), p.1894.

Tabe, L., Wirtz, M., Molvig, L., Droux, M. and Hell, R., 2010. Overexpression of serine acetlytransferase produced large increases in O-acetylserine and free cysteine in developing seeds of a grain legume. *Journal of experimental botany*, *61*(3), pp.721-733.

Taj, G., Agarwal, P., Grant, M. and Kumar, A., 2010. MAPK machinery in plants: recognition and response to different stresses through multiple signal transduction pathways. *Plant signaling & behavior*, *5*(11), pp.1370-1378.

Tangahu, B.V., Sheikh Abdullah, S.R., Basri, H., Idris, M., Anuar, N. and Mukhlisin, M., 2011. A review on heavy metals (As, Pb, and Hg) uptake by plants through phytoremediation. *International Journal of Chemical Engineering*, *2011*.

Tao, Y., Cheung, L.S., Li, S., Eom, J.S., Chen, L.Q., Xu, Y., Perry, K., Frommer, W.B. and Feng, L., 2015. Structure of a eukaryotic SWEET transporter in a homotrimeric complex. *Nature*, *527*(7577), pp.259-263.

Tepfer, M. and Casse-Delbart, F., 1987. Agrobacterium rhizogenes as a vector for transforming higher plants. *Microbiological sciences*, *4*(1), pp.24-28.

Tian, H., De Smet, I. and Ding, Z., 2014. Shaping a root system: regulating lateral versus primary root growth. *Trends in plant science*, *19*(7), pp.426-431.

Tian, H., Jia, Y., Niu, T., Yu, Q. and Ding, Z., 2014. The key players of the primary root growth and development also function in lateral roots in Arabidopsis. *Plant cell reports*, *33*(5), pp.745-753.

To, A., Joubès, J., Thueux, J., Kazaz, S., Lepiniec, L. and Baud, S., 2020. AtMYB92 enhances fatty acid synthesis and suberin deposition in leaves of Nicotiana benthamiana. *The Plant Journal*, *103*(2), pp.660-676.

Tohge, T., Nishiyama, Y., Hirai, M.Y., Yano, M., Nakajima, J.I., Awazuhara, M., Inoue, E., Takahashi, H., Goodenowe, D.B., Kitayama, M. and Noji, M., 2005. Functional genomics by integrated analysis of metabolome and transcriptome of Arabidopsis plants over-expressing an MYB transcription factor. *The Plant Journal*, *42*(2), pp.218-235.

UN. World Population Prospects. The 2019 Revision. Volume I : Comprehensive Tables. New York, United Nations, 2013.

UN, Draft resolution submitted by the Vice-Chair of the Committee, Ms. Farrah Brown (Jamaica), on the basis of informal consultations on draft resolution A/C.2/68/L.21, viewed on 24th March 2021, < http://www.fao.org/fileadmin/user_upload/GSP/docs/iys/World_ Soil_Day_and_International_Year _of_Soils __UNGA_Resolution_Dec._2013.pdf >

United Nations. 1975. Report of the World Food Conference, Rome 5-16 November 1974. New York.

United Nations. Universal Declaration of Human Rights (1948)

Urbanowicz, B.R., Catalá, C., Irwin, D., Wilson, D.B., Ripoll, D.R. and Rose, J.K., 2007. A tomato endo-β-1, 4-glucanase, SlCel9C1, represents a distinct subclass with a new family of carbohydrate binding modules (CBM49). *Journal of Biological Chemistry*, *282*(16), pp.12066-12074.

Ursache, R., Vieira-Teixeira, C.D.J., Tendon, V.D., Gully, K., De Bellis, D., Schmid-Siegert, E., Andersen, T.G., Shekhar, V., Calderon, S., Pradervand, S. and Nawrath, C., 2020. GDSL-domain containingå proteins mediate suberin biosynthesis and degradation, enabling developmental plasticity of the endodermis during lateral root emergence. *bioRxiv*.

USEPA 2021, Superfund: National Priorities List (NPL), viewed on 24th March 2021, < https://www.epa.gov/superfund/superfund-national-priorities-list-npl>

Vailleau, F., Daniel, X., Tronchet, M., Montillet, J.L., Triantaphylides, C. and Roby, D., 2002. A R2R3-MYB gene, AtMYB30, acts as a positive regulator of the hypersensitive cell death program in plants in response to pathogen attack. *Proceedings of the National Academy of Sciences*, *99*(15), pp.10179-10184.

Van Bavel, J., 2013. The world population explosion: causes, backgrounds and projections for the future. *Facts, views & vision in ObGyn*, *5*(4), p.281.

Van Ittersum, M.K., Van Bussel, L.G., Wolf, J., Grassini, P., Van Wart, J., Guilpart, N., Claessens, L., de Groot, H., Wiebe, K., Mason-D'Croz, D. and Yang, H., 2016. Can sub-Saharan Africa feed itself?. *Proceedings of the National Academy of Sciences*, *113*(52), pp.14964-14969.

Vangheluwe, N. and Beeckman, T., 2021. Lateral Root Initiation and the Analysis of Gene Function Using Genome Editing with CRISPR in Arabidopsis. *Genes*, *12*(6), p.884.

van Weringh, A., Pasha, A., Esteban, E., Gamueda, P.J. and Provart, N.J., 2021. Generation of guard cell RNA-seq transcriptomes during progressive drought and recovery using an adapted INTACT protocol for Arabidopsis thaliana shoot tissue. *bioRxiv*.

Vedamurthy, A.B., Bhattacharya, S., Das, A. and Shruthi, S.D., 2021. Exploring nanomaterials with rhizobacteria in current agricultural scenario. In *Advances in Nano-Fertilizers and Nano-Pesticides in Agriculture* (pp. 487-503). Woodhead Publishing.

Velasco, R., Zharkikh, A., Troggio, M., Cartwright, D.A., Cestaro, A., Pruss, D., Pindo, M., FitzGerald, L.M., Vezzulli, S., Reid, J. and Malacarne, G., 2007. A high quality draft consensus sequence of the genome of a heterozygous grapevine variety. *PloS one*, *2*(12), p.e1326.

Vermeer, J.E., von Wangenheim, D., Barberon, M., Lee, Y., Stelzer, E.H., Maizel, A. and Geldner, N., 2014. A spatial accommodation by neighboring cells is required for organ initiation in Arabidopsis. *Science*, *343*(6167), pp.178-183.

Vidal, E.A., Araus, V., Lu, C., Parry, G., Green, P.J., Coruzzi, G.M. and Gutiérrez, R.A., 2010. Nitrate-responsive miR393/AFB3 regulatory module controls root system architecture in Arabidopsis thaliana. *Proceedings of the National Academy of Sciences*, *107*(9), pp.4477-4482.

Voß, U., Wilson, M.H., Kenobi, K., Gould, P.D., Robertson, F.C., Peer, W.A., Lucas, M., Swarup, K., Casimiro, I., Holman, T.J. and Wells, D.M., 2015. The circadian clock rephases during lateral root organ initiation in Arabidopsis thaliana. *Nature communications*, *6*(1), pp.1-9.

Wang, Z., Gerstein, M. and Snyder, M., 2009. RNA-Seq: a revolutionary tool for transcriptomics. *Nature reviews genetics*, *10*(1), pp.57-63.

Wang, B., Luo, Q., Li, Y., Yin, L., Zhou, N., Li, X., Gan, J. and Dong, A., 2020. Structural insights into target DNA recognition by R2R3-MYB transcription factors. *Nucleic acids research*, *48*(1), pp.460-471.

Wang, Z., Tang, J., Hu, R., Wu, P., Hou, X.L., Song, X.M. and Xiong, A.S., 2015. Genome-wide analysis of the R2R3-MYB transcription factor genes in Chinese cabbage (Brassica rapa ssp. pekinensis) reveals their stress and hormone responsive patterns. *BMC genomics*, *16*(1), pp.1-21.

Watson, A., Ghosh, S., Williams, M.J., Cuddy, W.S., Simmonds, J., Rey, M.D., Hatta, M.A.M., Hinchliffe, A., Steed, A., Reynolds, D. and Adamski, N.M., 2018. Speed breeding is a powerful tool to accelerate crop research and breeding. *Nature plants*, *4*(1), pp.23-29.

WFP (World Food Programme). COVID-19 Pandemic, viewed on 22nd July 2021, < https://www.wfp.org/emergencies/covid-19-pandemic>

Wingenter, K., Schulz, A., Wormit, A., Wic, S., Trentmann, O., Hoermiller, I.I., Heyer, A.G., Marten, I., Hedrich, R. and Neuhaus, H.E., 2010. Increased activity of the vacuolar monosaccharide transporter TMT1 alters cellular sugar partitioning, sugar signaling, and seed yield in Arabidopsis. *Plant physiology*, *154*(2), pp.665-677.

Winter, D., Vinegar, B., Nahal, H., Ammar, R., Wilson, G.V. and Provart, N.J., 2007. An "Electronic Fluorescent Pictograph" browser for exploring and analyzing large-scale biological data sets. *PloS one*, *2*(8), p.e718.

Wu, Y., Ma, L., Liu, Q., Vestergård, M., Topalovic, O., Wang, Q., Zhou, Q., Huang, L., Yang, X. and Feng, Y., 2020. The plant-growth promoting bacteria promote cadmium uptake by inducing a hormonal crosstalk and lateral root formation in a hyperaccumulator plant Sedum alfredii. *Journal of hazardous materials*, *395*, p.122661.

Wuepper, D., Borrelli, P. and Finger, R., 2020. Countries and the global rate of soil erosion. *Nature Sustainability*, *3*(1), pp.51-55.

WULFF-ZOTTELE, C.R.I.S.T.I.Á.N., Gatzke, N., Kopka, J., Orellana, A., Hoefgen, R., Fisahn, J. and Hesse, H., 2010. Photosynthesis and metabolism interact during acclimation of Arabidopsis thaliana to high irradiance and sulphur depletion. *Plant, cell & environment*, *33*(11), pp.1974-1988.

WTO. WTO | Frequently asked questions: The WTO and COVID-19. 2021.

Xu, J., Meng, J., Meng, X., Zhao, Y., Liu, J., Sun, T., Liu, Y., Wang, Q. and Zhang, S., 2016. Pathogen-responsive MPK3 and MPK6 reprogram the biosynthesis of indole glucosinolates and their derivatives in Arabidopsis immunity. *The Plant Cell*, *28*(5), pp.1144-1162.

Xu, W., Dubos, C. and Lepiniec, L., 2015. Transcriptional control of flavonoid biosynthesis by MYB–bHLH–WDR complexes. *Trends in plant science*, *20*(3), pp.176-185.

Xuan, W., Band, L.R., Kumpf, R.P., Van Damme, D., Parizot, B., De Rop, G., Opdenacker, D., Möller, B.K., Skorzinski, N., Njo, M.F. and De Rybel, B., 2016. Cyclic programmed cell death stimulates hormone signaling and root development in Arabidopsis. *Science*, *351*(6271), pp.384-387.

Yadav, V., Molina, I., Ranathunge, K., Castillo, I.Q., Rothstein, S.J. and Reed, J.W., 2014. ABCG transporters are required for suberin and pollen wall extracellular barriers in Arabidopsis. *The Plant Cell*, *26*(9), pp.3569-3588.

Yamada, K., Kanai, M., Osakabe, Y., Ohiraki, H., Shinozaki, K. and Yamaguchi-Shinozaki, K., 2011. Monosaccharide absorption activity of Arabidopsis roots depends on expression profiles of transporter genes under high salinity conditions. *Journal of Biological Chemistry*, *286*(50), pp.43577-43586.

Yang, C., Song, J., Ferguson, A.C., Klisch, D., Simpson, K., Mo, R., Taylor, B., Mitsuda, N. and Wilson, Z.A., 2017. Transcription factor MYB26 is key to spatial specificity in anther secondary thickening formation. *Plant physiology*, *175*(1), pp.333-350.

Yanhui, C., Xiaoyuan, Y., Kun, H., Meihua, L., Jigang, L., Zhaofeng, G., Zhiqiang, L., Yunfei, Z., Xiaoxiao, W., Xiaoming, Q. and Yunping, S., 2006. The MYB transcription factor superfamily of Arabidopsis: expression analysis and phylogenetic comparison with the rice MYB family. *Plant molecular biology*, *60*(1), pp.107-124.

Yatusevich, R., Mugford, S.G., Matthewman, C., Gigolashvili, T., Frerigmann, H., Delaney, S., Koprivova, A., Flügge, U.I. and Kopriva, S., 2010. Genes of primary sulfate assimilation are part of the glucosinolate biosynthetic network in Arabidopsis thaliana. *The Plant Journal*, *62*(1), pp.1-11.

Yin, R., Han, K., Heller, W., Albert, A., Dobrev, P.I., Zažímalová, E. and Schäffner, A.R., 2014. Kaempferol 3-O-rhamnoside-7-O-rhamnoside is an endogenous flavonol inhibitor of polar auxin transport in Arabidopsis shoots. *New Phytologist*, *201*(2), pp.466-475.

Yoshimoto, N., Takahashi, H., Smith, F.W., Yamaya, T. and Saito, K., 2002. Two distinct high-affinity sulfate transporters with different inducibilities mediate uptake of sulfate in Arabidopsis roots. *The Plant Journal*, *29*(4), pp.465-473.

Yoshimoto, N., Inoue, E., Saito, K., Yamaya, T. and Takahashi, H., 2003. Phloem-localizing sulfate transporter, Sultr1; 3, mediates re-distribution of sulfur from source to sink organs in Arabidopsis. *Plant Physiology*, *131*(4), pp.1511-1517.

Yu, Q., Liu, S., Yu, L. *et al.* RNA demethylation increases the yield and biomass of rice and potato plants in field trials. *Nat Biotechnol* (2021). https://doi.org/10.1038/s41587-021-00982-9

Yuan, W., Zhang, D., Song, T., Xu, F., Lin, S., Xu, W., Li, Q., Zhu, Y., Liang, J. and Zhang, J., 2017. Arabidopsis plasma membrane H+-ATPase genes AHA2 and AHA7 have distinct and overlapping roles in the modulation of root tip H+ efflux in response to low-phosphorus stress. *Journal of experimental botany*, *68*(7), pp.1731-1741.

Zhang, H., Zhang, F., Yu, Y., Feng, L., Jia, J., Liu, B., Li, B., Guo, H. and Zhai, J., 2020. A comprehensive online database for exploring∼ 20,000 public Arabidopsis RNA-seq libraries. *Molecular Plant*, *13*(9), pp.1231-1233.

Zhang, H., San, M.L., Jang, S.G., Lee, J.H., Kim, N.E., Lee, A.R., Park, S.Y., Cao, F.Y., Chin, J.H. and Kwon, S.W., 2020. Genome-wide association study of root system development at seedling stage in rice. *Genes*, *11*(12), p.1395.

Zhao, S., Zhang, M.L., Ma, T.L. and Wang, Y., 2016. Phosphorylation of ARF2 relieves its repression of transcription of the K+ transporter gene HAK5 in response to low potassium stress. *The Plant Cell*, *28*(12), pp.3005-3019.

Zhou, M., Zhang, K., Sun, Z., Yan, M., Chen, C., Zhang, X., Tang, Y. and Wu, Y., 2017. LNK1 and LNK2 corepressors interact with the MYB3 transcription factor in phenylpropanoid biosynthesis. *Plant physiology*, *174*(3), pp.1348-1358.

Zhu, J. and Lynch, J.P., 2004. The contribution of lateral rooting to phosphorus acquisition efficiency in maize (Zea mays) seedlings. *Functional Plant Biology*, *31*(10), pp.949-958.

Zhu, N., Cheng, S., Liu, X., Du, H., Dai, M., Zhou, D.X., Yang, W. and Zhao, Y., 2015. The R2R3-type MYB gene OsMYB91 has a function in coordinating plant growth and salt stress tolerance in rice. *Plant Science*, *236*, pp.146-156.

Zhu, Q., Shao, Y., Ge, S., Zhang, M., Zhang, T., Hu, X., Liu, Y., Walker, J., Zhang, S. and Xu, J., 2019. A MAPK cascade downstream of IDA–HAE/HSL2 ligand–receptor pair in lateral root emergence. *Nature plants*, *5*(4), pp.414-423.

Zhu, Y., Klasfeld, S., Jeong, C.W., Jin, R., Goto, K., Yamaguchi, N. and Wagner, D., 2020. TERMINAL FLOWER 1-FD complex target genes and competition with FLOWERING LOCUS T. *Nature communications*, *11*(1), pp.1-12.

Zimmermann, P., Hirsch-Hoffmann, M., Hennig, L. and Gruissem, W., 2004. GENEVESTIGATOR. Arabidopsis microarray database and analysis toolbox. *Plant physiology*, *136*(1), pp.2621-2632.

Zobel, R.W., 2016. Arabidopsis: An adequate model for dicot root systems?. *Frontiers in plant science*, *7*, p.58.

Zouine, M., Maza, E., Djari, A., Lauvernier, M., Frasse, P., Smouni, A., Pirrello, J. and Bouzayen, M., 2017. TomExpress, a unified tomato RNA-Seq platform for visualization of expression data, clustering and correlation networks. *The Plant Journal*, *92*(4), pp.727-735.